9-2021

Optimal Incorporation of Non-Traditional Sensors Into the Space Domain Awareness Architecture

Albert R. Vasso

OPTIMAL INCORPORATION OF NON-TRADITIONAL SENSORS INTO THE SPACE DOMAIN AWARENESS ARCHITECTURE

DISSERTATION

Albert R. Vasso, Major, USSF

AFIT-ENY-DS-21-S-110

DEPARTMENT OF THE AIR FORCE
AIR UNIVERSITY

AIR FORCE INSTITUTE OF TECHNOLOGY

Wright-Patterson Air Force Base, Ohio

AFIT-ENY-DS-21-S-110

OPTIMAL INCORPORATION OF NON-TRADITIONAL SENSORS INTO THE SPACE DOMAIN AWARENESS ARCHITECTURE

DISSERTATION

Presented to the Faculty

Department of Aeronautics and Astronautics

Graduate School of Engineering and Management

Air Force Institute of Technology

Air University

Air Education and Training Command

In Partial Fulfillment of the Requirements for the

Degree of Doctor of Philosophy

Albert R. Vasso, BS, MS

Major, USSF

August 2021

AFIT-ENY-DS-21-S-110

OPTIMAL INCORPORATION OF NON-TRADITIONAL SENSORS INTO THE SPACE DOMAIN AWARENESS ARCHITECTURE

Albert R. Vasso, BS, MS

Major, USSF

Committee Membership:

Richard G. Cobb, Ph.D.
Chair

John M. Colombi, Ph.D.
Member

Bryan D. Little, Lt Col, Ph.D.
Member

David W. Meyer, M.S.
Member

ADEDEJI B. BADIRU, Ph.D.
Dean, Graduate School of Management

Abstract

The United States Government is the world's *de facto* provider of space object cataloging data, but is challenged to maintain pace in an increasingly complex space environment. This work advances a multi-disciplinary approach to better understand and evaluate an underexplored solution recommended by national policy, in which current collection capabilities are augmented with non-traditional sensors. System architecting and literature identify likely needs, performance measures, and contributors to a conceptualized Augmented Network. Multiple hypothetical telescope architectures are modeled and simulated on four separate days throughout the year, then evaluated against performance measures and constraints using optimization. Decision analysis and Pareto optimality identify a small, diverse set of high-performing architectures while preserving design flexibility. The efficacy of using the performance measures as proxies for reducing positional uncertainty is also explored. The results suggest a 3.5-times increase in average capacity, 55% improvement in coverage, and 3.5 hour decrease in the average maximum time a space object goes unobserved is achievable if decision-makers adopt the Augmented Network approach. A correlation between performance and positional uncertainty is found, suggesting top architectures can generally achieve a major Space Domain Awareness technical requirement without explicitly conducting an orbit determination routine on simulated collection data.

Acknowledgments

"Things are only impossible until they are not."

– J.L. Picard

I wish to express gratitude to the Committee for their guidance on the development and implementation of this research. I would also like to thank Ms. Jaclyn Schmidt from the AFIT Center for Directed Energy, Mr. Dave Vallado and many other employees from Analytical Graphics Incorporated, Dr. Tamara Payne from Applied Optimization, and analysts from the 14th Weather Squadron for their help in completing portions of this work. The developers of the various software routines which underpin and sped conclusion of this work are acknowledged for providing quality products, many times at no-cost, so that individuals can more readily enhance the collective body of knowledge. I reserve a special salutation for members of the local community—notably Mike, Mark, Dale, Kalen, Mat, and Rob—whose virtual friendships made execution during the pandemic more bearable. Finally, I would like to thank my family for their unwavering support throughout the past three years, their mentorship and kind words, and for ultimately empowering me to succeed in this and many other goals in my life. *Supra Summus*.

Albert R. Vasso

Table of Contents

Page

List of Figures

Page

List of Tables

Page

List of Acronyms

Acronym	Definition
AFB	Air Force Base
AFRL	Air Force Research Laboratory
AFSPC	Air Force Space Command
AFSPCI	AFSPC Instruction
AGI	Analytical Graphics Inc.
AIC	Astrodynamics Innovation Committee
AN	Augmented Network
ASW	Astrodynamic Support Workstation
BIGGO	Brazil-Internacional Gigante Global Observatorio
C2	Command and Control
C4I	Command, Control, Communications, Computer, and Information
CA	Conjunction Assessment
CAMO	Commercially Augmented Mission Operations
CAVENet	Correlation, Analysis, and Verification of Ephemerides Network
CCD	Charged Coupled Device
CSSI	Center for Space Standards and Innovation
CEO	Chief Executive Officer
CM	Clear Moonless
ComSpOC	Commercial Space Operations Center
COTS	Commercial Off-the-Shelf
CRN	Common Random Numbers
CSpOC	Combined Space Operations Center
DARPA	Defense Advanced Research Projects Agency
DIA	Defense Intelligence Agency
DISCO	Disaggregated Integral System Concept Optimization
DMSP	Defense Meteorological Satellite Program
DoD	Department of Defense
DS	Deep-Space
EBMC2	Enterprise Battle Management Command and Control
EDR	Energy Dissipation Rate
EO	Electro-Optical
FOR	Field of Regard
FOV	Field of View
GA	Genetic Algorithm
GAO	Government Accountability Office
GEO	Geosynchronous Earth Orbit
GEODSS	Ground-Based Electro-Optical Deep Space Surveillance System
GP	General Perturbations

Acronym	Definition
GPO	Geosynchronous Polar Orbit
GSO	Geostationary Earth Orbit
HEO	Highly Eccentric Orbit
HPC	High-Performance Computing
ISCCP	International Satellite Cloud Climatology Project
JMS	JSpOC Mission System
JP	Joint Publication
JSpOC	Joint Space Operations Center
KPPs	Key Performance Parameters
LEEDR	Laser Environmental Effects Definition and Reference
LEO	Low Earth Orbit
LSST	Large Synoptic Survey Telescope
M&S	Model and Simulation
MCAT	Meter-Class Autonomous Telescope
MEO	Medium Earth Orbit
METAR	Meteorological Aerodrome Reports
MODEST	Michigan Orbital Debris Survey Telescope
MODIS	Moderate Resolution Imaging Spectroradiometer
MOEs	Measures of Effectiveness
MOO	Multi-Objective Optimization
MOPs	Measures of Performance
MUA	Military Utility Assessment
NASA	National Aeronautics and Space Administration
NASIC	National Air and Space Intelligence Center
NDPP	Non-Traditional Data Pre-Processor
NE	Near-Earth
NFOV	Narrow Field of View
NOAA	National Oceanic and Atmospheric Administration
NPF	Normalized Pareto Front
NSDC	National Space Defense Center
NSGA-II	Non-Sorted Genetic Algorithm II
NSOSA	NOAA Satellite Observing System Architecture
O&M	Operations and Maintenance
OD	Orbit Determination
ODTK	Orbit Determination Tool Kit
OPCON	Operational Control
ORS-5	Operationally Responsive Space 5
Pan-STARRS	Panoramic Survey Telescope and Rapid Response System
PCFLOS	Probability of Cloud Free Line of Sight
PCFN	Probability of Cloud Free Night

Acronym	Definition
PU	Percent Unrealized
RA	Right Ascension
RAM	Random Access Memory
RCS	Radar Cross Section
RF	Radio Frequency
RSO	Resident Space Object
SADSS	Small Aperture Deep Space Surveillance
SBSS	Space-Based Space Surveillance
SDA	Space Domain Awareness
SFB	Space Force Base
SMC	Space and Missiles Systems Center
SME	Subject Matter Expert
SNPF	Sum of NPFs
SNR	Signal to Noise Ratio
SOI	Space Object Identification
SP	Special Perturbations
SPADOC	Space Defense Operations Center
SPCS	Space Control Squadron
SPD-3	Space Policy Directive 3
SPO	System Program Office
SQL	Structured Query Language
SSA	Space Situational Awareness
SSN	Space Surveillance Network
SSPU	Sum of Sum of PU
SST	Space Surveillance Telescope
STK	Systems Toolkit
STM	Space Traffic Management
SU	Sensor Utilization
TLE	Two-Line Element Set
TPMs	Technical Performance Measures
UDL	Unified Data Library
USG	United States Government
USSTRATCOM	United States Strategic Command
WFOV	Wide Field of View

OPTIMAL INCORPORATION OF NON-TRADITIONAL SENSORS INTO THE SPACE DOMAIN AWARENESS ARCHITECTURE

I. Introduction

General Issue

Reliance on space services is paramount for defense, civil, and commercial purposes. Space usage is projected to grow as responsive launches coupled with improvements in small-satellite technology lower barriers to space access, world actors solidify national space goals, and debris concerns are magnified. The need to maintain Space Domain Awareness (SDA), specifically the tracking and cataloging of Resident Space Objects (RSOs), will clearly increase. Currently, the United States Government (USG) provides the world's *de facto* SDA and Space Traffic Management (STM) services through the data gleaned from a worldwide network of USG and allied radars, telescopes, and satellites. However, the USG will be hard-pressed to maintain services due to both the increased volume of RSOs, new threats, and a failure to modernize equipment and processes.

Fortunately, recent technological advancements and realization of business cases have prompted commercial entities to field their own SDA tracking networks. Meanwhile, the USG has recognized that sensors atypically employed for space tracking such as large-scale civil and scientific telescopes may bring value to the SDA mission. The USG has publicly outlined how it will vet non-traditional sensor providers for incorporation into the SDA pipeline. However, no framework for assessing the performance of the hybrid USG/Non-traditional SDA architecture has been developed.

Problem Statement

Seeking to directly incorporate non-traditional data into the Space Surveillance Network (SSN) for use in Deep-Space (DS)[1] cataloging routines is proposed as the most impactful, actionable solution to the looming SDA challenge. However, system needs, requirements, performance measures, and capabilities of the future Augmented Space Surveillance Network, henceforth referred to as the Augmented Network (AN), are not extant. These are first inferred from literature review and engineering judgment, then utilized to develop a large-scale modeling and simulation (M&S) study which assesses alternative architectures. The end result employs system architecting, M&S, optimization, and decision analysis to explore and quantify the efficacy of the AN approach.

Research Objectives/Questions

This research seeks to answer the following questions:

1. Using system architecting, M&S, Multi-Objective Optimization (MOO), and decision analysis, how should the AN be optimally selected?
2. What are appropriate measures to gauge AN performance, and how should they be formulated to permit architectural comparisons?
3. How efficient and effective are non-traditional capabilities in augmenting USG SDA tracking?

[1] For the purposes of this study, DS is defined as the region in space in which RSOs have orbital periods greater than 225 min and a maximum of 24 hours. Cislunar trajectories are not considered.

Methodology

The methodology consists of seven sequential steps: developing the scenario, developing representative sites and sensors, translating AN needs into measures, developing the M&S to assess AN architectures, executing the M&S, analyzing M&S results, and assessing the efficacy of the performance measures as proxies for positional uncertainty. An iterative approach to this project is employed such that key parameters and assumptions are refined in successive, publishable revisions, eventually leading to the final product presented herein.

To advance the study, the following future scenario is assumed. A USG SDA System Program Office (SPO) is allocated $25M to incorporate DS metric data from multiple commercial, civil, and scientific providers directly into the SDA data framework. The SPO is unable to purchase all data from all providers. Desiring to incorporate observations so as to maximize AN requirement fulfillment, and to maintain operational control (OPCON) over processes, the SPO decides to select the commercial providers by purchasing fully-taskable sensors from various sites, while data from civil and scientific sensors collecting on RSOs is incorporated at no-cost. The fundamental issue becomes determining how to go about, and ultimately select, the optimal commercial sensors for incorporation in the existing SDA network. This is approached by conducting a large-scale M&S under realistic conditions using representative sensors and performance measures.

Representative networks consisting of ground- and space-based SDA sensors are developed by reviewing extant literature. The Department of Defense (DoD) network is modeled using the nine GEODSS sensors, the Space Surveillance Telescope (SST), and three space-based sensors. The National Aeronautics and Space Administration's

(NASA's) Meter-Class Autonomous Telescope (MCAT) represents the civil contributor, while a hypothetical large aperture sensor is developed as a scientific contributor. Four commercial companies with business cases, capabilities, and locations are designed based on parameters in open-source literature; three consist of ground-based small telescopes while one consists solely of space-based assets.

Review of policy, regulations, previous studies, and brainstorming generate likely AN needs and requirements, from which three architectural-level measures are chosen to quantify performance. These include the average number of observations per RSO, or average capacity; the average of the maximum time between observations per RSO; and coverage, a value which encourages geographically-distributed redundancy.

The SPO purchase decision is approached as an architectural optimization problem in which data from the USG, civil, and scientific sites are combined with any permutation of commercial sensors, yielding many architectural alternatives of differing performance. This large tradespace is smartly explored within the M&S. For each of four days, 25,000 random architectures are evaluated using the Non-Sorted Genetic Algorithm II (NSGA-II) heuristic method. Initial architectures are randomly seeded and subjected to the M&S. Better performers are identified and advanced with children architectures in successive generations during five trials. To enable a fair comparison, a set of high-performing architectures found on each day are cross-evaluated on all other days, ultimately resulting in 14,000 architectures for comparative analytical exploration.

To score each architecture during the M&S, the results of a Systems Tool Kit (STK) and Python-based optical collection scenario are employed. For each day, the Two-Line Element Sets (TLEs) for nearly 1,400 RSOs in Geosynchronous Earth Orbit (GEO),

Medium Earth Orbit (MEO), and Highly Eccentric Orbit (HEO) obtained from Space-Track are imported into an STK scenario along with ground sites and space-based observational satellites. Various STK reports are output to determine site-RSO accesses, while sensor parameters and relevant physics are fused together in Python to garner acceptable Signal to Noise Ratio (SNR) sensor-RSO accesses. A scheduling routine is developed and employed to simulate all sensors' intended collection of RSOs. This results in a database of sensor-RSO collections in time, from which every architecture pulls observational data to calculate the performance measures. 200 Monte Carlo runs are performed on each architecture to simulate cloud-out conditions by randomly excluding sites based on custom-computed weather probabilities; the averaged results are returned to the optimizer. Within each generation, all architectures are subjected to a MOO problem which seeks to optimize the performance measures while ensuring each architecture meets the $25M cost constraint.

Decision analysis is used to identify better performers from the 14,000 available architectures. Better architectures are defined as those which a non-dominated sorting routine ascribes to better Pareto fronts, such that those in the top 10% of fronts each day on all four days form the *best* set. Additional technical and managerial metrics are introduced to further reduce the set to a manageable size, referred to as the *best of best* set. A diverse set of architectures performing highly on all four days is thus identified, along with frequently- and less-frequently employed sensors and general trends which are useful for a decision-maker.

An additional topic of interest involves determining if the architectural performance measures are a reasonable proxy for architectural-wide RSO position uncertainty, such that

a better architecture as quantified by the M&S equates to an architecture with a lower network-wide RSO position uncertainty associated with each RSO in the study. Lower network-wide positional uncertainty is an implicit, if not explicit, need in Space Domain Awareness problems. The benefit of this proxy, should its utility be proven, is the simplification of architecture analysis by foregoing the need to conduct an exhaustive and intractable search on every RSO-sensor pair to determine covariance impacts. Because regulations and intuition suggest a relationship, validating the veracity of this claim aids architects and M&S developers in planning.

The core M&S is extended by creating two sets of the same RSOs; the first with positional information based on TLE data denoted the *assumed set*, and the second with positional information based on simulated certainty in position called the *truth set*. The schedule derived from the core M&S is used as the baseline in a collection scenario, while the time and locations of *truth* RSOs are used to simulate observational data. For all RSOs seen by each architecture, an orbit determination (OD) routine is run based on this data to determine the final covariance at the end of each day. This is compared to covariance information derived from the *assumed* set, and a metric is formed to express for median architectural position uncertainty. Architectural performance determined from the M&S using both Pareto front information and a weighted sum is compared to the median uncertainty to analyze the efficacy of the proxy.

Assumptions/Limitations

Because the manner in which the USG may choose to incorporate non-traditional sensors is unknown, an assumption is made that the USG would pursue the procurement

of fully-taskable commercial sensors to expedite a solution to the problem. Determining how the USG might in fact best approach the selection of sites and/or data based on the plethora of purchase options provided by commercial companies is out of scope for this work and left for future research.

A cost constraint of $25M is levied based on review of the SDA budget. Ground-based commercial sensor costs are adapted based on publicly-available pricing for ExoAnalytic turn-key sensors. Non-traditional site locations and sensor parameters are based on representative capabilities in the literature. All commercial-related data is based on open-source information, and no network devised in the study is reflective of any particular company's capabilities.

An assumption is made that all data is properly formatted and ingestible into the USG's system of record. While the USG has made strides to accept new data formats, work remains on improving the ability of the system to ingest a larger volume of data. It is also assumed that a near-future SDA system will be able to accommodate this volume of data due to improved processes.

The study is purposefully limited to the optical collection of RSOs in the DS regime for cataloging only. While including characterization or Space Object Identification (SOI) capabilities would make the problem more complete, simulating photometric returns and allocating the scheduling tradeoff between cataloging and characterization is thought to add an unnecessary layer in addressing the core research questions. It is assumed, without proof, that there is a positive correlation between improved cataloging and improved characterization.

Near-Earth (NE) collection is omitted due to the computational burden of propagating thousands more RSOs, the need to simulate radar capabilities, and the complexity of the NE/DS scheduling problem. DS contributions from radar sites such as Eglin and the S-band Space Fence as well as Radio Frequency (RF) detection capabilities are omitted. The study also neglects contributions from any potential allied sensors with exception of the Canadian Sapphire platform.

Because the USG intends to execute OPCON over the commercial sites, a routine mimicking the tasking and scheduling of the SSN and the commercial sites is employed. It is assumed each telescope requires 30 seconds to collect an observation and slew; therefore, each day is broken into 2,880 finite intervals. A stochastic algorithm suggestive of the centrally-tasked, decentrally-scheduled process used by DoD is developed without utilizing extensive scheduling theory techniques such as integer programming due to computational limitations. Notably, to aid execution the scheduling is run once on all sensors *en masse* to generate a database from which any architecture's pertinent observations may be pulled to compute network-wide metrics. This compromise is necessary as the scheduling of hundreds of thousands of individual architectures adds inordinate time and data handling complexities.

In the core M&S, it is also assumed that all scheduled RSOs meeting physics-based constraints, namely brightness, appear in their propagated positions and are successfully collected. An SNR of 6 is set as a minimum collection threshold for the physics-based constraint. For the proxy efficacy study, RSO covariance information is based on general values found in literature and Monte Carlo simulations for uncertainty comparisons are excluded due to innate computational complexity.

Implications

This study qualitatively outlines how to architect the inclusion of sensors into the SSN for SDA collection gains. Final results quantify the magnitude of these improvements while highlighting key decision analysis factors useful for related studies. The efficacy of using the core performance measures as a proxy for positional uncertainty reduction also aids developers in understanding if a likely technical requirement is in fact incidentally fulfilled during a typical M&S. This work ultimately aids decision-makers charged with evaluating the utility of non-traditional capabilities and identifies how to better capture overall performance.

Dissertation Overview

A thorough literature review outlining the fundamental disciplines of the problem; SDA processes, capabilities, and challenges; and related research is presented. The methodology introduced above is next discussed. Analytical results are presented, then major conclusions are summarized.

Due to the large scale of this multi-disciplinary M&S, many of the fundamental assumptions used in the Methodology section are merely referenced as covered in the Literature Review. A reader with no background in the subject matter is highly encouraged to review the entire section[2] prior to the Methodology. However, a reader with an SDA background wishing to swiftly move through this document may do so by reviewing the Challenges to USG SDA, Non-Traditional SDA Capabilities, and Literature Gap sections

[2] Admittedly, many of the studies in the Relevant Research section are provided as holistic SDA M&S background which, if felt to be relevant, are cited in the Methodology section. Reviewing Moomey's [33], Raley's [71], and Colombi et al.'s [93] approaches provide the most relevance to the problem at hand.

before proceeding to the Methodology, with the caveat that some understanding of the problem may be lost.

II. Literature Review

Chapter Overview

The fundamental disciplines of system architecting, optimization, optical collections, astrodynamics, and modeling and simulation are first detailed. Current SDA processes, challenges to these processes, and non-traditional capabilities are then discussed. Relevant literature which informs the methodology is then outlined, and the literature gap intended to be filled is identified.

System Architecting

Introduction

A system may be defined as "a collection of hardware, software, people, facilities, and procedures organized to accomplish some common objective" [1, p. 3] while systems engineering may be thought of as "an interdisciplinary approach and means to enable the realization of successful systems" [1, p. 9]. Buede & Miller assert the system engineering design process consists of: defining the problem to be solved; defining and evaluating alternate concepts for solving the problem; defining the system level design problem to be solved; developing the system functional, physical, and allocated architecture; developing the interface architecture; and defining the qualification system for the system [1, p. 48].

Crawley et al. state that an architecture is "an abstract description of the entities of a system and the relationship between those entities…[which] can be represented as a set of decisions" [2, Ch. 1]. Maier & Rechtin define the discipline of systems architecting as the art and science of creating and building complex systems through use of qualitative heuristic principles and quantitative analytical techniques [3, p. 426]. The system architect

thus seeks to first loosely define a system's parameters, identify and prioritize trades, and evaluate alternatives based on desirable performance.

Needs, Requirements, and Measures

Key to system architecting is the needs-to-goals framework, which consists of identifying stakeholders and beneficiaries; characterizing needs of the stakeholders; interpreting needs as goals; prioritizing goals; and developing metrics [2, Ch. 11.1]. Needs are often expressed in ambiguous terms and consist of necessities, wants, and desires for improvements [2, Ch. 11.3]. Goals are similar to high-level requirements, and can be traded against other product and system attributes in the design phase.

The attainment of goals and requirements must be measured. Measures of Effectiveness (MOEs) are qualitative measures defined as "how well a system carries out a task or set of tasks within a specific context" [1, p. 174]. Subordinate to specific MOEs are Measures of Performance (MOPs), or "specific system propert[ies] or attribute[s] for a given environment and context [which is] measured within the system [such as] accuracy, timeliness, distance, throughput, workload, and time to completion" [1, p. 174]. Roedler & Jones define Technical Performance Measures (TPMs) as measuring "attributes of a system element within the system to determine how well the system or system element is satisfying specified requirements" while Key Performance Parameters (KPPs) are a "subset of the performance parameters representing the most critical capabilities and characteristics" [4, p. 6].

Bullock & Deckro summarize work by Kirkwood which delineates measures as being either natural or constructed [5, pp. 706–707]. Natural measures have "a universal interpretation that directly measures the system purpose" while a constructed measure is

"defined for a specific context". Using a natural measure which directly considers parameters is ideal, but if this is not possible a constructed measure which directly considers parameters should be used. Should either be unattainable, using indirect or proxy measures must be performed. This situation is depicted in Table 1. Identifying, constructing, and employing the most reliable and impact measures is fundamental to the completion of the SDA architecting problem at hand.

Table 1. Measure types [5]

	Natural	Constructed
Direct	- Commonly understood measures directly linked to strategic objective - Example: profit	- Measures directly linked to the strategic objective but developed for a specific purpose - Example: gymnastic scoring
Proxy	- In general, use measures focused on an objective correlated with the strategic objective - Example: GNP (economic well-being)	- Measures developed for a specific purpose focused on an objective correlated to the strategic objective - Example: student grades (intelligence)

Decision-Making

Knowledge of needs, requirements, and measures allow the system architect to define potential system architectures. The discipline of decision analysis aids the evaluation of alternatives. Parnell et al. define decision analysis as "a philosophy and a social-technical process to create value for decision makers and stakeholders facing difficult decisions involving multiple stakeholders, multiple (possibly conflicting) objectives, complex alternatives, important uncertainties, and significant consequences" [6, Ch. 1.1].

While several decision analysis methods are extant, a common approach employs Value-Focused thinking [6, Ch. 3.6]. Value-Focused thinking starts by considering

decision-maker values and objectives prior to identifying alternatives to avoid limiting options prematurely. Next, gaps in valued objectives are qualitatively and quantitatively defined. Finally, decision opportunities are identified, and the values are used to evaluate alternatives.

Using a hierarchy in which objectives are ascribed weighted values and combined into an overall score is a typical approach to evaluating alternatives. Buede & Miller show that rank-ordered objectives may be assigned values by interpolating from linear and exponential curves [1, pp. 402–403]. Parnell asserts that weights should be selected, in descending order of favor, by: direct interviews with senior decision makers and key stakeholders; inferring senior decision-maker views from documents; and using data from stakeholder representatives [6, Ch. 7.7]. An alternative to the weighting scheme which employs optimization is described in the next section.

Optimization

Introduction

Optimization may be defined as "a procedure of finding and comparing feasible solutions until no better solution can be found" [7, p. xvii]. In the case of system design, Arora posits that a solution can be more readily located by formulating an optimization problem in which "a performance measure is optimized while all other requirements are satisfied" because "analyz[ing] and design[ing] all possibilities can be time-consuming and costly" [8, pp. 3–4].

A simple single-objective optimization problem, historically termed a *program*, may be cast as:

$$
\begin{aligned}
&minimize\ \ f = x_1 - 3x_2^2 + 4x_3^3 \\
&subject\ to \\
&\quad x_1 \leq 3 \\
&\quad 2 \leq x_2 \leq 5 \\
&\quad 2 \leq x_3
\end{aligned}
\tag{2.1}
$$

where *f* represents the objective function to be minimized or maximized and x_1, x_2, and x_3 are decision variables or optimality criteria which, in the case of system design, represent performance attributes. Equations after the *subject to* statement represent constraints which must be fulfilled. Many times, there are implied constraints or *side bounds* on decision-variables which must also be considered. For example, if the decision variable x_1 represents mass, classical physics compels the quantity to be greater than or equal to zero. Thus this constraint should be reformulated so that a realistic, or *feasible*, solution is returned.

Any feasible solution to the optimization problem is termed an *optimal*. A *local optimal* is the best solution in some neighborhood of solutions, while a *global optimal* is the best solution to the problem [9, p. 124]. The mathematical behavior of the equations in the program generally determine the technique used to solve the problem, where linear programs are usually solved more easily than non-linear and integer programs. The nature of advanced routines, which are computationally complex and time-consuming, is such that a succession of better optimals are returned while a global optimum may never be identified. The optimals form around one or more clusters of local optima; therefore, the decision-maker many times is faced with conducting a trade-off in performance attributes.

Often it is practical to solve a constrained problem using unconstrained solution techniques by merging the objective function $f(\boldsymbol{x})$ and constraints into one *composite function* [8, Ch. 11.7]. This approach penalizes unfulfilled constraints so that feasible solutions are more favorable. The program can be transformed from

$$\begin{aligned} &minimize\ \ f(\boldsymbol{x}) \\ &subject\ to \\ &\quad h_i(\boldsymbol{x}) = 0;\ \ i = 1\ to\ p \\ &\quad g_i(\boldsymbol{x}) \leq 0;\ i = 1\ to\ m \end{aligned} \tag{2.2}$$

into

$$minimize\ \ \Phi(\boldsymbol{x}, \boldsymbol{r}) = f(\boldsymbol{x}) + P(h(\boldsymbol{x}), g(\boldsymbol{x}), \boldsymbol{r}) \tag{2.3}$$

where $\Phi(\boldsymbol{x})$ is the composite function, $\boldsymbol{x}$ is a vector containing all decision variables, $h_i(\boldsymbol{x})$ includes all equality constraints from *i* to *p*, $g_i(\boldsymbol{x})$ contains all inequality constraints from *i* to *m*, and **r** is a vector of penalty parameters. Two common methods employing this technique are the Penalty Function method and the Barrier Function method.

The Penalty Function method penalizes the objective function by adding a value whenever the constraints are violated. This is illustrated using the common quadratic loss function

$$\Phi(\boldsymbol{x}) = f(\boldsymbol{x}) + r\left\{\sum_{i=1}^{p}[h_i(\boldsymbol{x})]^2 + \sum_{i=1}^{m}[g_i^+(\boldsymbol{x})]^2\right\} \tag{2.4}$$

where *r* is a scalar penalty and $g_i^+(\boldsymbol{x}) = \max\left(0, g_i(\boldsymbol{x})\right)$. It can be seen that if the equality constraint is not satisfied or the inequality is violated a penalty is added. Routines will iterate through infeasible regions when the cost and/or constraints may be undefined, so if the iteration terminates prematurely the final solution may not actually be feasible.

The Barrier Function method aims to create a barrier around the feasible solution region and prevent infeasible solutions from being returned. This method is valid only for inequality-constrained problems and requires a feasible starting point. One common formulation is the inverse barrier function

$$\Phi(\boldsymbol{x}) = f(\boldsymbol{x}) + \frac{1}{r}\sum_{i=1}^{m}\frac{-1}{g_i(\boldsymbol{x})} \tag{2.5}$$

while another is the log barrier function

$$\Phi(\boldsymbol{x}) = f(\boldsymbol{x}) + \frac{1}{r}\sum_{i=1}^{m} log(-g_i(\boldsymbol{x})) \tag{2.6}$$

Arora notes that both the Penalty and Barrier Function methods approach the optimal value as *r* increases. However, a larger penalty increases computational time. Both methods also become ill-behaved at the boundary of the feasible set.

Multi-Objective Optimization

Many real-world problems require a solution amongst competing goals. Mathematically, these may be modeled and solved using MOO. MOO problems are ones in which two or more objective functions are to be minimized or maximized subject to constraints. A MOO problem may be cast as:

$$
\begin{aligned}
&minimize\ \ f_1 = x_1 - 3x_2^2 + 4x_3^3 \\
&minimize\ f_2 = 4x_1 + 5x_2 - x_3^3 \\
&subject\ to \\
&\quad x_1 \leq 3 \\
&\quad 2 \leq x_2 \leq 5 \\
&\quad 2 \leq x_3
\end{aligned}
\tag{2.7}
$$

However, the concept of minimizing multiple objective functions poses two new dilemmas: how much the researcher cares about balancing the minimization between the objective functions, and how the final results can be compared to find the best solution. One technique to represent the final result is to effectively convert the problem into a scalar objective problem by weighting each objective *f* by a value *w,* then summing the product of each objective with each weight such that

$$
\begin{aligned}
&F(x) = w_1 f_1(x) + w_2 f_2(x) + \cdots + w_n f_n(x) \\
&\sum_{1}^{n} w_n = 1
\end{aligned}
\tag{2.8}
$$

The optimals can thus be compared by comparing the final values for *F(x)*. However, this approach requires *a priori* knowledge of the weights [10, p. 103]. If weights are assumed arbitrarily, many additional solutions in the design process will be effectively eliminated.

An alternative approach, stated by Arora as "the predominant solution concept in defining solutions for multi-objective optimization problems," is to employ Pareto optimality [8, p. 777]. Figure 1 illustrates this concept for a program with two objective functions being simultaneously minimized, where each point on the curve indicates an optimal. Clearly, the best solution is the one in which both objective functions are the

lowest possible and approach the origin or *utopia point*, but this point is generally infeasible. In the search for the best optimals, the concept of *non-domination* is key. An optimal is non-dominated when it outperforms all other optimals in all objective values. The set of non-dominated optimals are referred to as Pareto optimals, and form the best Pareto Front.

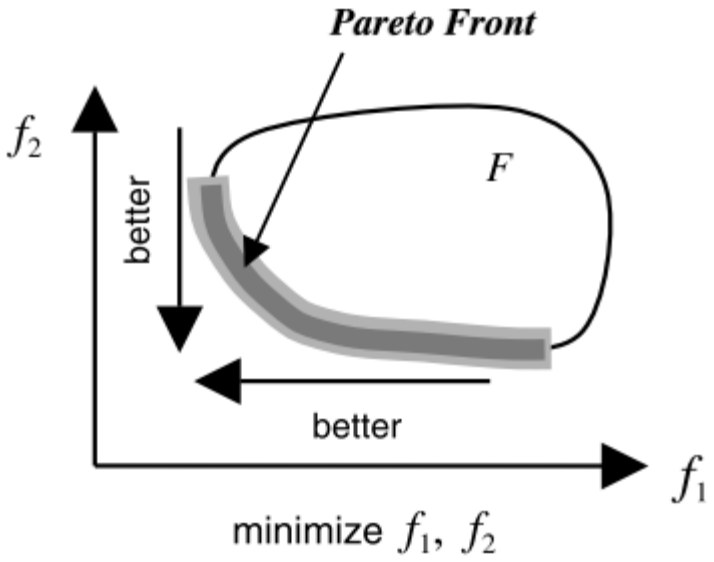

Figure 1. Pareto optimality [11, p. 191].

Applications to Architecting

In regards to the decision-making techniques discussed in the previous section, the weighted sum method maps decision-maker priorities to weighting functions and applies them to the objective function values, resulting in a final score for each alternative. Crawley et al. instead recommends using MOO to evaluate a system's design tradespace, which includes "numerous architectures, represented at lower fidelity and evaluated with a few simple key metrics," and considering Pareto and near-Pareto optimal solutions for

exploitation [2, Ch. 15.2]. Evaluation is expected to find clusters which suggest "families of architectures that achieve similar performance in one or more metrics".

In some cases, a system must be assessed over multiple time periods. Epoch-Era Analysis posits that high-performing solutions common to all periods have greater value [12, p. 3]. Figure 2 illustrates this scenario for a set of 49 architectures assessed on two days by two hypothetical measures, both of which are to be minimized. Architecture performance is plotted, where the numbers indicate each architecture and Pareto fronts are shown by dashed lines. Inspection indicates the number of fronts and architecture performance differs between days. Architectures which perform in the top 20% front on both days are highlighted in red, and represent those with greater value.

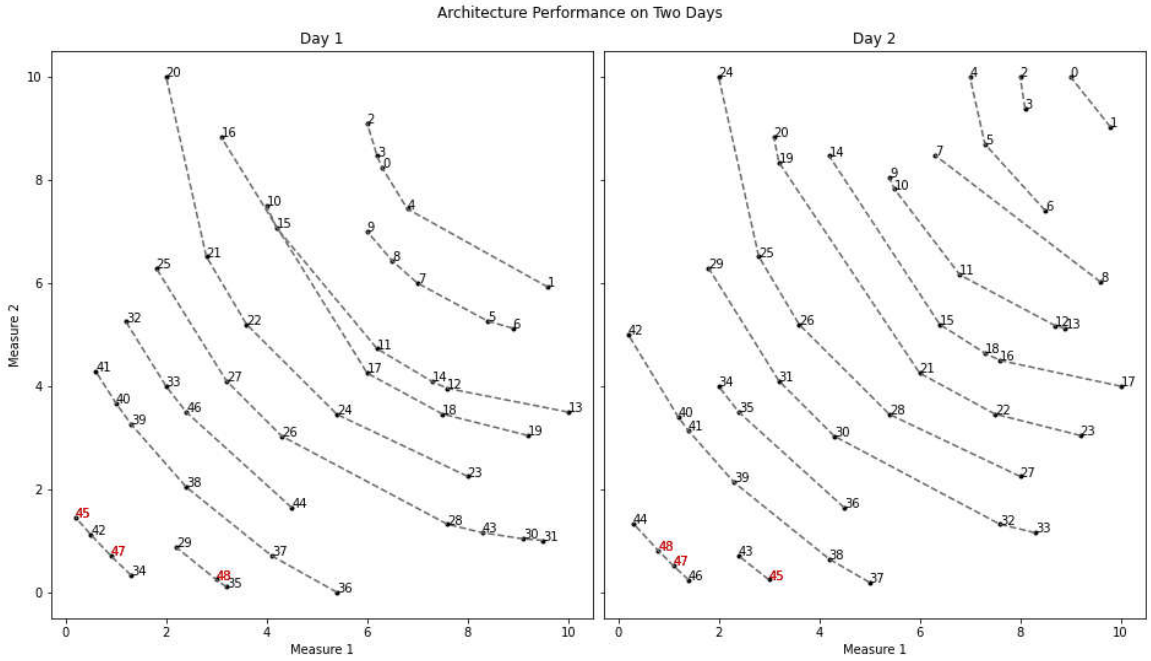

Figure 2. Comparison of architectural performance on two different days. Red architecturess are top performers on both days and have greater value.

Evolutionary Computation and the Genetic Algorithm

Evaluating optimization problems requires the use of search methods. Arora categorizes global optimization search methods as being either deterministic or stochastic [8, pp. 709–710]. Deterministic methods exhaustively search over the entire set of solutions, while stochastic methods use variations of random searching. Evaluating MOO problems with large tradespaces has inherent complexity, which makes purely deterministic search time-prohibitive. Stochastic methods are therefore preferred. Nature-inspired or evolutionary computation techniques such as Genetic Algorithms (GAs), Particle Swarm Optimization, Simulated Annealing, and Ant Colony Search are typically used in the evaluation of such problems.

The use of evolutionary computation offers several advantages [11, Ch. 1.2]. Foremost is a simple approach consisting of four steps: initializing the population with individuals, varying individuals randomly, evaluating fitness, applying selection criteria, and continuing with the randomization until termination criteria are met. Second is the ability to outperform classical approaches such as gradient-based methods. Additionally, the ease of apportioning parts of the problem to other computer processors via parallelization helps speed execution time.

The GA is a commonly-employed technique for optimization problems. Arora provides an overview of its processes [8, Ch. 17.1] which is depicted in Figure 3. First, the design space is recast as a set of *chromosomes*, or strings, representing characteristics as *genes*. Individual characteristics of chromosomes are called *genes*, and the possible values genes can take on are *alleles*. Chromosomes are typically cast as binary strings, making each allele a bit consisting of zeros and ones. As an example, the design space for forming

a telescope network from any of three ground sites consists of 2^3 or eight permutations. Each permutation may be represented by a chromosome with the choice to use or not use each site represented by three separate binary bits. Thus the total chromosomes are represented as {0, 0, 0}, {0, 0 1}, {0, 1, 0}, {0, 1, 1}, {1, 0, 0}, {1, 0, 1}, {1, 1, 0}, and {1, 1, 1}. The null case may be omitted if at least one site is desired.

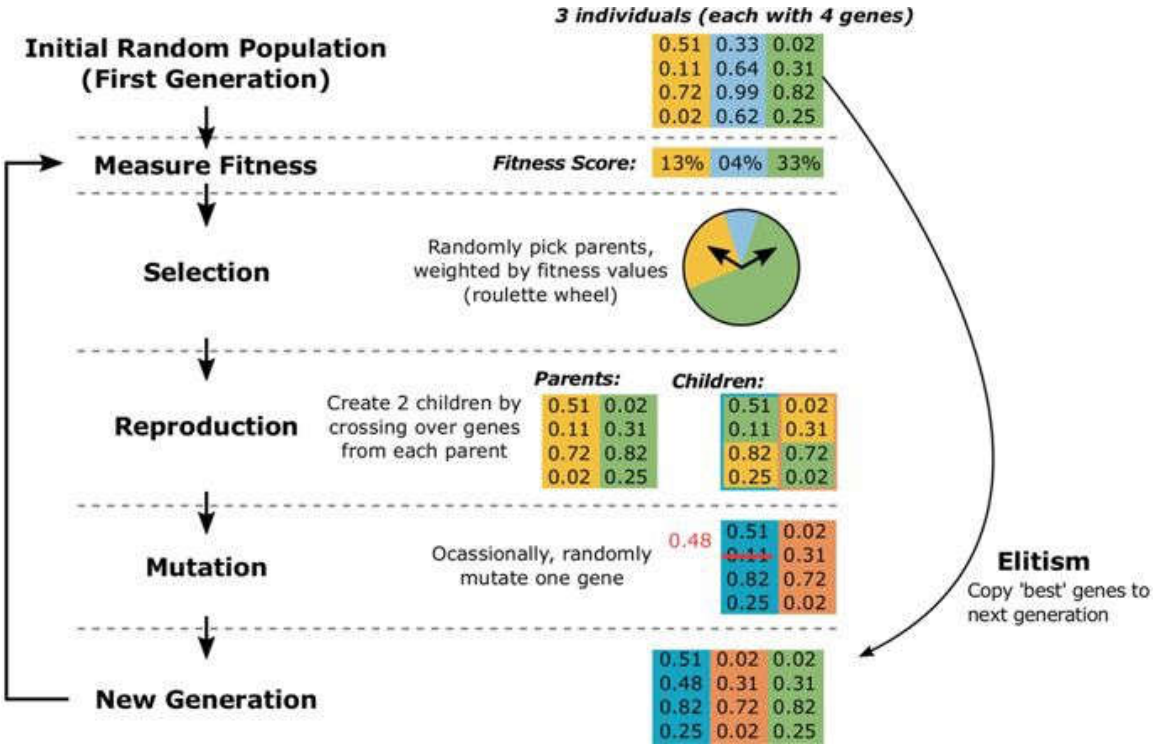

Figure 3. Genetic algorithm process for a population of non-binary chromosomes [13].

An initial population from the designs may be selected at random, or the population is seeded by known or suspected high-performing designs. For constrained problems which do not employ a penalty function, a check to ensure the designs' feasibility should be conducted prior to selection for the initial population. The optimization problem is then solved for each design in the population, and a *fitness function* is used to define the relative importance of the design amongst the others.

After the initial population's values are computed, the reproduction stage begins. Designs are selected based on their fitness and placed into the new population. Then, certain pairs of chromosomes undergo crossover, in which characteristics of the designs are exchanged. Typically, the chromosomes are cut once or twice and the substrings are swapped. A few members of the resulting population undergo mutation by selecting a random location on the strings and changing the values. In the binary case, a simple bit flip is conducted. This process continues for several generations until the number of generations set by the algorithm elapse or no further improvement is noted.

Consideration should be given to several subtle but important choices in the GA: population sizing; the number of generations; and crossover and mutation rates. Opinions in literature differ regarding how to pick these quantities, especially sizing the population. Arora maintains that the population should be sized to a "reasonable number for each problem" and depend on the number of decision variables, the number of possible designs, and the number of allowable discrete values for each problem [8, p. 746]. Haupt & Haupt assert that a GA performing Pareto optimization needs a large population in order to define the Pareto Front, but noted the GA optimizes quickest with small population sizes and relatively high mutation rates [14, pp. 101, 132]. Reeves developed a mapping, depicted in Figure 4, defining the minimum population size based on the length of the design chromosome and number of alleles while noting that small populations are sufficient for binary strings [15]. Harvey suggested that a minimum size of 30 to 100 individuals is practical based on experience [16]. Lastly, personal opinions from several researchers on the optimal population size for differential evolution, a related evolutionary algorithm, included set numbers such as 30-60, 100, or 250-500; rules of thumb such as ten times the

number of criteria; and deciding via trial and error by running the problem multiple times with successively increasing population sizes and ultimately using the lowest population size which yields solution consistency with the higher populations [17].

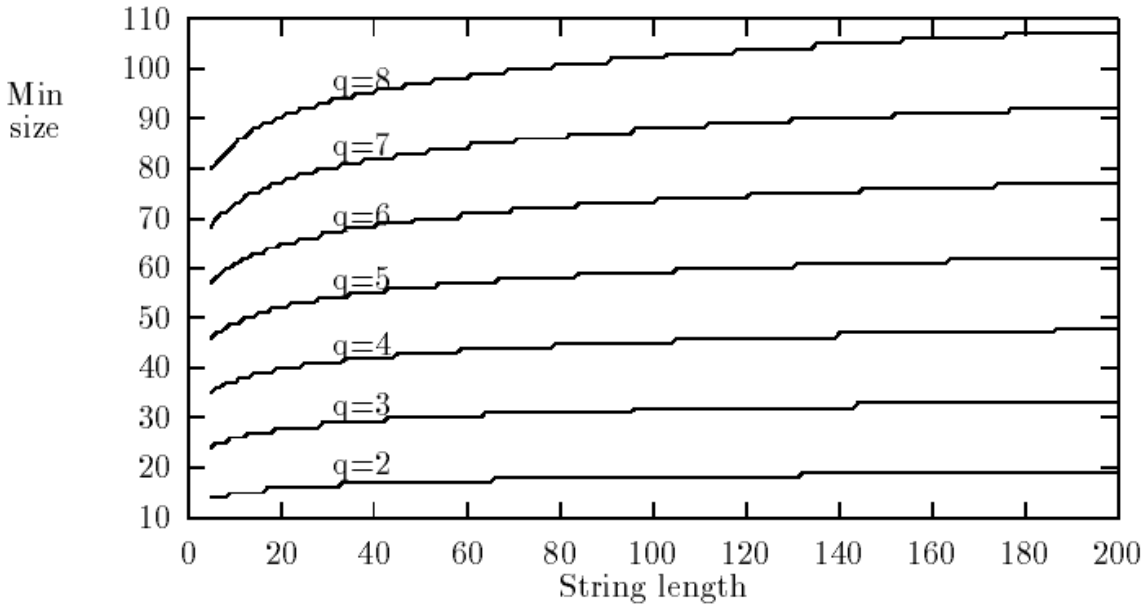

Figure 4. Minimum population sizes for 99.9% confidence of all alleles represented, where q is the number of alleles possible in a gene; $q = 2$ for binary problems [15].

Choosing the correct number of generations is also important. More generations improves confidence in the final optimals, or may reveal additional optimals in a very large tradespace. However, conducting more generations increases computational time and may yield diminishing returns. Researchers have noted that performing trial runs on problems to determine an appropriate cutoff may be useful.

Lee emphasizes the importance of selection pressure, crossover, and mutation [11, Ch. 2.6]. Selection pressure is "the degree to which the best individuals are favored" where a higher pressure implies higher convergence rate of the GA. A balance must be struck between a rate which is high enough to speed the algorithm, but low enough to prevent

convergence to a coarse solution. Lee deems crossover to be controversial due to its disruptive nature, and asserts that traditional GAs use one-point crossover. Lastly, Lee states that mutation rate is more critical than crossover rate, and that a binary problem usually performs bit flipping randomly at a rate of 0.1% to 5%.

Eiben & Smith explain how to handle constraints when using an evolutionary algorithm by using either indirect or direct methods [18, Ch. 12.4]. Indirect constraint handling requires recasting the constraints to form a penalty function as described previously, which returns a wildly infeasible value the algorithm will not choose to advance. Constraints may also be handled directly in one of two manners. Either the algorithm may be written such that infeasible solutions can never be generated, or any infeasible solutions returned may be approximated with nearby feasible solutions which are assumed to be close enough to the infeasible solution.

NSGA-II

NSGA-II was developed by Deb in 2002 to specifically address research community concerns about the limitations of multi-objective evolutionary algorithms [19]. It implements a fast non-dominated sorting approach and combines parent and offspring populations in the mating pool to select the best solutions based on fitness and spread. It has since gained favorable acceptance within the optimization community.

Goel's depiction of the algorithm is provided in Figure 5 [20]. The initial population, referred to as the parent population, is created and each individual is evaluated. All individuals are ranked using non-dominated sorting, where Pareto optimals form the best front and poorer individuals are grouped into weaker fronts. The selection process uses a binary tournament to randomly select two individuals from the parent population

and advances the individual from the better non-domination front. Should the individuals be in the same non-domination front, the *crowding distance*, which measures the density of individuals near one particular individual, is used to select the winner. Individuals in less-crowded regions are deemed more favorable.

Crossover and mutation are then applied; although no particular method is prescribed, Deb used single-point crossover and bit-flip mutation for his trials of binary programs in his original paper. The resulting child population is then evaluated. The parent and child populations are then combined, and *elitism* is used to select the best individuals from the two to form a new parent population. If the number of generations or another stopping criteria is unmet, the algorithm continues to the selection stage and repeats.

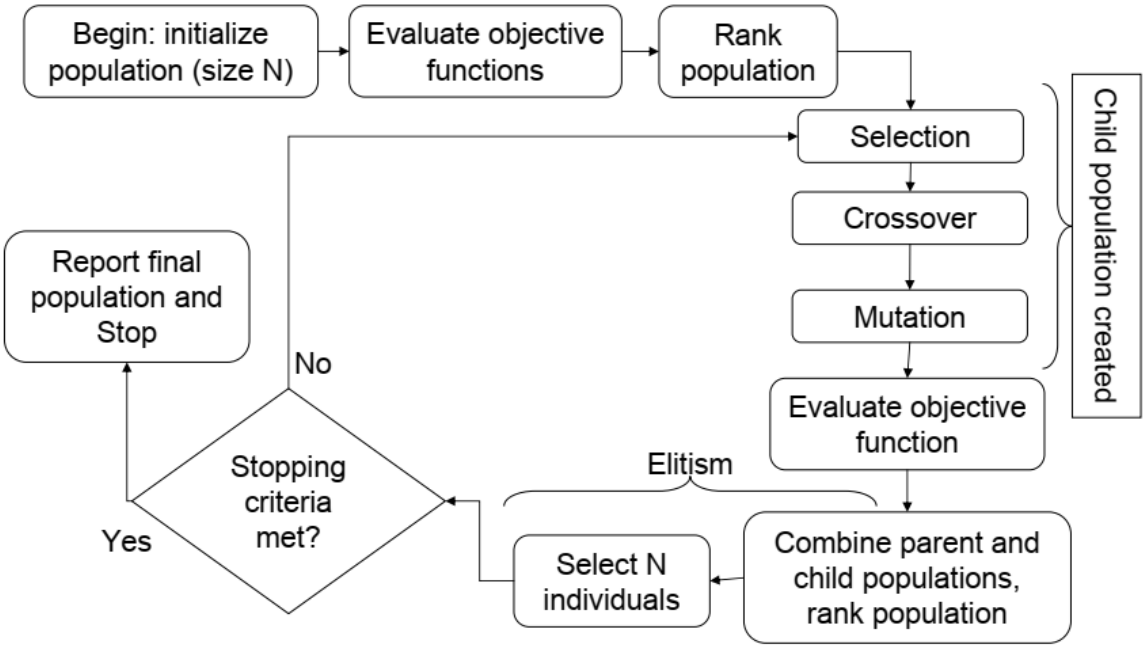

Figure 5. Flowchart for NSGA-II [20].

Application

The use of optimization is highly important in this research. The overarching framework for identifying best-performing AN permutations must employ a heuristic method such as the GA because evaluating the entire tradespace is prohibitively difficult. Likewise, the measures computed for any one AN permutation are best compared to those of other permutations by using MOO techniques. The next section introduces the physics-based principles powering the evaluation of each AN permutation.

Optical Collection

Introduction

This section will cover an architect's approach to designing a network. Choosing site locations and the physics of an optical collection are discussed. Telescope operations are then reviewed. Lastly, scheduling techniques to best employ limited telescope resources are highlighted.

Designing a Network

There are several considerations when designing a space surveillance network. The ultimate aim of fielding a network is to perform OD on the highest-quality data available, which improves the knowledge of RSO states. This is made possible by the following factors as outlined by Vallado [21, pp. 828–831]. Geometric dispersion of observations such that multiple sensors obtain observations at different times, and collecting a large quantity of data, aids a better fit in OD routines. Employing multiple phenomenologies, such as both radar and optical tracking, combines the advantages of range and angles-only information which minimizes covariance. Additionally, higher availability of sensors

naturally allows more collections; factors such as maintenance downtime, weather, and tasking priority must also be considered. Herz more succinctly posits that "improvements in orbit estimation accuracy can be realized by achieving diversity of measurement type, orbital separation of measurements, favorable observation geometry, and observational merit" [22, p. 1].

Ackermann et al. outlines additional physics-based and business considerations [23]. Foremost is the weather at the site. Cloudy conditions prohibit light collection; therefore, sites in cloudier areas have less tracking time. Better atmospheric visibility and stability are desirable. Minimizing the amount of artificial sky brightness is desirable to improve the ability to discriminate on the dimmest RSOs. The researchers assert ideal sites are at high elevations with very dry air and cloud-free skies, distant enough from large population areas to minimize artificial brightness but close enough to have access to infrastructure and utilities, and located near the equator to minimize seasonal variations in observing hours.

Physics of Optical Collections

Overview

Shell outlines an optimal collection scenario in his paper for monitoring orbital debris, stating the general process involves the optical system, the detector, the RSO, and the atmosphere and/or background[3] [24]. Ultimately, the RSO's illumination must meet a certain SNR threshold at the telescope's sensor array for a track to be considered successful. Howell defines the SNR for a Charged Coupled Device (CCD) as

[3] Shell's approach is largely adopted and supplemented with other authoritative equations for this research.

$$SNR = \frac{e_s t}{\sqrt{e_s t + n_p(e_b t + e_d t + e_r^2)}} \tag{2.9}$$

where e_s is the total number of photoelectrons per second collected from the RSO, t is the time in seconds, n_p is the number of pixels being considered, e_b is the total number of photoelectrons per pixel per second from the background or sky, e_d is the total number of dark current electrons per pixel per second, and e_r^2 is the total number of electrons resulting from read noise [25, pp. 73–74]. Typical thresholds for SNR success range from 2.5 to 6 depending on the techniques used and the observer's desired confidence in collection. The sky brightness may be empirically measured or estimated and consists of both ambient light and sources such as zodiacal background, moonlight, and earthshine.

The dark noise and read noise are properties of the sensor, while the number of pixels used in the calculation are set by the observer. The sky brightness may be empirically measured or estimated. Typical contributions for sky brightness include ambient conditions and the moon.

Signal Calculation

The signal at the detector may be expressed in photoelectrons as

$$e_s = \eta \tau_{opt} A \tau_{atm} E_{RSO} t_{sig} \tag{2.10}$$

where η is the sensor's quantum efficiency, τ_{opt} is the system's optical transmittance, A is the telescope's aperture (m), τ_{atm} is the atmospheric transmittance at the site, E_{RSO} is the irradiance of the RSO (photons/s-m^2), and t_{sig} is the signal integration time (s). η and A are taken from sensor specifications, while τ_{opt} is assumed to be 0.9 for all sensors. τ_{atm} at zenith may be derived from empirical data or atmospheric models; τ_{atm} varies by elevation θ, and for a known zenith value $\tau_{atm,zen}$ may be approximated by

$$\tau_{atm} = \left(\tau_{atm,zen}\right)^{sec(\pi/2-\theta)} \tag{2.11}$$

For a typical silicon-based sensor operating at 625 nm, the irradiance is given by

$$E_{RSO} = 5.6x10^{10}10^{-0.4m_{RSO}} \tag{2.12}$$

in units of photos/s-m^2, where m_{RSO} is the RSO's visual magnitude (M_v). When approximated as a uniform sphere, an RSO's visual magnitude is given as

$$m_{RSO} = m_{sun} - 2.5log\left[\frac{d^2}{R^2}\rho p(\psi)\right] \tag{2.13}$$

where d is the RSO diameter, R is the range to the RSO from the sensor, ρ is the reflectance, and $p(\psi)$ is the solar phase angle function. The solar phase angle ψ is the angle between the sun, RSO, and sensor. $p(\psi)$ can be calculated by considering equal contributions of specular and diffuse light such that the visual magnitude is

$$m_{RSO} = m_{sun} - 2.5log\left[\frac{d^2}{R^2}\left(\frac{\rho_{spec}}{4}\right) + \rho_{diff}p_{diff}(\psi)\right] \tag{2.14}$$

An alternative approximation of m_{RSO} is pertinent. If orbital information and the RSO's standard M_v at 1000 km altitude and 50% illumination, $M_{v_{RSO,std}}$, are known from a catalog of values then M_v at the sensor may be approximated using Schmunk's adaptation of Matson's formula [26, p. 27]

$$m_{RSO} = M_{v_{RSO,std}} + 5\log_{10}(R) - 15 \ - 2.5\log_{10}\left[\sin(\psi) + \left(\pi - \frac{\pi\psi}{180}\right)\cos(\psi)\right] \tag{2.15}$$

where R is the range to the RSO (km) and ψ is the sun-RSO-site or phase angle (rad).

The maximum signal integration time may be approximated as the transit time through a single pixel on the detector such that

$$t_{sig,max} = \frac{x}{f\omega} \tag{2.16}$$

where x is the detector's pixel size (m), f is the focal length (m), and ω is the RSO's angular rate (rad/s). For an RSO in GEO traveling at 15 arcsec/s, $\omega = 7.3 \times 10^{-5}$ rad/s. Angular velocities in other regimes must be calculated directly.

Background Calculation

The background contribution e_b in photoelectrons per pixel may be expressed as

$$e_b = \frac{\eta \tau_{opt} \pi L_b x^2 t_{int}}{1 + 4(f/d)^2} \tag{2.17}$$

where L_b is the background radiance (photons/s-m^2-sr), t_{int} is the integration time (s), and d is the telescope's aperture diameter (m). For a silicon-based sensor, the background radiance is calculated by

$$L_b = (5.6x10^{10})10^{-0.4M_b}\left(\frac{180}{\pi}\right)^2 3600^2 \tag{2.18}$$

where M_b is the background radiance at the site in units of M_v/arcsec^2. M_b may be empirically measured or modeled.

Background Calculations for Ground-Based Telescopes

For ground-based sensors, major sources of background radiance include ambient light and moonlight. These quantities may be modeled by combining the brightness for the site on a clear moonless (CM) night, typically around 21 M_v/arcsec^2 at zenith for observatory-level conditions, with an approximation of the changing lunar brightness in units of nanoLamberts (nL) such that

$$B = B_{site,CM} + B_{lunar} \tag{2.19}$$

In their foundational model of lunar brightness Krisciunas & Schaefer [27] provide the relation between M_b and B as

$$M_b = \left(\frac{1}{0.92104}\right)\left[-ln\left(\frac{B}{34.08}\right) + 20.7233\right] \quad (2.20)$$

To first order, the brightness during umbra on a clear moonless (CM) night may be assumed constant at a given elevation angle. Shell empirically derived the radiance at a site as a function of elevation and a known zenith quantity; on a clear moonless night this may be used to represented the brightness at the site by using the relationship

$$L_{Bsite,CM}(\theta) = L_{Bsite,CM\ zen}(-0.6118\theta^3 + 2.6249\theta^2 - 3.8585\theta + 2.9482) \quad (2.21)$$

where $L_{Bsite,CM\ zen}$ is calculated using the L_b equation. $L_{Bsite,CM}(\theta)$ may be recast as $B_{site,CM}$ by substitutions in the previous equations.

Krisciunas & Schaefer's model of lunar brightness uses various empirically-derived factors which fundamentally require knowledge of the atmospheric extinction coefficient k, sky position zenith angle ρ, the lunar phase angle α, the lunar zenith angle Z_m, and the RSO's zenith angle Z as measured from the site[4]. k is empirically derived, assumed, or estimated in atmospheric modeling software; ρ is the angle formed by the site-moon and site-RSO vector; α is the angle formed by the sun-moon-earth geometry, and the zenith angle is computed by

$$Z = \frac{\pi}{2} - \theta \quad (2.22)$$

B_{lunar} is calculated using the Rayleigh scattering function $f(\rho)$, the illuminance of the moon outside the atmosphere I^*, and the distance of the moon $X(Z)$ based on zenith angle such that

[4] Krisciunas & Schaefer use degrees instead of radians, which requires care when employing the angles in the non-trigonometric portions.

$$
\begin{gathered}
B_{lunar} = f(\rho) I^{*} 10^{-0.4kX(Z_m)}\left[1 - 10^{-0.4kX(Z)}\right] \\
f(\rho) = 10^{5.36}[1.06 + cos^2(\rho)] + 10^{6.15 - \frac{\rho}{40}} \\
I^{*} = 10^{-0.4(3.84 + 0.026|\alpha| + 4\times10^{-9}\alpha^4)} \\
X(Z) = (1 - 0.96 sin^2 Z)^{-0.5}
\end{gathered}
\tag{2.23}
$$

Background Calculations for Space-Based Sensors

Dressel [28, Ch. 9.7] asserts that zodiacal light, moonlight, and earthshine are major background contributors for space-based sensors, which may be calculated in nL by

$$B = B_{zodiacal} + B_{lunar} + B_{earth} \tag{2.24}$$

Zodiacal background varies by helicocentric ecliptic latitude and longitude, with values between ~21-25 M_v/arcsec^2; several sources approximate this quantity as 22 M_v/arcsec^2. Moonlight and earthshine vary by the RSO-Telescope-Moon and RSO-Telescope-Earth angles, respectively, which may be approximated by interpolation of Dressel's results.

Number of Pixels Calculation

Evans et al. [29, p. 182] provide a method to estimate the number of pixels n_p a point source will occupy on a focal plane. Given the sensors' focal ratio $f/\#$, pixel pitch $x_{\mu m}$ in μm, and sensor wavelength λ in μm and assuming the diameter of a point spread function, the number of pixels may be estimated by

$$n_p = \frac{2.44(f/\#)\lambda}{x_{\mu m}} \tag{2.25}$$

Other Approximations

In selecting the telescopes for the study in the Methodology section, the Field of View (FOV) and plate scale are pertinent quantities. A telescope FOV in degrees is calculated in each dimension dim by

$$FOV_{dim} = \frac{Pixels_{dim}x}{f}\left(\frac{180}{\pi}\right) \tag{2.26}$$

The plate scale ps in arcsec/pixel is calculated by

$$ps = \frac{206265x_{um}}{10^6 f} \tag{2.27}$$

Cloud Conditions

Clouds inhibit ground-based collections; thus, having some measure of real-time conditions and knowledge of general trends is prudent. Hourly sky conditions are typically reported along with other weather quantities in standard Meteorological Aerodrome Reports (METARs) by ground-based weather sensors [30]. The sky is broken into eighths and conditions reported with a height, but without direction. For example, sky coverage of 3/8 oktas at 3,500 feet is reported as SCT035, where SCT is an abbreviation for scattered. Half the sky obscured equates to 4/8 oktas. Cloud coverage may also be computed using space-based observations, data from which is made available in databases such as NASA's International Satellite Cloud Climatology Project (ISCCP) and Moderate Resolution Imaging Spectroradiometer (MODIS) projects. When aggregated by location and time, useful trend information for optical collections may be generated.

Telescope Operations

There are three main approaches to tracking RSOs using telescopes: staring, sidereal tracking, and rate tracking [31]. Campbell notes staring is useful for fast moving detection using a wide FOV (WFOV) sensor with a fixed orientation. Sidereal tracking is used to keep the star background stationary, such that stars appear as point sources while RSOs appear as streaks on the detector. This permits using stars to determine accurate sensor pointing. Rate tracking follows the RSO, requiring *a priori* knowledge of the RSO, and causes stars to appear as streaks. Rate tracking is useful for collecting on dim RSOs. The choice of integration time in any method is also important, especially for faster RSOs [32, p. 1]. RSOs in GEO have angular rates on the order of tens of arcsec/s, while MEO RSOs have rates from tens to hundreds of arcsec/s. The exposure must be long enough to capture the light as the RSO travels across the FOV.

The choice of telescope in any network is key. Larger apertures, better cameras, and high-quality software enable better results but typically must be traded off for cost. An owner/operator would be prudent to make their decision based on collection requirements. Moomey estimates that 77% of GEO RSOs are brighter than 16 M_v or more [33]; Ackermann & Zimmer report that communications satellites in GEO have a M_v between 10.5-13.5 and the difference between a glinting and non-glinting 1U CubeSat at GEO is 12-21 M_v [34, p. 188]. If the goal is to collect solely on bright RSOs, this may be performed by smaller telescopes. Collecting on dimmer and/or more distant targets will require rate tracking, a larger aperture, and/or advanced processing techniques, which is typically more expensive.

Scheduling

The 2004 edition of Strategic Command Document 505-1 (SD 505-1) Volume 2 states that for the "most accurate orbit determination, observations should be taken at different positions on a satellite's orbital path…ideally, cover[ing] the full 360 degrees of an orbit" [35, p. 10]. It further states that since this is not realistic, sensor tasking and scheduling must be conducted. Determining which RSOs to track, when to track them, and with which sensors is a fundamental operational challenge. The Air Force Space Command (AFSPC) Astrodynamics Innovation Committee (AIC) defines this goal as "allocate[ing] resources appropriately in order to gain as much information as possible about a system…[and] optimiz[ing] system performance while simultaneously meeting as many, if not all, of the requirements as possible" [36, Ch. 3.4].

The principal concern for SDA scheduling scenarios is collecting prioritized RSOs to a requisite capacity and/or geometric diversity, by particular sensors with finite access times and capability limitations, so that uncertainty in RSO positions is minimized. There are several commonly-employed scheduling methods in the SDA academic and operational communities which attempt to resolve this problem with more or less rigor. Less rigor is not necessarily worse, however, as more advanced techniques are shown to substantially increase computational requirements.

The Greedy Scheduler represents the algorithm with least rigor. Site-RSO access intervals are determined, and RSOs are prioritized in some manner. Access intervals and sites are stepped through, and the first RSO meeting collection constraints from the prioritized list is scheduled and its priority sent to the back of the queue. Forcing functions may also be employed to meet problem objectives. While extremely fast, this method does

not consider optimal placing of resources. An improved routine may break RSOs into categories and assign a particular number of observations per night to be collected.

A much more advanced technique employs a pure Scheduling Theory problem. A pseudo optimization program is developed to enforce collection desires and constraints. The DoD's Special Perturbations (SP) Tasker algorithm discussed in the US SDA section uses this method. Unfortunately, these problems typically employ integer programming which requires advanced solution techniques through use of solvers, are computationally expensive, and are slower to solve. Newer techniques include scheduling based on projecting which observations will result in lower overall covariance or which observations will maximize overall information gain.

More advanced techniques do not necessary equate to demonstrable improvements. In his thesis, Dararutana executed an SDA collection scenario using both United States Strategic Command's (USSTRATCOM's) legacy SD 505-1 Greedy scheduling routine and a binary integer program [37]. The integer program was so time-consuming that the researcher rescaled his 3,000 RSO problem to 190 RSOs to obtain a comparison. After doing so, he found execution time increased by a factor of 10 while the number of unique RSOs collected only increased by 2%.

Application

Accurately capturing the physics of the problem is essential to performing a valid M&S. It also powers the ability to create an optimized schedule based on likely sensor collection capabilities. As the purpose of telescopic collections is to turn photonic collections into useful information, a discussion on how observational data is used to solve the OD and orbit propagation problems is next discussed.

Astrodynamics

Introduction

OD is described as the process by which knowledge of an RSO's motion relative to the center of mass of the Earth is obtained [38, p. 1]. An RSO's *state* is the set of parameters required to predict future motion, which could consist of the position and velocity or equations of motions. This is typically represented by the state vector $\vec{X}$. If the equations of motion are known, the differential equations can be used to find the state at any other time.

Uncertainty is an important concept in OD problems. Due to limitations in sensor capabilities, approximations in equations and models, and measurement errors the true state of an RSO is rarely known. The overall uncertainty of the state is represented by the RSO's *covariance*, more appropriately termed the variance-covariance matrix which consists of the variances on each measured quantity. Tapley et al. describe the problem of estimating the state as "determining the best estimate of … a spacecraft whose initial state is unknown, from observations influenced by random and systematic errors, using a mathematical model that is not exact" [38, p. 2].

Orbit Determination

OD may be said to begin as soon as observations are collected. A telescope watches for an RSO and, assuming a sidereal collection, a streak is generated. The streak is processed and both endpoints are used to get two observations [21, p. 273]. For optical observations, a minimum of three observations is required to form a *tracklet* and compute an orbit [39, p. 117]. Once observations are computed, they are roughly correlated by

solving for certain orbital elements and comparing the results to those in a known catalog in Initial Orbit Determination [21, p. 273].

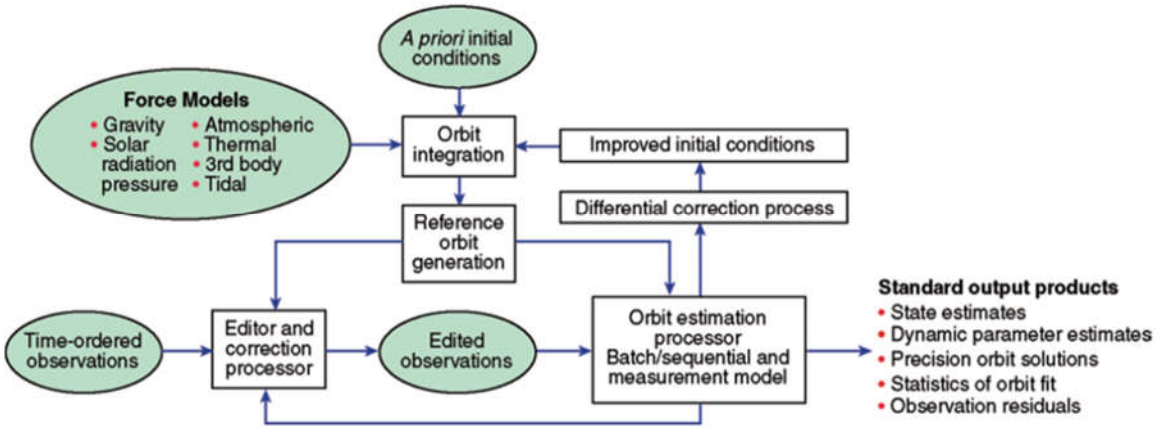

Figure 6. Flowchart for OD [40, p. 245].

A more rigorous statistical orbit determination process appears in Figure 6. When many observations are available, the trajectory is approximated to give the best agreement with the observations. This is first accomplished by finding the equations of motion, then linearizing them about a reference trajectory. The approach is valid as long as the reference trajectory stays close to the true trajectory [38, p. 9]. The vector containing all observations, Y, is expressed as [38, p. 10,173]:

$$Y = Hx + \epsilon$$

where

$$Y = \begin{bmatrix} Y_1 \\ \vdots \\ Y_i \end{bmatrix}, \text{ the observations}$$

$$H = \begin{bmatrix} \widetilde{H}_1 \Phi_1 \\ \vdots \\ \widetilde{H}_i \Phi_\mathrm{i} \end{bmatrix}, \text{ the measurement matrix}$$

$$\epsilon = \begin{bmatrix} \epsilon_1 \\ \vdots \\ \epsilon_i \end{bmatrix}, \text{ the noise matrix}$$

$$Y_i = \begin{bmatrix} \partial \rho_i \\ \partial \theta_i \end{bmatrix}, \text{ the expected measurements} \qquad (2.28)$$

$$\widetilde{H}_i = \begin{bmatrix} \left[\frac{\partial \rho_i}{\partial X_i}\right] & \left[\frac{\partial \rho_i}{\partial Y_i}\right] & 0 & 0 & 0 \\ \left[\frac{\partial \rho_i}{\partial \theta_i}\right] & \left[\frac{\partial \rho_i}{\partial \theta_i}\right] & 0 & 0 & 0 \end{bmatrix}, \text{ the measurements' Jacobian}$$

$$\epsilon_i = \begin{bmatrix} \epsilon_\rho \\ \epsilon_\theta \end{bmatrix}, \text{ noise errors}$$

$$\rho_i = \sqrt{(X - X_s)^2 + (Y - Y_s)^2} + \epsilon_\rho, \text{ errors in range}$$

$$\theta_i = \tan^{-1}\left(\frac{Y - Y_s}{X - X_s}\right) + \epsilon_\theta, \text{ errors in elevation}$$

Φ is the state transition matrix

(X, Y) and (X_s, Y_s) are the RSO and site coordinates

Two common techniques are employed to estimate the state variable **x**. Batch Least Squares incorporates all measurements at once to estimate the state. Tapley et al. note that the method has existed since the time of Gauss, but has the following shortcomings: all observation errors are weighted equally despite accuracy of observations differing; no allowance is given for observation errors that may be correlated; and the method does not use any statistical information [38, p. 176]. The most common alternative to Batch Least Squares is Sequential Estimation, in which observations are processed successively and measurements updated immediately. The Kalman Filter is the most common Sequential Estimation technique.

An improvement to Batch Least Squares incorporates weighting of sensor biases and noise when processing the data in a routine suitably named Batch Weighted Least Squares (BWLS). Vallado's implementation of this routine[5] uses differential correction to reduce the computational complexity of matrix operations, as outlined in Figure 7 [21, Ch. 10.4], [41]. A list of time-tagged observations on an RSO of a standard observational type, such as azimuth and elevation, are submitted to the routine. An initial estimate of the desired state is made. All observations are processed per one iteration of a loop, which sequentially propagates the estimated state to each observation's time, forms residuals, runs a least squares routine, and forms a matrix which is used to estimate the state at the end of the iteration. Iterations continue until convergence criteria are met. Upon conclusion, the final state and covariance are available.

[5] As with most routines in his textbook, Vallado makes this example available on the CelesTrak webpage in multiple programming languages.

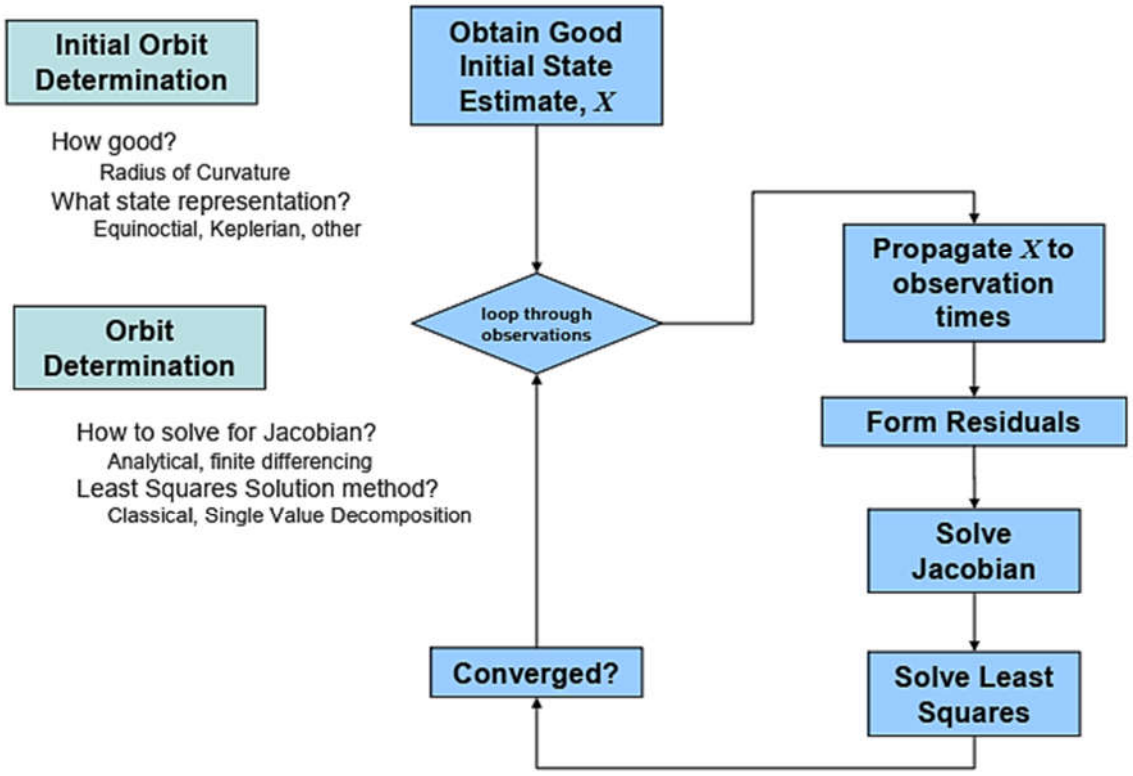

Figure 7. Vallado's BWLS differential correction OD routine [41, p. 2]

Orbit Propagation

When orbital parameters and uncertainty are known, physics-based models may be used to estimate an RSO's position forward or backward in time. From this predictive information, an RSO's future location may be projected, inferring behavior, capabilities, and the potential for a collision with another RSO. There are two principal methods of propagating orbital parameters.

The first approach merely uses equations of motion derived from the Two-Body Problem. This is acceptable for lower-fidelity work, especially in regimes between Low Earth Orbit (LEO) and cislunar where other forces are less prevalent. The second approach uses perturbation theory, which slightly modifies the equations of motion to add more rigor to the evaluation. General Perturbations (GP) uses analytical techniques to obtain

approximate solutions by using a reference solution with a perturbation [38, p. 45]. The most common GP methods use Simplified General Perturbations 4 (SGP4). SP techniques solve the equations of motion numerically. While GP techniques give a coarser solution, their adequacy over short-term time intervals for non-maneuvering, non-critical orbits many times outweighs the computational intensity and time required for a SP solution.

Application

Using appropriate propagation techniques aids in the validity of the problem. Conducting OD on a series of observations permits an estimate of the final state and uncertainty. Chiefly, the use of both techniques become paramount in the study towards the end of the research comparing architectural performance as measured by the core M&S to some level of architectural-wide positional uncertainty.

Modeling and Simulation

Introduction

Law defines a *model* as a set of assumptions about a system based on mathematical or logical relationships, and a *simulation* as the numerical evaluation of a model in order to estimate its true characteristics [42, p. 1]. Law asserts that most real-world systems are too complex to allow realistic models to be evaluated analytically, so simulation is used to assess different outcomes. The discipline of M&S therefore attempts to estimate the system's *state*, or "the collection of variables necessary to describe [the] system at a particular time, relative to the objectives of [the] study" [42, p. 3].

There are several key characteristics of modeling and simulation. Static simulations are invariant with respect to time, while dynamic simulations evolve. Models

and simulations may be deterministic or stochastic, where approaches with randomness and/or probabilities increase stochasticity. Law notes that since stochastic approaches produce output that are themselves random, they must "be treated as only an estimate of the true characteristics of the model" [42, p. 6]. Lastly, approaches may be viewed as continuous or discrete, where a discrete simulation's variables change instantaneously at separate points in time and those of a continuous simulation do not.

All M&S approaches are approximations, which implies results are themselves at best approximations. Any model of a real-world system is inherently limiting; in fact, validating a model is posited as one of the most difficult problems a simulation analyst faces [42, pp. 246–247]. Balancing the desire to capture reality to the appropriate degree with the execution time and cost in resources proves a particular challenge.

Designing a M&S

Law outlines a 10-step process for the design of a simulation study [42, p. 67]. It includes: formatting the problem; collecting data and defining a model; validating the assumptions are correct; constructing the software program; running test cases; validating the model; experimenting with the model and executing a final run; analyzing results; and using the results. Law also provides guidelines for determining the level of detail to include in a model [42, p. 249]:

- Define the specific issues to be investigated and the MOPs
- Understand stakeholder needs
- It is not always necessary to model each component of the system in complete detail
- Use SMEs and sensitivity analysis to help determine the level of model detail and which factors have the greatest impact of desired MOPs

- Start with a moderately detailed model which can be refined later if needed
- Do not have more detail than is necessary to address the issues of the study unless they are required to make the model more credible, and the level of detail should be consistent with the type of data available
- If the number of aspects of interest in the study is large, use a coarse simulation model or analytic model to first identify which factors have a significant impact on system performance, then build a detailed model which emphasizes these factors

Implementing a M&S

Since any stochastic simulation produces estimates of true characteristics for only the given set of input parameters, additional work must be done to improve understanding of the results. Two ways to improve the understanding of the model's performance are to minimize variance in the experimental conditions and to perform several independent runs of the model. The Common Random Numbers (CRN) approach seeks to compare alternative configurations under similar experimental conditions. This enhances confidence that the differences are in fact due to the system configuration and not the variation in the experiment [42, p. 588]. For example, in a comparison of the performance of two telescope networks with several common ground sites, the weather availability of ground sites may be simulated by computing the probability of clear weather at the sites. Computing the availability prior to scheduling and comparing both networks adheres to CRN because both networks will be simulated under like conditions. Computing the availability separately for each network being simulated does not adhere to CRN because the networks will be compared using different starting conditions.

The second method of improving the understanding of a model's performance is by conducting multiple trials. Re-running an element of a stochastic simulation a certain number of times and considering its performance by a measure of central tendency is preferable to a single run. Such measures of central tendency include the mean, median, maximum, minimum, variance, coefficient of variation, and skewness. Law recommends running at least three to five replications of any stochastic simulation, where a higher number of replications improves confidence in results. Alternatively, iterations may be performed until the change in the output achieves the user-defined confidence interval [42, p. 506].

Complex problems require multiple simulations, and multiple simulations increase computational time. Fortunately, computer technology is sufficiently advanced such that individual processors may be linked together to perform *parallel processing* of operations. Different portions of a single simulation may be spread over multiple processors, which can reduce the total execution time up to a factor of the number of processors [42, p. 62]. Modern-day supercomputers such as the DoD Supercomputing Resource Center's High Performance Computing (HPC) facility employ this technique. Specifically, HPC's Mustang login node alone boasts 576 Intel Xeon Platinum 8168 processors operating at 2.7 GHz with 12 nodes, each node possessing 384 Gb of memory [43]. When parceling out portions of the problem, thought must be given to the synchronization of parallel operations in order to avoid causality concerns in the main program, as well to avoid a bottleneck in computation. Additionally, care must be taken to minimize additional randomness such as by ensuring random values used in all processors are computed from the initial seeds.

It is prudent to determine an appropriate number of random simulations, or Monte Carlo trials, to perform instead of making a blanket assumption. Oberle's percent error-based approach using the Central Limit Theorem states that the minimum number of simulations to adequately represent a problem may be found by taking a sample with a large number of Monte Carlo trials, assuming the sample standard deviation and averages are close to the those of the population, and calculating

$$m = \left(z_{\alpha/2} \frac{100s}{\varepsilon Y_{avg}} \right)^2 \tag{2.29}$$

for each measure, where $z_{\alpha/2}$ is the z statistic, ε is the percent error, s is the sample standard deviation, and Y_{avg} is the sample average [44, p. 25].

Application

Balancing the rigor and reality of the M&S with the time and effort required to achieve results is a fundamental challenge. An SDA M&S must adequately model the physics of an optical collection using astrodynamics and simulate observational data using some amount of stochasticity. A review of US SDA practices helps illuminate the choices which should be made in this endeavor.

US Space Domain Awareness

Introduction

Since 1957 nation-states, academic institutions, commercial entities, and hobbyists have exerted vast effort in tracking man-made objects in Earth orbit. This concept is referred to as SDA[6]. Joint Publication 3-14 (JP 3-14), Space Operations, declares that SDA

[6] The term *SDA* replaced the term *Space Situational Awareness (SSA)* in 2019, which itself had previously replaced the term *space surveillance*.

is “dependent on integrating space surveillance, collection, and processing; environmental monitoring; [the] status of US and cooperative satellite systems; [the] understanding of US and multinational space readiness; and [the] analysis of the space domain” [45, pp. II–1].

RSOs may be classified as actively operated or defunct satellites; spent rocket bodies; or debris, and range from the size of paint flecks to a school bus. Active satellites perform missions such as communications, intelligence gathering, remote sensing, and scientific monitoring and typically require years to develop at high cost with limited ability to fix after deployment. In 2018 Lal et al. reported the DoD tracks 23,000 RSOs larger than 10 cm, with 16,000 alone in LEO, and over 90% of all RSOs being inactive [46, p. 1,9]. The possibility of collisions between two RSOs in which one, both, or neither are maneuverable is real and alarming. Therefore, knowledge of RSO locations and behavior is essential to maintain owner/operator situational awareness of the risks to their mission objectives.

The Space Environment

The space environment may be considered by reviewing the orbital regimes and fundamental forces, which are summarized in Table 2. LEO comprises the distance between the lowest permissible orbit at 200 km and extends to around 2000 km altitude. LEO is used by weather, remote sensing, scientific, experimental, human spaceflight, and imagery satellites. Navigational satellites mostly comprise MEO around 20,000 km altitude. GEO occurs around 36,000 km altitude and is defined as orbits with a period matching the Earth’s sidereal day. A Geostationary Earth Orbit (GSO) is a further subset of GEO with zero inclination and zero eccentricity. The major residents at GSO are large communications satellites, which typically are in near-Geostationary orbits. HEO RSOs

have a low perigee and a high apogee. A typical application is the Molynia orbit, which takes advantage of a peculiarity of the Earth's gravitational perturbations to keep the orbit plane from precessing and effectively permits an RSO to loiter over a position while at apogee. This orbit is useful for communications and intelligence purposes.

Table 2. Orbital regimes, adapted from [47, p. G-4] and [21, p. 31].

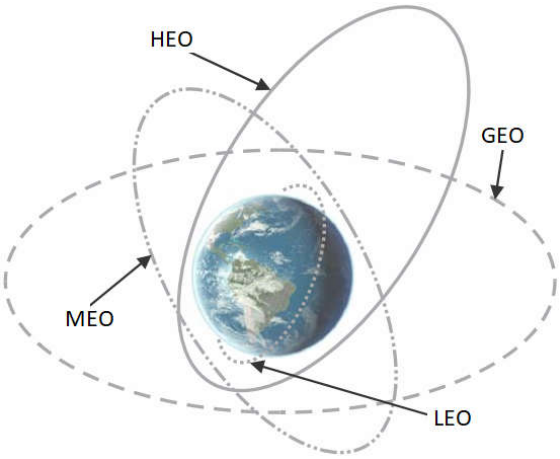

	LEO	MEO	HEO	GEO
Altitude (km)	200-2000	20,000	400, 40,000	36,000
Speed (km/s)	7	4	10, 3	3
Period (hrs)	1.5	12	12	24
Forces				
$F_{g,e}$	X	X	X	X
F_D	X			
F_B	X		X	
$F_{g,3rd}$		X	X	X
F_{SRP}		X	X	X

There are several forces which impact an RSO's motion, but their dominance is dependent on the regime. In all regimes, Earth's gravity, $F_{g,e}$, dominates the motion. In LEO, atmospheric drag, F_D, and Earth's magnetic field, F_B, perturb the natural orbital motion. Both drag and Earth's magnetic field decrease with altitude such that in higher regimes only solar radiation pressure, F_{SRP}, from solar photons and third-body gravitational effects, $F_{g,3rd}$, from the Sun and Moon are important perturbations to consider [21, p. 31]. Accurate modeling of these forces is imperative in high-accuracy orbital propagation and OD. It should also be stated that RSOs in LEO may be expected to re-enter the atmosphere naturally over several years due to drag, while RSOs in higher regimes may remain in orbit essentially indefinitely. The difficulty of modeling drag, which varies due to solar

conditions, as well as the permanence of debris at higher altitudes, puts additional onus on the space tracking mission.

For the purposes of US space tracking, the space environment is typically broken into NE and DS. SD 505-1 Volume 1 defines DS RSOs as those with periods greater than or equal to 225 minutes, or approximately 5875 km altitude for an RSO in a circular orbit [48, p. 10]. Definitions on GSO differ. SD 505-1 Volume 2 defines GSO to be an orbit with a period between 1100-1800 minutes [35, p. 27]. Space-Track, the USG's clearing house for orbital parameters, states that its Geosynchronous Report considers only RSOs with periods between 1430-1450 minutes while the report itself only lists RSOs with mean motion between 0.99 and 1.01 revolutions per day and eccentricity less than 0.01 [49]. Academic literature generally defines GSO within the context of particular studies. Flohrer estimates the largest components of the positional uncertainty for RSOs in MEO, HEO, and GEO to be 0.131 km, 1.367 km, and 0.432 km, respectively [50, p. 3].

The Space Surveillance Network

The USG uses a worldwide system of ground- and space-based telescopes and ground-based radars to perform SDA via an architecture known as the SSN. The components of a notional architecture are depicted in Figure 8. Sensors collect data using various phenomenologies, which is collated and stored in a central database. Algorithms are then run on the data to develop information, which leads to tasking of sensors to improve knowledge. Finally, information is disseminated to various customers.

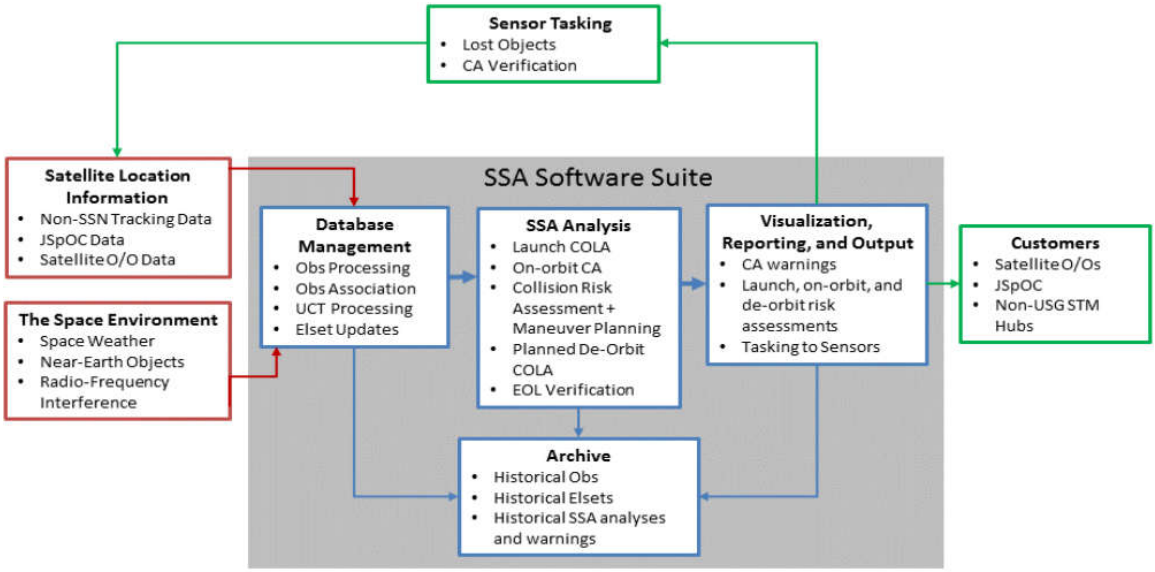

Figure 8. Elements of a conceptual SDA system, adapted from Nightingale [51, p. 62].

There are two major use cases for the data gleaned from this network: RSO cataloging, tracking, or metrics generation; and RSO characterization or Space Object Identification (SOI). Cataloging consists of using observational data and orbital mechanics to predict the current and future location of one or many RSOs. Cataloging is typically conducted using narrowband radar for NE RSOs due to the power requirements for long-distance returns as well as the inability to perform fast telescope slewing on faster-moving NE RSOs using legacy systems. Non-resolved Electro-Optical (EO) collections are typically used to track DS RSOs, although certain sensors such as the Eglin radar may be used to improve orbit estimates. Characterization, however, seeks to infer an RSO's behavior by analyzing changes and/or peculiarities in the data. Typical characterization methods include reviewing light intensity (photometry) or Radar Cross Section (RCS) returns over time and analyzing EO and radar imagery. Further discussion of characterization is omitted as cataloging is the main thrust of this research.

The sites comprising the SSN are depicted in Figure 9. Space-based contributors such as Space Based Space Surveillance (SBSS), Operationally Responsive Space 5 (ORS-5), and Sapphire should be noted, as well as pending capabilities such as the Defense Advanced Research Projects Agency (DARPA) SST being placed in western Australia and the S-band Radar Fence. Estimated capabilities of optical sensors provided by Ackermann appear in Table 3.

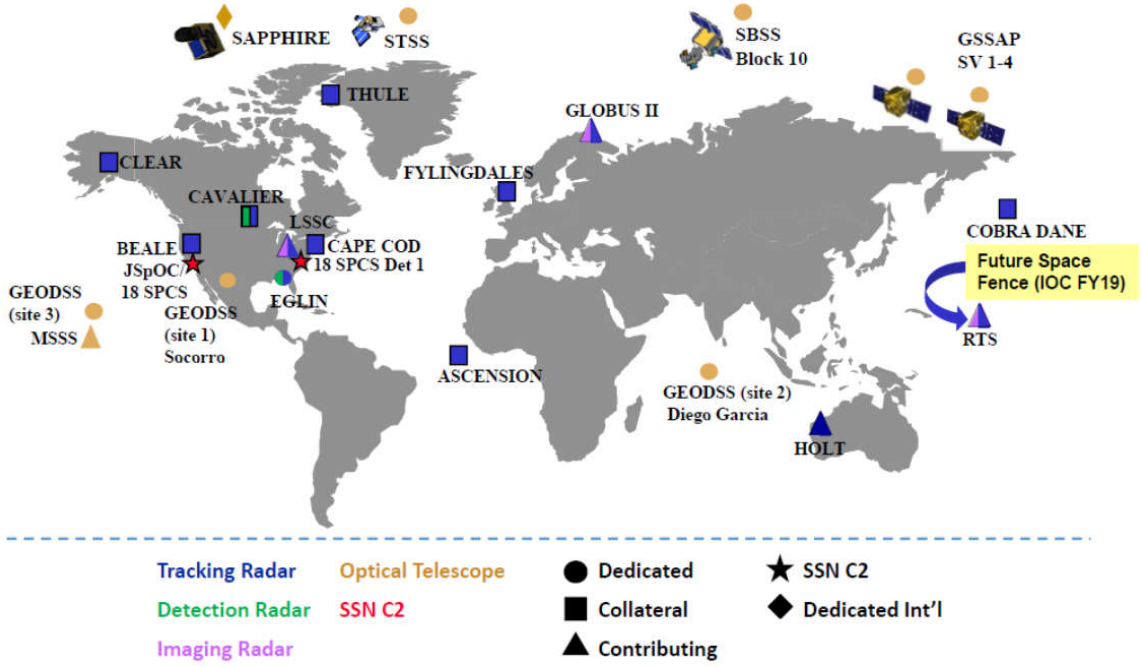

Figure 9. The Space Surveillance Network[7] [46, p. A-2].

[7] SST is denoted as HOLT in this diagram. ORS-5 is omitted. The S-band fence is now operational.

Table 3. Estimated SSN optical sensor capabilities [52].

	GEODSS	SST	SBSS	ORS-5	Sapphire
Location	3 x Soccoro 3 x Maui 3 x Diego Garcia	Western Australia	SSO 630 km	LEO equatorial	SSO 786 km
Aperture (m)	1	3.5	0.30	0.10	0.15
Visual Magnitude	18	19.5	16.5	16.5	15
FOV	2.05°	3.5°	2° x 4°	>5°	1.4° x 1.4°
Focal Length (m)	2.15	3.5	0.85		0.55
Focal Ratio	2.15	1	2.83		3.63
Other	CCD, 1960 x 2560 pixels on 24 um ptich		2 MP CCD, 2200 x 1044 pixels on 27 um pitch		

Although USSTRATCOM is responsible for executing the SDA mission, many of the sensors are owned by different organizations. All sensors are delineated as either dedicated, contributing, or collateral platforms [48, Ch. 1.3]. Dedicated sensors are owned by USSTRATCOM with a primary mission of SDA. Collateral sites are subordinate to USSTRATCOM units but have other primary missions such as missile warning, intelligence collection, and range support. Lastly, contributing sites are under agreements to support the SSN but are not under USSTRATCOM operational control. Allied partners also contribute to the SSN, such as by operating ground sites such as Diego Garcia and Fylingdales or by sending data from allied sensors such as the Canadian Sapphire platform.

Figure 10 depicts the dataflow of cataloging information within the SSN as of 2011. Weeden provides background on the SSN's data system [53, pp. 6–15]. The core of the SSN consists of the Space Defense Operations Center (SPADOC) and the Correlation, Analysis, and Verification of Ephemerides Network (CAVENet) systems. The systems

were previously operated out of the Cheyenne Mountain complex in Colorado Springs, CO but are now operated by the 18th Space Control Squadron (18 SPCS) at Vandenberg Space Force Base (SFB), CA[8]. SPADOC and CAVENet are used to process observations on RSOs, maintain the catalog, and use the catalog to perform conjunction assessments and detect threats. SPADOC's limited processing power permits it to only perform calculations using general perturbation theory; additional work is conducted on CAVENet via its Astrodynamic Support Workstation (ASW). ASW updates and maintains a higher accuracy catalog using special perturbation theory-derived state vectors and covariance information which is used for more refined work such as conjunction assessments and sensor tasking. Observations flow from all sensors into the systems, and OD is performed when a certain threshold of positional accuracy is met. The two resulting products are state vectors and TLEs, the later using traditional Keplerian orbital parameters.

[8] System operations were transitioned from the Cheyenne Mountain complex to the Joint Space Operations Center (JSpOC), later renamed the Combined Space Operations Center (CSpOC). The SDA and STM missions were moved from the JSpOC several years ago to 18 SPCS. Legacy documents and stakeholders unaware of the transition cite JSpOC instead of 18 SPCS as the manager of SDA and STM services.

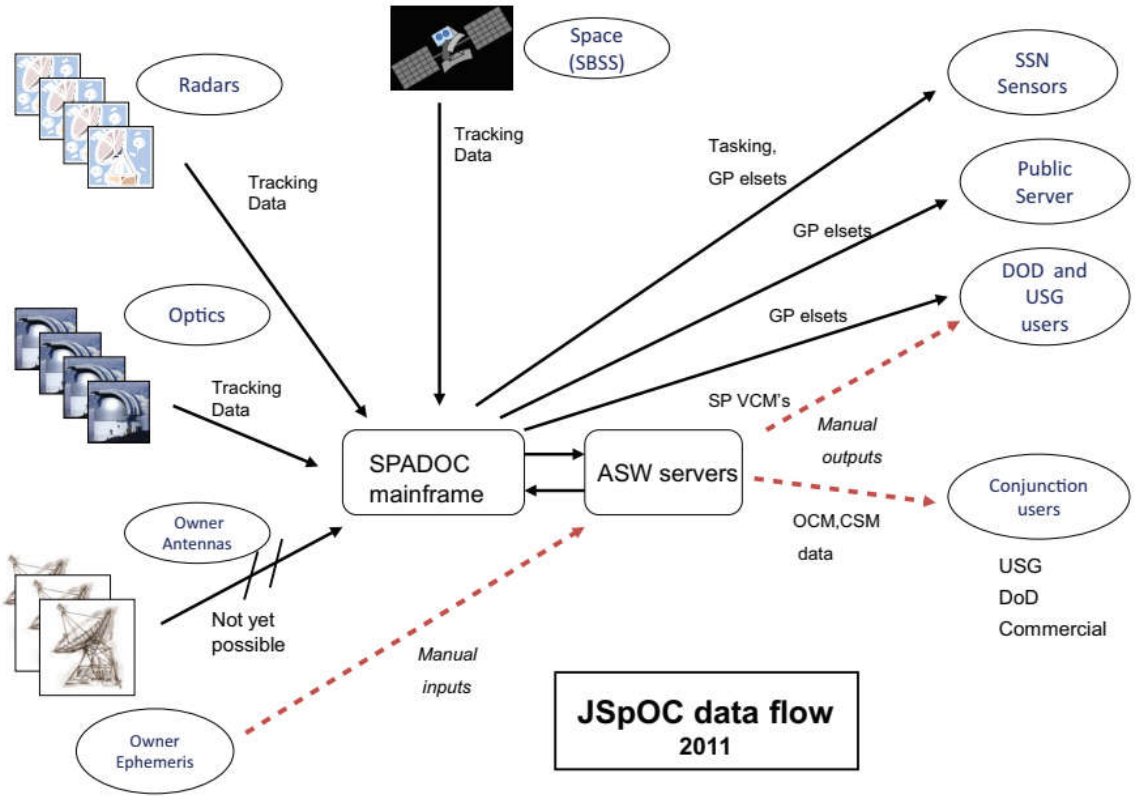

Figure 10. SDA data flow [54, p. 45].

SDA has traditionally been a nation-state activity, and the US has historically been reluctant to disclose high-accuracy catalog information due to concerns that capabilities may be derived. The 2009 Iridium/Cosmos collision, however, has been cited as the turning point in which providing limited conjunction assessment data was felt to outweigh operational security concerns [54, p. 50]. That same year, USSTRATCOM instituted the SSA Sharing Program, allowing private citizens to make an account on Space-Track and receive basic orbit tracking data. Data from the high accuracy catalog, which is much more precise and includes state covariance information, is only available via special sharing agreement [55, pp. 6–7].

After the Iridium/Cosmos collision, the DoD began active coordination with RSO owners/operators to ensure greater community awareness of conjunction threats. The DoD has in effect become the world's major broker of free basic space tracking data and unofficial coordinator for parties with conjunction concerns. This general process has been deemed STM, defined as "the planning, coordination, and on-orbit synchronization of activities to enhance the safety, stability, and sustainability of operations in the space environment" [56]. In 2018, President Trump issued Space Policy Directive 3 (SPD-3), National Space Traffic Management Policy, which recognized that "the contested nature of space is increasing the demand for DoD focus on protecting and defending U.S. space assets and interests" and necessitated turning over the STM mission to the Department of Commerce. SPD-3 asserts that the Secretary of Defense will maintain authority over the space catalog, and the definition of STM implies that the DoD will still conduct the foundational SDA mission while the majority of stakeholder engagement becomes the responsibility of the Department of Commerce.

Tasking and Scheduling

The AFSPC AIC concluded that sensor management[9] is a stochastic dynamic programming or deterministic optimization problem which is "notoriously difficult to solve". The pseudo optimization program defines a cost or utility function that assigns resources (sensor observation times) against tasks (collection of data on RSOs), and is structured so that information gain, or less uncertainty in the state, is maximized. This

[9] AFSPC AIC notes that the term *sensor management* has become widely adopted in literature, implying an equivalency to the term *scheduling* as used in the field of Scheduling Theory. This differs from the SDA mission's definition of *scheduling* as the allocation of the time intervals for an RSO-sensor pairing.

function is then minimized subject to constraints such as the line of site between the sensor and target.

DoD breaks the sensor management problem into two parts: tasking and scheduling. The DoD performs centralized tasking at the headquarters level, then decentralizes scheduling to the sensors. Tasking consists of assigning RSOs to be observed by one or more sensors, while scheduling is the time-based lineup of RSOs each sensor plans to collect. This process is employed instead of a centralized tasking and centralized scheduling approach due to computational burdens on the centralized computer, the inability to control the tasking of contributing and collateral sensors, and the challenges of sensor-specific constraints [36, Ch. 3.4], [57, p. 384].

Specifics of the SSN sensor tasking process are detailed in SD 505-1 Volume 2, Wilson, and Miller dating from 2004, 2004, and 2007 respectively [35], [57], [58]. The three documents present different processes, and while Miller's work on the SP Tasker is the most current, it is a scholarly study and not regulation. However, a review of more recent literature surmises that the spirit of Miller's work is, in the least, directly utilized. In 2016 the AFSPC AIC indicated Miller's adaptations are employed, and the 2019 AFSPC Instruction 10-610 (AFSPCI 10-610) guidance referenced that the SP Tasker "is being used to manage sensor workloads and generate a list of RSOs and tracking requirements for each sensor based on catalog needs and expected fulfillment from sensors" [59, p. 12]. The DoD's proclivity to use legacy processes suggests Miller's paper provides valid insight into the current tasking approach. A short summary of the first two documents is provided followed by Miller's work. Information on scheduling routines, which are site-specific, was not found in literature.

SD 505-1 Volume 2 defines a category and suffix system which is used to classify the importance of any RSO. Categories set the priority for taking observations and is determined in part by TLE quality and age. Category 1 is used for highest-priority special events; Category 2 is used for high priority special events and RSOs with old TLEs; and Categories 3-5 are for routine tracking. Suffixes define the amount of observational data required and the frequency of data collection on an RSO. For DS sensors, the regulation requires tracks to be scheduled so that the maximum quality of observations is made and notes sites should sample different parts of the orbit on different attempts. In his research on alternative SSN schedulers, Dararutana used the following category breakouts and suffixes after consulting with 18 SPCS depicted in Table 4 [37, p. 35]:

Table 4. Categories and suffixes from the 2003 version of SD 505-1.

Category	% Catalog
1	0.01%
2	20%
3	5%
4	25%
5	50%

Suffix	Definition
A	- Radars take all possible obs on all passess for maximum of 50 obs per pass - Opticals take all possible obs for a maximum of 50 obs per shooting period
B	- Radars take 10 obs on all passes, centered at max available elevation or on boresight - Opticals take 10 obs per shooting period
C	- Radars take 5 obs on all passes, centered at max available elevation or on boresight - Opticals take 5 obs per shooting period
D	- Radars take 3 obs on all passes, centered at max available elevation or on boresight - Opticals take 3 obs per shooting period
E	- Radars take 1 obs on all passes, centered at max available elevation or on boresight - Opticals take 1 obs per shooting period

Wilson reported that the first SSN tasking routine was deployed in 1993 on SPADOC. By 2004, the routine optimized data collection by minimizing the observations needed to maintain TLEs for all NE and DS RSOs. Sensor tracking capacity, viewing

limits, and outages were taken into account before prioritizing each RSO within the five categories according to orbital period and inclination. A Greedy algorithm then iterated through the list and tasked sensors to view each RSO. Sensor selection used a weighting method which included ranking, number of passes, orbit distribution, loading, and probability of acquisition. The orbit distribution weight was used to spread out observations across different areas of the orbit, with GEO RSOs using longitude as its metric. Tasking was usually run 12 hours early to allow each site enough time to schedule collections.

Miller developed an improved routine, recognizing the Greedy algorithm did not permit lower-ranking RSOs to be collected frequently and did not consider if RSOs met sufficient SNR before tasking. First, he used higher accuracy catalog data, requiring running the tasker on the CAVENet system which earned the new algorithm the moniker SP Tasker. In lieu of categories, he used empirical data from a research study which sought to determine the number of tracks per day on RSOs required to meet accuracy requirements as a function of the Energy Dissipation Rate (EDR) of the RSOs. EDR is defined as the amount of atmospheric drag an RSO experiences; the study found RSOs could be categorized into 11 bins with the majority having no drag (Bin 0, 24%) and very minor drag (Bin 1, 51%).

Wilson's Greedy algorithm was replaced with a marginal analysis optimization problem which seeks to maximize the number of tracks allocated from sensors to RSOs subject to sensor capacity and opportunities to track the RSOs. The utility functions are set to be concave so that adding additional tracks from RSOs decreases marginal returns, averting challenges with Greedy algorithms selecting only high-priority RSOs, and

considers the required tracks per day based on the RSO's EDR. A comparison of tasking results using the SPADOC GP tasker and SP Tasker showed demonstrable improvement in the amount of unique RSOs collected nightly and a 20% increase in catalog accuracy. The program is represented as:

Maximize

$$U = \sum_{j=1}^{n} U_j(x_{1j}, \dots, x_{mj})$$

Subject to

$$\sum_{j=1}^{n} x_{ij} \leq c_i \text{ for } i = 1 \; to \; m \text{ and } x_{ij}, c_i \text{ integers}$$

$$0 \leq x_{ij} \leq d_{ij} \text{ for } i = 1 \; to \; m, j = 1 \text{ and } n, x_{ij}, d_{ij} \text{ integers}$$

Where

$$U_j(x_{1j}, \dots, x_{mj}) = R_j \left[\sum_{i=1}^{m} E\left(\frac{x_{ij}}{R_j}\right) \right]^a$$

$$E(x_{ij}) = \sum_{k=1}^{x_{ij}} P_{ij} k \qquad (2.30)$$

$$0 < a \leq 1$$

$x_{ij}$is number of tracks allocated from the i^{th}sensor to the j^{th} RSO

c_i is daily tracking capacity of i^{th} sensor

d_{ij} is number of daily opportunities to track the j^{th} RSO by the i^{th} sensor

m is the number of sensors

n is the number of RSOs

$R_j$is required tracks/day to meet accuracy requirements based on EDR

$P_{ij}$is probability of i^{th} sensor tracking the jth RSO on the k^{th} daily pass

E is the expected number of received tracks for allocating and attempting

a is a tuning parameter, empirically determined to be 0.25

Cataloging

Once orbital parameters are available, 18 SPCS uses astrodynamical software to propagate multiple RSOs into the future. The available information is used to determine when the RSO will likely be trackable again, which feeds into the next tracking cycle. DoD performs high accuracy catalog screenings in DS every 24 hours, and NE every 8 hours. Ephemerides are calculated for high-interest screenings on demand, every 12 hours for DS RSOs, and every 8 hours for NE RSOs [46, p. 43].

18 SPCS takes extrapolated GP ELSETs from the high-accuracy catalog, stores as TLEs without covariance, and provides them on Space-Track. Lal asserts that "because [the TLEs] do not have covariance, they may not be optimal for advanced analysis and risk assessment; however, they are accurate for fairly long periods of time" [46, p. A-4]. Limited covariance information is provided to registered owners/operators. STM efforts are also conducted as a public service for the world. Conjunction Assessments (CAs) are run to determine the probability of collisions between RSOs; if CAs exceed acceptable limits, 18 SPCS alerts owners/operators.

Application

Incorporating DoD processes and capabilities into the M&S adds confidence that the problem being solved is as close to reality as possible. However, merely reviewing current processes only partially aids in understanding the problem. There are multiple issues facing DoD SDA which lead to major considerations in the M&S. These challenges are outlined in the next section as a precursor to solutions which involve use of non-traditional SDA capabilities.

Challenges to USG SDA

Introduction

The USG SDA mission is currently challenged by several factors. The volume of new RSOs in orbit, projected to be in orbit, and detectable by newer sensors is increasing—which necessitates increased tracking and conjunction assessments. New threats from foreign actors is requiring increased and novel approaches to SDA. Lastly, the USG is unable to quickly improve mission execution due to reliance on legacy processes. A summary of these challenges is provided, and potential solutions are addressed in the next section.

Volume of New RSOs

Historically, the number of RSOs in orbit any given year has increased since the dawn of the Space Age. Recently, though, access to space has become dramatically more affordable and available. Additionally, looming technology is expected to improve RSO detection capability. In short, the RSO population is increasing and is expected to substantially increase in the near future.

The miniaturization and cost reduction of hardware has permitted previously unattainable missions to be developed. The increased frequency of ridesharing small payloads with a larger satellite, made possible by the adoption of standards such as Cubesat, is allowing more actors and their platforms to get to space. Launch services have blossomed over the past decade, with three separate billionaires developing medium- and heavy-lift capabilities while dozens of small launch vehicle startups have been founded. The demand for space services is also growing, especially in commercial imagery and

communications. Notably, several companies are actively devolving and fielding constellations of hundreds to thousands of small satellites in LEO.

Along with more RSOs is the potential for increased debris. Despite proactive measures, such as adhering to the NASA Orbital Debris Mitigation Guidelines, more RSOs in orbit will likely contribute more debris due to launch operations, outgassing, anomalies, and the increased probability of conjunctions. The unexpected explosion of the Defense Meteorological Satellite Program 13 (DMSP-13) in 2015 alone created a cloud of 147 new trackable RSOs in the highly-utilized sun-synchronous orbit [60]. A collision similar to the 2009 Iridium-Cosmos conjunction may be expected to add nearly 2000 trackable pieces of debris to the catalog [61, p. 2].

The NASA Orbital Debris Program Office has also estimated there are over 500,000 RSOs with at least a 1 cm diameter which are currently not tracked [46, p. 23]. New capabilities are expected to improve the threshold for RSO detection, most notably by the SST and the S-band Radar Fence. The National Research Council estimated that the space catalog will exceed 100,000 RSOs when the S-band Radar Fence's exquisite capabilities are fully realized [54, p. 1]. Further miniaturization of satellites will only increase the burdens of tracking.

New Threats

The emergence of China as a competitor; a resurgent Russia; and less-than-peaceable actions by nations such as Iran, North Korea, and India necessitate increased vigilance in the space domain. In 2019 the Defense Intelligence Agency (DIA) and the National Air & Space Intelligence Center (NASIC) both published factbooks on adversarial

capabilities and intentions. The possibility of warfare is space is now openly discussed by policy-makers and literature.

DIA reports that China and Russia are both developing on-orbital capabilities that can achieve reversible and nonreversible effects against other space assets [62, p. iii]. These orbital threats include kinetic kill vehicles, radiofrequency jammers, lasers, chemical sprayers, high-power microwave beam, and robotic mechanisms [62, p. 10]. Conducting both the tracking and characterization missions on adversarial RSOs is essential to maintain awareness in the space environment, as depicted in Figure 11.

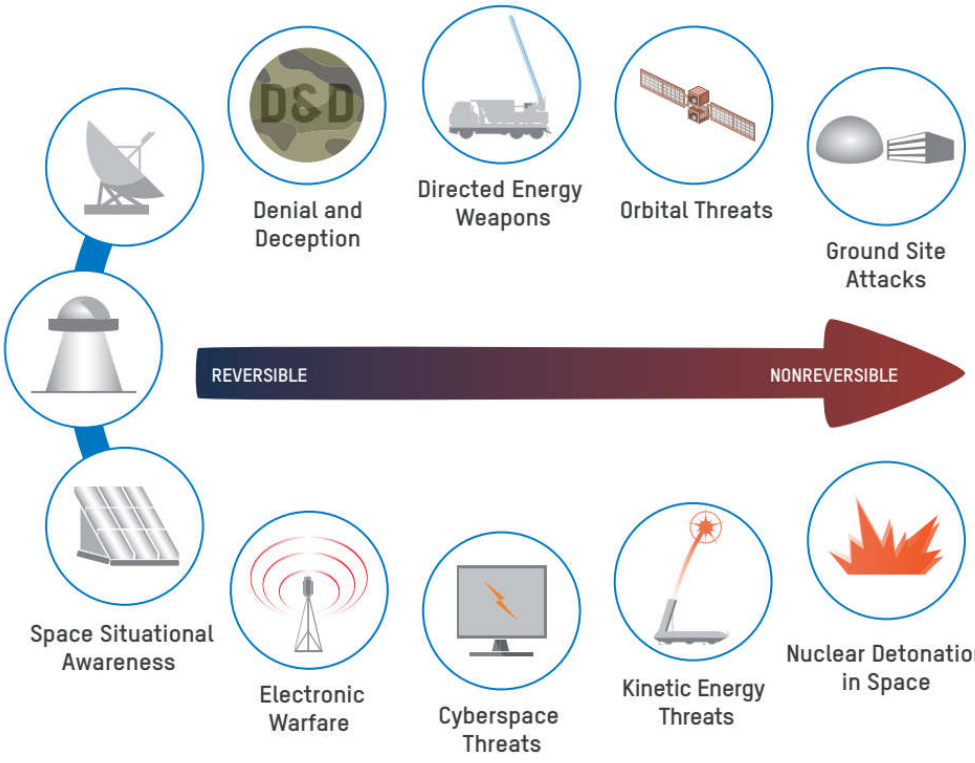

Figure 11. Space asset threat spectrum [62, p. 36].

Reliance on Legacy Systems

In his 2017 speech to the Multi-Domain Command and Control Conference, then Commander of AFSPC, Gen John Raymond, opined [63]:

> Today the system that we have, which is called SPADOC (Space Defense Operations Center)—anybody ever hear of SPADOC? I can't wait until we can take a hammer to SPADOC and just blow it to bits. It's an old clunker and it's a catalog system: it's not a warfighting command and control system. It's not a multi-domain system. It's full, it's tired, and it's limping across the finish line until we can get this thing called JMS (Joint Space Operations Center Mission System) up.

Since Gen Raymond's speech, however, JMS has failed to materialize, leaving DoD and hence the world in a precarious position when it comes to SDA. The SPADOC system was developed in the 1980s and CAVENet was developed in the early 2000s and are still being used for daily operations. Both systems have been described as antiquated, proprietary and user-unfriendly. Weeden estimated their processing capabilities to be 2-3 orders of magnitude below that of a mid-2000s web server, and described instances where replacement parts could only be procured via eBay [53, pp. 14–15].

In 2011 Morton outlined several requirement documents and efforts since the 1990s to upgrade SDA systems, culminating in JMS. JMS was intended to use modern hardware to enable higher speed, higher volume processing as SPADOC was found to have performance limitations after 710,000 observations per day with a 20,5000 RSO catalog [64, p. 6]. Clark, reporting from Breaking Defense, cited that the $1B upgrade was cancelled in 2019 [65]. He also interviewed Brian Weeden and cited a test report surmising the program struggled with replacing systems performing real-time missile warning without impacting critical daily operations, as well as incorporating an increased volume of data from new sensors such as the S-band Radar Fence.

Erwin, reporting for SpaceNews, quoted then-Col Stephen Purdy from the Space and Missile Systems Center as saying that JMS's catalog updating will be replaced with agile software while tactical operations will be merged with the existing Enterprise Battle

Management Command and Control (EBMC2) program [66]. Purdy stated both efforts will later be merged into the Space Command and Control (Space C2) program. The Government Accountability Office (GAO) has also reported that the new Space C2 data repository will be populated with data from various commercial, civil, military, and intelligence sensors and be made available for various applications [67, p. 10].

Call to Action

The need for increased SDA has long been recognized by the USG. The 2011 Technology Horizons study listed persistent SDA as a high-priority technology area which would be needed by 2030 [68, p. 135]. The 2017 National Security Strategy called upon renewing key capabilities in space to address global challenges, asserting that "the United States considers unfettered access to and freedom to operate in space to be a vital interest" [69, p. 31]. Actions by the Trump administration to reactivate United States Space Command and spin off AFSPC into the sixth branch of the military attest to the growing importance of the space domain.

The publication of SPD-3 in 2018 represents the call to action for improving SDA and STM practices. The document asserts that "as the number of space objects increases…[the current] limited traffic management activity and architecture will become inadequate" and directed executive departments to pursue: improvements in observational data, algorithms, and models; developing new hard and software to support data processing and observations; mitigating the effect of orbital debris; improving SDA data interoperability; and enabling greater data sharing". Agencies were also directed to improve SDA coverage and accuracy by seeking to minimize deficiencies in SDA capability, "particularly coverage in regions with limited sensor availability and sensitivity

in detection of small debris" through data sharing, data purchase, or the provision of new sensors; developing better tracking capabilities; and developing the standards and protocols for creation of an open architecture data repository.

The most comprehensive response to this order found in open source literature is AFSPCI 10-610, SSA Metric Data Integration Guidelines for Non-Traditional Sensors[10]. Released in Jul 2019, it provides authoritative guidance on utilizing commercial SDA capabilities, stating that the "intent is to improve SDA through the utilization of a wide variety of sensor data and ephemeris data, of varying fidelity and accuracy, from an array of USG, non-DoD, commercial, civil and foreign data providers" while emphasizing that "the quality and compatibility criteria for new data sources should be set as broadly as possible".

AFSPCI 10-610 admits that the "overall process for accepting non-traditional data sources is constrained by (1) current technical limitations of the command and control systems in their ability to ingest and process non-traditional data and by (2) the quality standards data must meet to be blended with SSN data for use in automated mission processes" [59, p. 5]. Concerns were also raised that ingesting data from outside sources provides avenues for cyber intrusion and "introduces new risks by allowing data sources that have greater potential to degrade SSA processing functions if the data is not well understood or is mishandled by the processing system" [59, pp. 17–18]. To that end, the Non-Traditional Data Pre-Processor (NDPP) has been developed. The system "translates the external non-traditional data source observation format" into the SPADOC format. Lal

[10] As of writing, the document has not been re-released as a Space Force regulation but is assumed authoritative.

et al. assert this will "allow non-SSN data to be validated, verified, and used operationally" and is already used to bring in ephemeris data from satellite owners/operators in a limited manner [46, p. A-5]. Further discussion on measures AFSPCI 10-610 recommends for categorizing non-traditional sensor performance appears in the Relevant Research section later in this chapter.

Non-Traditional SDA Capabilities

Introduction

A projected increase in RSOs, the emergence of new threats, and the failure to modernize the USG cataloging system make the impetus for improving SDA paramount. Employing non-traditional capabilities drawn from the commercial and scientific sectors may provide the disruptive innovation needed to help the US maintain its space superiority. This section provides an introduction to non-traditional SDA; outlines representative commercial and scientific SDA capabilities; and concludes with a summary of the opportunities and challenges facing the USG.

In 2018 Lal et al. researched global trends in SDA and STM while interviewing several commercial SDA stakeholders. They concluded that "due to perceptions related to lack of transparency with DoD data, and motivated by the desire for increasing self-reliance, some countries and companies either by themselves or through consortia are developing their own SSA catalogs" [46, p. 40]. The ability to develop such catalogs for DS tracking has in part been spurred by improvements in optical sensing technology with a reduction in parts cost, permitting adequate telescopes for SDA to be purchased as

Commercial Off-the-Shelf (COTS) items [46, pp. 30–31]. The researchers asserted that [46, pp. 37–38]:

> There is growing recognition that the entry point for SDA need not be based on exquisite and expensive technology. Having several, geographically distributed, even lower-quality ground-based optical sensors can enable the development of an effective sensor network for certain missions that rivals the USG network…[this also helps] augment sensors affected by weather impact[s], and offer[s] redundancy in the system that helps if a sensor fails. Using this emerging paradigm, space-based objects can be detected more frequently, enabling more effective and timely tracking.

Because satellite owners/operators and governments value additional SDA data, multiple worldwide commercial networks rivaling DoD's coverage at the expense of lower fidelity now exist. Additionally, assets employed or formerly employed for scientific space-related endeavors are being time-shared, repurposed, and adapted for RSO tracking and characterization.

Over the past few years, the DoD has implemented several programs to explore augmentation of the USG SDA processes with commercial data. In 2016 the National Space Defense Center (NSDC) solicited commercial capabilities to "augment the Government's ability to detect and characterize space threats and improve integration between DoD, intelligence community, interagency, and nongovernmental space assets" [70, p. 2]. The solicitation sought to utilize both tracking and characterization data.

DARPA executed the comprehensive OrbitOutlook program from 2012 to 2017. In his 2016 report, Raley acknowledged that the "data volume to produce reliable orbital estimates has far surpassed the pace of the traditional government sensor acquisition process" and posited using a consolidated system fusing DoD, civil, commercial, academic, and hobbyist SDA observations as a solution [71]. A demonstration which merged data

from Space-Track and seven SDA providers using over 100 worldwide sensors was conducted. To overcome eventual concerns with accepting data from only certified sensors into the SSN, OrbitOutlook instituted a data-focused validation process which identified abnormal noise and outlier characteristics before checking if non-traditional tracking data was similar to Space-Track's TLEs.

Erwin, reporting for SpaceNews, summarized more recent efforts [72]. The Commercially Augmented Mission Operations (CAMO) program was started as a partnership between the Space and Missiles Systems Center (SMC) and the Air Force Research Laboratory (AFRL) to assess the utility and value of commercial data from three vendors. The partnership led to the creation of the Unified Data Library (UDL), which seeks to develop a repository to host commercial data and make it more readily available for military and civilian users. In Aug 2019, SMC began development of the SSA Marketplace, an electronic storefront to "streamline the manner in which commercial SDA data is purchased". It is unclear if any of the data from these efforts was intended to, and actually did, flow into the SPADOC and ASW systems for incorporation in orbit determination.

Commercial Capabilities

In 2016 Nightingale et al. conducted research and interviewed stakeholders regarding future civil SDA scenarios. Over a dozen entities performing roles as data providers, developers of database management and analysis software, and providing SDA services were identified. The study concluded [51, p. 27]:

> Companies today appear to be able to not only provide data and software as individual components, but also provide SSA services that are increasingly comparable to, or according to some companies interviewed, even superior to

> DoD's. Some companies have developed full commercial RSO databases using commercial, scientific, and international data. These databases are not yet on par with [DoD's], but they are expected to be within a few years.

A review of multiple sources and discussions with the SDA community elicited five major providers: Analytical Graphics Inc. (AGI), ExoAnalytics, Numerica, LEO Labs, and Rincon. LEO Labs and Rincon, whose contributions are largely made using radar observations on LEO RSOs and passive RF detection, respectively, are omitted from this review.

AGI may be considered the first commercial SDA provider. The company, perhaps known best inside DoD circles as the developers of the STK software, manages a substantial research arm called the Center for Space Standards and Innovation (CSSI). CSSI's purpose is to pursue and advocate for SDA improvements. AGI is also involved in the CelesTrak program, which aggregates tracking data from multiple sources and provides free TLEs on its public webpage.

Recognizing the need for more precise location data than available for owners/operators of GEO communications satellites, AGI began development of its own surveillance network. Operations are overseen in the AGI Commercial Space Operations Center (ComSpOC) and observations are compiled into the SpaceBook catalog. The Space Data Association, a grouping of commercial satellite owners/operators interested in highly-refined positional data, maintains their operations through the ComSpOC catalog [46, pp. 41–42].

In 2014, Oltrogge & Houlton outlined AGI's vision to "create a timely, accurate and complete [catalog] of space objects via the commercial ComSpOC…[using] a sensor network which is sufficiently diverse, both geographically and phenomenologically" and

employs telescopes, radars, and radio telescopes with a focus on GEO RSO tracking [73, p. 22]. Optical telescopes were stated to have been placed to take advantage of cloud-free locations in the southern hemisphere and southwestern US with an anticipated visual magnitude between 16-18 M_v and FOV 0.5°-1° for single telescope systems and 2π steradians for all-sky-staring optical systems. Radar capabilities were believed to be able to capture RSOs between 5-10 cm diameter up to 700 km altitude and larger diameters in MEO. The network is illustrated in Figure 12.

Figure 12. AGI network [74, p. 2].

ExoAnalytic Solutions Inc. has deployed its own worldwide telescope network consisting of over 230 sensors at 25 worldwide locations as of 2018 [75]. It is depicted in Figure 13. The company has developed its own catalog of 2000 RSOs with altitudes greater than 10,000 km and claims to routinely achieve accuracies better than 0.25 arcsec in ideal

conditions. ExoAnalytic posits that by combining observations from multiple sensors at one site they routinely achieve detection sensitivity as low as 21 M_v.

Figure 13. ExoAnalytic network [75].

ExoAnalytic provides an extensive list, with prices, of its SDA services on its public webpage [76]. As of Feb 2020, the following options were being offered:

- Monthly subscriptions for observational data from the network based on tiers, where each tier provides 360° GEO survey coverage down to 18 M_v for a varying number of dedicated sensors, percent availability per RSO, and angular persistence for GEO belt coverage, ranging from $90K to $1.4M per month
- Software licenses for proprietary SDA tools
- Space catalog data for $787K to $1.2M per month; the underlying observations can be purchased for additional fees
- Analytical reports summarizing GEO RSO behaviors for $240K to $415K per month
- Bulk historical observational data for around $1 per observation and $12 per observation for frame-stacked data. Historical data is data which is at least two months old. There is an $80K minimum purchase order on bulk historical data.
- Data from dedicated telescopes, delivered the next day, for $18K to $50K per month, or $165K per month for higher quality data

- Data from dynamically taskable telescopes, delivered within 15 minutes, for $30K to $50K per month
- Two turn-key sensor packages. For $500K, one 14 in telescope with 1° FOV capable of observing RSOs down to 18.5 Mv with accuracy 0.2 arcsec. For $5.5M, ten 14 in telescopes with 1° FOV capable of observing RSOs down to 20 M_v with accuracy of 0.2 arcsec. Both purchases include camera, computer equipment, image processing suite, telescope and camera control module, installation, and one week of training.

The Numerica Corporation has also deployed a network of small telescopes across the world. The network consists of "small-aperture, wide FOV sensors that provide persistent coverage of a large swath of the night sky, and medium-aperture telescopes that provide increased detectability and resolution but with a smaller FOV" [77, p. 1]. Numerica has been working with AFRL to build a custom DS catalog with accuracy meeting or exceeding the DoD catalog. The majority of cataloged RSOs are in the 10-15 M_v brightness range. The network is depicted in Figure 14.

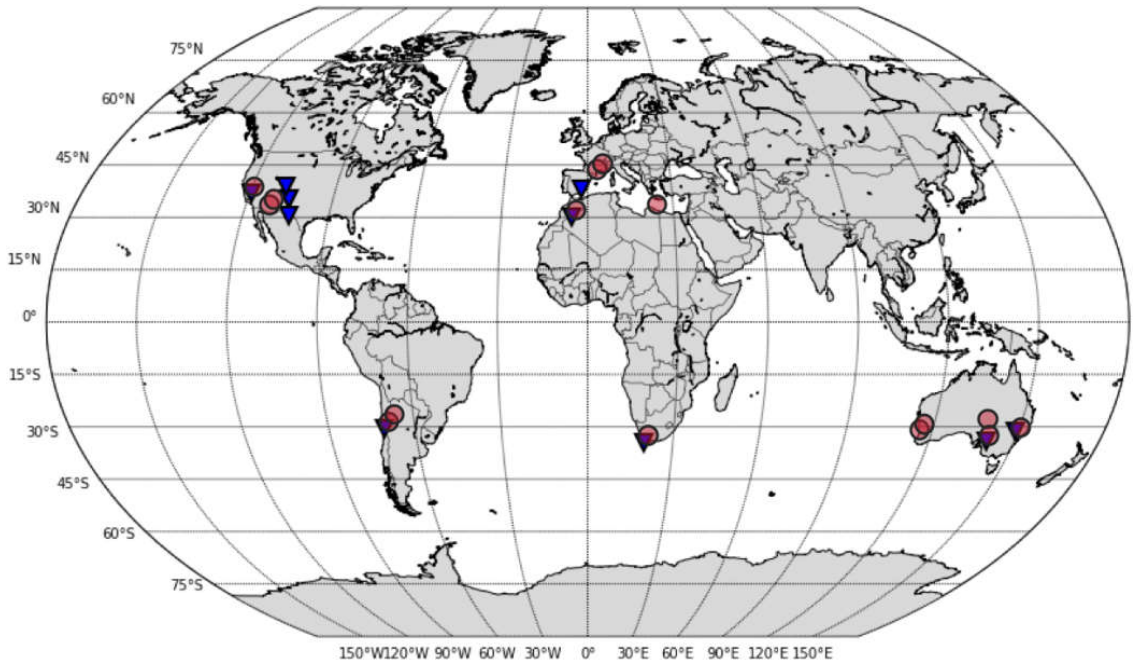

Figure 14. Numerica network [77].

As of 2018, the network consisted of 15 sites across the world to provide 100% coverage of all DS orbital regimes. The telescopes were designed using COTS components along with custom-developed parts to provide robustness. 15 medium-aperture telescopes of 0.3-0.4 m performing rate tracking are augmented with ten robotic sensor arrays conducting continuous collection of all RSOs in GEO or across swaths.

Commercial space-based optical capabilities are not extant, but are looming on the horizon. Lal et al. suggested companies such as Planet will seek to leverage their capabilities to collect SDA data as it is serendipitously gathered via the sensors used to maintain their large constellations' autonomous operations [46, p. 31]. The Space Development Agency's push for a defensive space architecture will likely further the need for space-based sensing. The most promising business case rests with NorthStar Earth and Space, a Canadian startup developing a 40-strong constellation of 700 kg satellites carrying

hyperspectral and infrared cameras for Earth observation and visible cameras to monitor LEO, MEO, and GEO RSOs [78]. Preliminary analysis suggested the constellation be in a 86.4° inclined Walker constellation of four planes with 10 satellites in circular orbits at an altitude of 550-575 km, with one variation including a plane to be equatorial "for observation of GEO belt assets and objects for [the] SDA mission" [79], [80].

Scientific Capabilities

In 2018 Lal et al. indicated a "recent development has been the repurposing of existing sensors previously used for astronomy and other scientific research" [46, p. 31]. Such sensors may be employed by the USG by accepting data on any or all RSOs they have collected, making agreements with sensor owners/operators to track particular RSOs at particular parts of the orbit, and by processing serendipitous data collected by the sensors.

An example of scientific sensors whose data may be easily incorporated into the SSN are those used by NASA for orbital debris measurements [81]. NASA employs the 1.3 m Eugene Stansbery MCAT system on Ascension Island to statistically characterize orbital debris at all altitudes and has advocated for its inclusion as a contributing sensor to the SSN. NASA previously used the 0.6 m Michigan Orbital Debris Survey Telescope (MODEST) at the Cerro Tololo Inter-American Observatory in Chile which routinely detected RSOs down to 17.5 M_v which could conceivably also be utilized.

Bellows demonstrated that ephemeris positional updates can be obtained using metric data from RSO streaks gathered serendipitously by astronomical telescopes which are observing other DS targets [82, pp. iv, 39]. He cited two particular sensors, the Panoramic Survey Telescope and Rapid Response System (Pan-STARRS) and the Large

Synoptic Survey Telescope (LSST) which are designed to detect faint RSOs, routinely collect serendipitous observations, and would provide advantages to DoD. Using data from Pan-STARRS, which is co-located with the Maui GEODSS telescopes, was posited as a way to free up DoD tasking. LSST, an 8.4 m telescope being deployed in Chile [83], was noted for its employment plan which calls for observing the entire western half of the GEO belt once every three days and making observations publicly available on the internet, which would be used for SDA purposes. This and similar work implies serendipitous data from other observatories may be utilized to improve the SDA mission; a cursory review has identified over 40 telescopes with a 3 m or greater aperture extant or in development, six of which are greater than 8 m [84], [85].

Opportunities and Challenges

There are major advantages to the use of commercial SDA. Stottler put forth the following benefits from use of commercial SDA data: improving the number and geographic diversity of sites; increasing capacity; cost-effectiveness; allow for tracking and characterization; and more immediate responsiveness to tasking which can be used to search for newly lost RSOs, conduct post-launch observations, and track lower priority RSOs and free up DoD assets for other missions [86]. Nightingale also noted the DoD can capitalize on "the rate of innovation in new types and technologies" from commercial sources [51, p. 19].

General non-traditional data is also advantageous. Bellows' work implies that data otherwise left on the cutting-room floor from telescopes with better viewing capabilities than that of the USG may be used for little to no cost, provided serendipitous data is in fact available. AFSPCI 10-610 also acknowledges that even data of lesser quality "may still

have utility to other SDA missions due to unique characteristics of the data source" and may aid "launch processing, maneuver detection, reentry, new object discovery and lost object processing" [59, p. 17].

Despite the clear advantages, there are several challenges with incorporating non-traditional data. First regards timeliness; while a several-day delay in obtaining observations on routine RSOs is acceptable, high-priority RSOs require quicker timelines. Processes will need to be in place to expedite data handling. Next is the inability to not only directly task and control non-traditional sensors, but in some cases an absence of incentive for non-traditional providers to deliver information to the USG. For example, convincing a scientific telescope's owner/operations, which typically tracks asteroids, to modify its scheduling to accommodate a collection on a very dim exquisite RSO may be difficult. The USG would also be cautioned to avoid relying exclusively on high-quality and/or unique observations from non-traditional sensors that do not share DoD's core interests as unique data sources may become unavailable at a later time.

Perhaps the most important concerns deal with the data itself. In 2016 Lal et al. stated 18 SPCS "currently ingests little non-SSN data, due to computer system limitations and security concerns" [46, p. 19]. Ingesting, sorting, and actioning the quantity of data available from non-traditional means to the maximum extent possible requires modern software which is not reflected in DoD's current architecture. Data integrity is also an issue; Bellows notes "inclusion needs to be accomplished using a method that ensures the data is trustworthy, usable, and will not corrupt the data that has already been validated by the SSN" [82, p. 3]. Data from less reputable sources with different accreditation may result in injecting incorrect data and cyber intrusions. The legal question of liability may

also arise when data from a non-traditional source is included and actioned on, or not actioned on, in an event such as a conjunction assessment.

Relevant Research

Introduction

All fundamental aspects of the project have been reviewed: system architecting, optimization, optical collection, astrodynamics, modeling and simulation, US SDA processes, challenges to USG SDA, and non-traditional SDA capabilities. These disparate components must be integrated to devise a study which accurately models and simulates a representative AN using physics-based assumptions and scheduling theory; uses appropriate measures to evaluate performance; applies optimization to deduce high-performing architectures, and is reflective of the projected operating environment. In devising such a study, it is instructive to review the approaches of previous researchers for insight and any adaptability to the problem at hand.

Literature was reviewed to elicit past studies which sought, in all or part, to augment or provide an alternative to the USG SDA architecture; described use of requirements and measures; performed optimization; and considered the scheduling problem. Architectural studies from non-SDA disciplines were also reviewed. Relevant research is presented in the categories of SSN augmentations and alternatives, related architectural studies, and SDA requirements.

SSN Augmentations and Alternatives

Optimal GEODSS Siting (Warren, Elio, 1991)

In 1991 Warren studied the optimal placement of a new GEODSS sensor to be operated from one of 12 Canadian sites based on the most favorable environmental considerations [87]. In his tradespace Warren required five conditions be met: the Sun be at least 6° below the horizon; the surface wind speed be less than 25 knots; the temperature be greater than -50° C; the satellite elevation be at least 15° above the horizon; and there be a 5-minute CFLOS between the RSO and the sensor. The probabilities for all five conditions were computed for each month of the year for all 12 sites using a simulated representative RSO in MEO and one simulated representative RSOs in five GEO belt longitudes. The joint probabilities for the conditions were then computed and compared. The study recommended the site at Moose Jaw be selected due to its high Probability of Cloud Free Line of Sight (PCFLOS) over all months, winds typically under 25 knots, and its southern location allowing year-round operations. Several months later Elio conducted follow-on research adapting Warren's approach to determine the optimal placement of a new GEODSS site amongst 14 worldwide locations [88]. The study recommended any of four sites in Australia as optimal locations.

Space Observation Network Study (Payne et al., 1998)

In 1998 Payne et al. researched augmenting GEODSS with a ground-based small telescope network and space-based space surveillance system for tracking and characterization needs 25 years into the future with emphasis on the number, placement, and cost of the telescopes [89]. The study used a four-tier approach: identify current requirements, tasks, and MOEs/MOPs; develop sensor concepts; analyze performance in

context of the requirements; and provide costing results. The quantity, location, and visual magnitude of future RSOs were extrapolated using contemporary trends.

For the ground-based study, two scenarios were tested: GEODSS primarily to provide SOI with limited metric contributions and using the small telescopes for metric tasking; and using GEODSS to perform SOI only and the small telescopes to provide all metrics. Task-based and search-based strategies were also compared. The small telescopes were assumed to be co-located with the five GEODSS sites; at the time, the Moron, Spain site was still operational and a fifth future site in Australia was anticipated. Four generic small telescope designs were considered; detectors were designed to match the FOV and spot size while the apertures were sized to obtain an SNR of 10 at 17 M_v in a one second integration time. The final specifications employed a FOV between 0.5° to 4° using a 40 cm aperture.

The total number of small telescopes needed at each site was found by estimating the total number of tracks per day occurring in longitude regions and dividing by the number of tracks per day estimated to be collected by a small telescope. For the task-based approach, 24 small telescopes were found to be required for the GEODSS performing SOI and limited metrics scenario while 33 small telescopes were required for the GEODSS using SOI only scenario. For the survey-based approach, 31 small telescopes were found necessary.

The space-based study sought to determine the number, orbit, and cost of space-based telescopes needed for LEO and DS metrics 25 years into the future. An iterative approach was used to determine the best orbit, optimal aperture size, and number of satellites in the space-based constellation before comparing with the required tracks per

day. RSO attributes such as brightness, range, and relative velocity were considerations in the iteration. A constellation of four 895 kg satellites with a 25 cm aperture at 1000 km altitude inclined at 90° in a sun-synchronous orbit was determined to best meet objectives at lowest cost.

Mechanism for Evaluating Space Surveillance Networks (Andrews & Raup, 1998)

Andrews & Raup conducted a follow-on to a 1998 Massachusetts Institute of Technology Lincoln Laboratory future concepts study to investigate the benefits of adding space-based sensors to the SSN [90]. Their 1999 paper outlined the process used to perform the evaluation of trade-offs for a mixture of ground and space-based sensors in the SSN by 2010. Noting the lack of requirements for a future system, they decided to conduct evaluations by considering the SSN's utility in hypothetical future focuses which included DoD performing traditional SDA; DoD use of space control; the USG focusing on civil missions; and use of commercial contributions. The four focuses were scalable such that a future scenario could consist of a set such as {0.25, 0.25, 0.25, 0.25} instead of only extrema.

The researchers broke their evaluation into three parts. First, input requirements were identified. These consisted of determining all future network concepts; capturing user needs such as timeliness, data completeness, and data fidelity; and then identifying the range of potential operating environments. Next, the researchers developed quantifiable scoring metrics. Lastly, they employed classical decision theory to develop a figure of merit which helped identify better-performing networks.

Each candidate network's capabilities were evaluated against performance parameters. The performance parameters were then converted to a continuous 0 to 5 range

using non-linear scaling functions which imposed boundaries on parameter performance. Networks were assigned a final score using the weighted sum method in which performance parameters were weighted based on relative importance then summed. The networks were then compared between the four future focuses. The researchers omitted conclusions from the document.

SSN Optical Augmentation (Andress, 1999)

Andress provided an after initiative report on the SSN Optical Augmentation effort conducted by the Air Force Space Battlelab in 1999 [91]. The project sought to demonstrate the potential for remote, autonomous collection and reporting of tracking data to augment GEODSS using low-cost COTS technology. The end goal was to demonstrate that the SSN's capacity and performance could be improved by offloading routine tracking from the more-capable telescopes to the smaller telescopes, allowing the former to focus on more difficult missions such as SOI or exquisite metrics generation. A second objective was to demonstrate the value of using geographically-dispersed sensors.

A two-week demonstration was conducted at Edwards AFB, CA using a 40 cm telescope with a German equatorial mount. Although no data was flowed into the operational SSN system, conclusions were made based on potential incorporation of the data. The small telescope's acquisition rate, throughput, and accuracy was found to be similar to that of GEODSS and it was able to track 70% of all DS RSOs. The investigators claimed success when the small telescope collected observations autonomously during a period when weather prohibited collection at two other GEODSS sites. Based on the trial, the investigators recommended procuring three small telescopes with a 1° FOV and improved tracking mounts then deploying them to sites in Australia, Europe, and

Southwest Asia to create coverage overlaps and improve capacity. The total cost for the three telescopes was estimated to be $5-7M with an Operations & Maintenance (O&M) cost of $6 per RSO, which compared favorably to the $15-38 per RSO cost incurred by GEODSS.

OrbitOutlook (Raley, 2012-2017)

This project was previously described in the SSN section of this chapter and is mentioned here only for completeness.

Cost and Performance Comparison for GEO SDA Architectures (Morris et al, 2014)

Morris et al. performed a relative comparison of the performance and total cost to field different space-based GEO SDA architectures [92]. Four options were evaluated: traditional dedicated large satellites; hosted SDA payloads; microsatellites with high-quality sensors; and a low cost, low quality CubeSat constellation. The four architectures were constructed in STK and a single day scenario was run and analyzed. Table 5 shows the architecture specifications and results.

Table 5. Architectural specifications and performance adapted from document.

	Large Sats	Microsats	Hosted Payloads	CubeSats
Specs	4 sats GEO belt 30 cm/3° FOV 42,000 km range 15 yr life	16 sats GEO belt 15 cm/3° FOV 20,000 km range 5 yr life	16 sats Uneven GEO belt 15 cm/3° FOV 20,000 km range 5 yr life	27 sats GEO +500 km 5 cm/30° FOV 5,000 km range 1 yr life
Mean Coverage	48%	47.5%	51.3%	38.5%
Mean Max Gap	21.2 hrs	11.5 hrs	15.6 hrs	30 hrs
Access	90%	96%	93.5%	79.2%
Relative Perf	2.4	3.0	2.6	2
Relative Cost	0.75	1.0	0.50	0.15

Average coverage, access, and average maximum time between observations were used as measures to compare performance between the architectures. Coverage was defined as the amount of time an RSO was viewed while access was defined as how many unique RSOs were observed. Relative performance was determined by normalizing the measures and summing the three values for each architecture. Cost for each architecture was determined by estimating spacecraft construction, launch, operations, and replenishment costs over an assumed program lifetime of 15 years. Relative total cost was determined by normalizing the costs for each architecture. A comparison of relative performance vs relative cost illustrated that the CubeSat constellation would likely have the lowest quality at lowest cost, but that a hosted payload constellation would outperform a traditional large satellite constellation in both cost and performance.

Aiding GEO SSA with COTS Telescopes (Moomey, 2015)

In 2015 Moomey developed a framework to determine if a large-scale employment of small-aperture COTS telescopes could augment the SSN's observing capacity of the

GEO belt without degrading the quality of orbit estimates [33]. He hypothesized that the resultant Small Aperture Deep Space Surveillance (SADSS) architecture could be used to collect on lower-priority RSOs. Using a systems engineering approach, he identified mission requirements, MOEs, MOPs, and design parameters for the system based on the AFSPC Commander's priorities. He then used extant data to determine the distribution and brightness of GEO RSOs and used it to size telescopes in a point solution. Lastly, he simulated observations from a similar telescope and converted the astrometric data into orbital parameters, demonstrating that quality comparable to 18 SPCS TLEs is possible.

The development of SADSS requirements are discussed in the SDA Requirements section. Moomey assumed that high-value GEO RSOs are brighter than 16 M_v and analyzed RSO brightness data as a function of size, reflectivity, and lighting angle to determine a 16 M_v RSO roughly corresponds to a 4 m^2 target. The percent of GEO RSOs with this area was estimated to be 77% based on extant RCS values, which was deemed an acceptable collection threshold. Assuming an SNR of 2.5 for minimum detectability, the minimum aperture diameter to collect on a 4 m^2 target was computed to be 22 cm. COTS hardware employing a 25 cm aperture with a 7.5 s sample rate and 1.4° x 1.4° FOV was ultimately selected for each telescope in the network.

Moomey chose to operate all telescopes in rate-track mode instead of the SSN's typical sidereal mode because he believed it was more advantageous to increase the probability of detecting RSOs during poor weather and improve custody on particular RSOs. This necessitated using approximately 60 telescopes at five separate sites. The five sites chosen were the three GEODSS sites, Ascension Island, and the future SST location in Australia with the thought that this would provide the surest security,

maintenance, and communications for operations. After validating the COTS telescopes could accurately perform orbital updates, it was estimated that up to two hours of track time per night per GEODSS telescope could be saved by offloading bright collections to SADSS. The final architecture was estimated to cost $3.5M per site before installation, comparable to the cost of operating one GEODSS site in a year.

Examination of Approaches to Optical Detection & Tracking (Ackermann et al., 2015)

In 2015 Ackermann et al. proposed an optical network to track GEO RSOs as an alternative to the SSN's optical sites, outperforming the SSN in terms of latency, coverage, and cost [52]. The researchers estimated the capabilities of GEODSS, SST, ORS-5, SBSS, and Sapphire, then estimated the optical-only SSN's performance. They posited the following measures as important: maximum latency, or the maximum time to wait between an RSO being reacquired by the network; sky coverage efficiency, or the fraction of time RSOs in each GEO position are visible to any sensor in the network, averaged over all orbital positions; instrument sensitivity; and system cost per observation. Review of the data found a global network of ground-based telescopes best searched broad areas of the sky for dim RSOs; space-based sensors in equatorial LEO demonstrated low latency and medium sensitivity; and space-based sensors in near-GEO orbit would aid in collecting on RSOs which are solar excluded for the space-based equatorial LEO sensors.

Based on the analysis, expert knowledge, and additional modeling, the researchers put forth a network of ground and space-based sensors to outperform the SSN. The ground network consisted of 16 total 1 m telescopes in pairs at eight sites; ten total 2 m telescopes in pairs at five sites; two ORS-5-like satellites in equatorial LEO spaced 180° in-plane; and three Sapphire-like satellites 500 km below GEO spaced 120° in-plane. Ground sites are

illustrated in Figure 15 and were chosen in part for their geographic diversity, proximity to the equator, high elevations, and distance to existing or nearby infrastructure. It was concluded that the observational latency of the proposed network would be lower than that of the SSN at a $1B construction cost and $64M annual O&M cost.

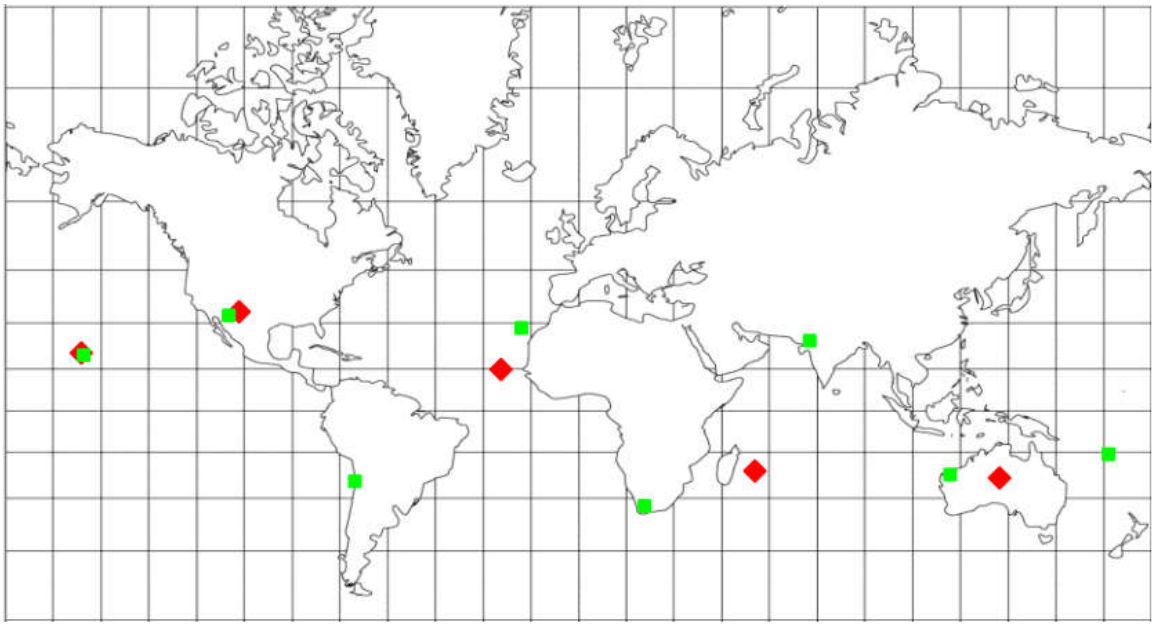

Figure 15. Alternative network. Diamonds are 2 m sites; squares are 1 m sites [52].

Multi-Objective Optimization of GEO SDA Architectures (Stern & Wachtel, 2017)

In 2017 Colombi et al.[11] implemented a methodology to select the optimal locations and aperture sizes of ground and space-based sensors to track GEO RSOs as an alternative network to the SSN [93]. Noting that previous studies did not strive for optimality due to a lack of computing power and methods to explore large tradespaces, they employed heavy use of optimization and M&S on a HPC to design their network. The study was limited to around 800 GEO RSO with all RSOs assumed collectable by sensors. No orbit updates were conducted during the M&S.

[11] For reference, it is noted that Stern & Wachtel's thesis work underpins this article.

The researchers identified maximizing the network's detection capability, minimizing the latency, and minimizing cost as the most important architectural needs. Measures used for these quantities were the mean of the mean detectable RSO size, the mean of the maximum observation time gap per RSO, and the total system cost, respectively. The tradespace of permissible sensors included:

- 9 ground sites with 0-4 telescopes each with aperture sizes from 0.5-4.0 m in 0.5 m increments
- 1-2 LEO sun-synchronous satellite planes with 0-2 satellites per plane at an altitude of 500-1000 km in 100 km increments and apertures in the set {0.15, 0.30, 0.45, 0.60, 0.75, 0.90, 1.00}
- 0-4 LEO equatorial satellites at an altitude of 500-1000 km in 100 km increments and apertures in the set {0.15, 0.30, 0.45, 0.60, 0.75, 0.90, 1.00}
- 0-4 near-GEO satellites at altitudes from the set {-1000, -500, 0, +500, +1000} km relative to GEO, and apertures in the set {0.15, 0.30, 0.45, 0.60, 0.75, 0.90, 1.00}

Considering all permutations of sensors was deemed unrealistic; a heuristic method was used to sidestep evaluating all architectures. The NSGA-II variant of the GA was selected and run using the Inspyred Python package after consultation with an SDA optimization SME. A 28-gene real-coded chromosome was used to represent the architectures. The architectures' performance was simulated on both Vernal Equinox and Summer Solstice; the former to test northern hemisphere sites during the shortest night and the latter to test performance when RSOs are in eclipse for over an hour.

Four separate trials of the following routine were performed on both days, each on separate processors of the HPC. An initial population of 96 architectures was selected

randomly; the population was sized based on prior analysis by Reeves. All architectures were subjected to an optical collection M&S which consisted of propagating RSOs over each 24 hour period, scheduling collections at sensors, and collating data on tracked RSOs. The results were used to calculate the three system measures. The measures were used as optimality criteria in the following MOO problem which employed a penalty function to enforce constraints:

Minimize

$$p_i(X) = f_i(X)v_i(X) \text{ for } 1 \leq i \leq 3$$

Where

$$\begin{gathered}
f_1(X) = \frac{1}{n_{RSOs}} \sum_{1}^{n_{RSOs}} \left(\frac{1}{n_{obs}} \sum_{o=1}^{n_{obs}} d_{RSO,o} \right) \\
f_2(X) = \frac{1}{n_{RSOs}} \sum_{1}^{n_{RSOs}} \left[max_{1 \leq o \leq n_obs} \left(t_1 - t_{start}, \ldots, t_{end} - t_{n_{obs}} \right) \right] \\
f_3(X) = \sum_{n_{Sat}} C_{sat} + \sum_{n_{Tel}} C_{Tel} + 10 \left(\sum_{n_{Sat}} C_{satOps} + \sum_{n_{Tel}} C_{telOps} \right) \\
+ \sum_{n_{Launch}} C_{launch} \\
v_1 = \begin{cases} 1 & if\ f_1(X) \leq 100\ cm \\ C & otherwise \end{cases} \\
v_2 = \begin{cases} 1 & if\ f_1(X) \leq 90\ min \\ C & otherwise \end{cases} \\
v_3 = \begin{cases} 1 & if\ f_1(X) \leq \$3B \\ C & otherwise \end{cases} \\
C \text{ is a large constant}
\end{gathered} \tag{2.31}$$

The architectures were compared using NSGA-II's Pareto optimality and distance-based sorting routine. Architectures were selected to advance based on binary tournament selection and subjected to crossover and mutation as described in the NSGA-II section of this chapter. The routine continued for 100 generations.

The optical collection M&S was conducted using Python and STK Connect, the command-line version of STK. Python called STK Connect to input the GEO RSOs TLEs from Space-Track into an STK scenario file and propagate the orbit, without covariance information, for 24 hours. All sites and observer satellite system constraints were modeled in STK. Ground sites were modeled with a solar exclusion angle of 40°, lunar exclusion angle of 10°, minimum elevation angle of 20°, and set to operate only in umbra. Observer satellites were subjected to a 40° solar exclusion angle and 5° lunar exclusion angle. All ground and space-based sensors were constrained to observing RSOs which are only solar illuminated.

Site-RSO access reports were generated to determine all astrodynamically possible collection windows. It was assumed that 30 seconds was sufficient for any sensor to compute an observation and slew to the next target; therefore, the 24 hour scenario was broken into 2,880 discrete intervals. A lookup table of all sensors vs the 2,880 30-second intervals was formed, indicating if a site-RSO access was possible during the interval. All RSOs were assumed bright enough to be collected by all sensors. RSOs were rank-ordered by their latency for use in the scheduler.

When an architecture was selected, a Greedy scheduler simulating a centralized tasking/centralized scheduling routine was run on all sensors in the network. PCFLOS data was first used to randomly determine if the weather at any ground site was poor; if it was, these sites were eliminated from consideration. The scheduler then stepped through every 30 sec interval, then each site or satellite. The corresponding entries in the lookup table were used to get the accessible RSOs, and the most latent RSO was selected for observation and its latency reset. For architectures with multiple sensors at the ground site, the

successive accessible RSOs with highest latent were scheduled. It was assumed that all scheduled RSOs were in fact collected by the sensors.

After all collections were scheduled, the optimality criteria were calculated. The minimum detectable size was estimated by backsolving the following SNR equation

$$\mathrm{SNR}\Delta = \left| \frac{((\psi \cdot (S \cdot \pi r_{\mathrm{rso}}^2) \cdot \tau_{\mathrm{opt}} \cdot \tau_{\mathrm{atm}} \cdot A_{\mathrm{RCVR}}/R^2) \cdot \eta \cdot \lambda_{\mathrm{avg}})/(h \cdot c) \cdot t_{\mathrm{INT}}}{\sqrt{((\psi \cdot (S \cdot \pi r_{\mathrm{rso}}^2) \cdot \tau_{\mathrm{opt}} \cdot \tau_{\mathrm{atm}} \cdot A_{\mathrm{RCVR}}/R^2) \cdot \eta \cdot \lambda_{\mathrm{avg}})/(h \cdot c) \cdot t_{\mathrm{INT}} + n(N_{\mathrm{sky}} + N_d) \cdot t_{\mathrm{INT}} + N_r^2}} - 6 \right| \quad (2.32)$$

where the ΔSNR was assumed to be 0.1, an SNR of 6 was used, and physical parameters of sensors and sites were known *a priori*. Table 6 summarizes sensor parameters used for this computation. Latency was calculated by looking at the maximum time gap for every RSO, then averaging across all RSOs. Cost was computed using cost-estimating relationships based on the telescope aperture size and an estimated 10-year mission life for satellites which included operations and launch costs.

Table 6. Sensor parameters, adapted from the report.

	Ground	**SSO**	**Eq LEO**	**Near-GEO**
Instantaneous FOV (arcsec/pixel)	2	2	2	2
Quantum Efficiency	0.65	0.65	0.65	0.65
Optical throughput	0.9	0.9	0.9	0.9
Integration Time (s)	1	1	5	1
Spectral range (nm)	400-800	400-800	400-800	400-800
Aperture Diameter (m)	0.5-4	0.15-1	0.15-1	0.15-1
Obstruction diameter	0.3 x ap dia	0.3 x ap dia	0.3 x ap dia	0.3 x ap dia
Read Noise (e^-/pixel)	12	12	12	12
Dark noise (e^-/pixel)	6	6	6	6
Background apparent magnitude (M_v/arcsec^2)	21.1	22	22	22
RSO avg angular velocity (arcsec/s)	15	30	5	15

The routine was completed in three days on the HPC. Because Pareto optimality returns clusters of high-performers instead of global optimals as in a weighted sum approach, the researchers ascribed values to the optimals in post-processing to compare results. Architecture optimality criteria were combined into a single value by either equally weighting the objectives or by using weights to minimize detection and latency regardless of cost. The near-optimal architectures consisted of 19 worldwide telescopes, typically with a 1 m aperture; four observer satellites in equatorial LEO with a 45 cm aperture; and four observer satellites in near-GEO with a 60-90 cm aperture at a cost of $1.5-2.9B. The architectures were found to outperform both the SSN and the Ackermann architectures.

Optimal GEO SDA Architecture with Direct Ascent Vehicle Tracking (Bateman, 2018)

The core methodology developed by Stern & Wachtel was adapted by several researchers to investigate additional problems. Bateman studied the performance and design of an optimal SDA architecture tasked to perform additional collection on a Direct Ascent vehicle [94]. He also sought to improve Stern & Wachtel's baseline methodology and incorporate data mining to better understand design implications. AGI's Astrogator module was used to design the Direct Ascent vehicle's trajectory. His scheduler placed focus on assigning sensors to always observe the Direct Ascent vehicle and tightened the RSO diameter constraint from 100 cm to 75 cm.

Increased computational power was available, and the population size in NSGA-II was increased from 96 to 468 and number of generations was decreased from 100 to 80 due to the larger population sufficiently evaluating the tradespace. Computation time per generation was sped from 45 to 22 minutes. Six trials were run on parallel processors to evaluate 227,000 architectures in two days.

Bateman chose to evaluate one day per month from Jan to Jun, which included Vernal Equinox and Summer Solstice, per trial. After NSGA-II concluded and the optimal architectures were identified, a comparison was conducted by assigning a value to each architecture using weighting on the optimality criteria. Equal weighting; maximum performance; and minimum latency weights were considered. Each measure was also scaled based on the upper bounds. The resulting formulation was:

$$Value(X) = w_1 u_1\big(f_1(X)\big) + w_2 u_2\big(f_2(X)\big) + w_3 u_3(f_3(X))$$

where

$$u_i\big(f_i(X)\big) = \begin{cases} 1 - \dfrac{f_i(X)}{bound_i} & if\ f_i(X) \le bound \\ 0 & otherwise \end{cases} \tag{2.33}$$

$$\sum_{i=1}^{3} w_i = 1$$

and f_i are the objective functions, X is the architecture, and w_i represent the weights. Bateman only reported equally-weighted values in his work. The researcher found better architectures have at least three GEO observer satellites, at least two equatorial LEO observer satellites, and have ground sites at Siding Spring, Paranal, Mount Graham, and Mauna Kea while few architectures employ ground sites at Diego Garcia and Haleakala.

A strong correlation was found between aperture diameter on the GEO observer satellites and the detectable RSO size of each architecture. Bateman posited that an architecture meeting cost and latency requirements that does not meet the detection threshold should focus on increasing the apertures of their platforms for the best performance boost. The final set of best architectures based on the equally-weighted solutions were simulated without the Direct Ascent vehicle in order to determine the effect

on the network. The mean of the maximum observation time gap was found to increase by 1-3 minutes due to the Direct Ascent vehicle.

Optimal GEO SDA Architecture with GPO Observer Satellites (Felten, 2018)

Felten extended work by Stern & Wachtel and Bateman with an increased tradespace and refined methodology [95]. Notably, he investigated the utility of Geosynchronous Polar Orbit (GPO) observer satellites placed in an 89° inclined orbit at 36,000 km altitude, hypothesizing they would minimize the effect of the solar exclusion angle and improve access to GEO RSO collections. The number of possible observer satellites per orbit was also extended while LEO sun synchronous observer satellites, found to be infrequently selected in previous research, were removed from consideration. Ground sensor capabilities were also extended from umbra to include twilight conditions. An improvement in satellite cost estimating was also implemented.

18 trials were performed for three separate days each month from Jan to Jun to include the complete Earth-Sun geometry. A GA was used with a population size of 192 for 50 generations to explore the tradespace. In lieu of finding all Pareto optimals then calculating value scores in post-processing, Felten normalized the optimality criteria and applied equal weighting to calculate a single value score for each architecture during the GA run. This resulted in a single best optimal architecture for each simulated day.

It was determined that the best architectures frequently chose GPO observer satellites over equatorial LEO and near-GEO options. The most common architectural elements from the top performers were combined to conclude the best architecture consists of 13 1 m ground telescopes, five 1.5 m ground telescopes, and two planes of six 0.15 m

aperture GPO satellites capable of detecting 26.9 cm RSOs with an average latency of 48.6 min for a cost of $1.1B.

Related Architectural Studies

Architectural design studies from non-SDA disciplines were surveyed to consider a breadth of perspectives. The approaches of three studies had relevance in the forming the proposed methodology. Additional studies reviewed included architecting a distributed imaging satellite system [96] and improving the Air Force Satellite Control Network [97].

Optimization of Disaggregate Space Systems (Thompson, 2015)

Thompson developed a framework for designing a disaggregated space system using system architecting, modeling, and optimization [98]. His Disaggregated Integral System Concept Optimization (DISCO) methodology consisted of: developing the reference architecture; developing the optimization/assessment models; and evaluating solutions then updating the architecture. His framework is depicted in Figure 16. Notably, a Monte Carlo analysis was employed on top of a GA with multiple trials to better assess the effects of the probabilistic elements in the system.

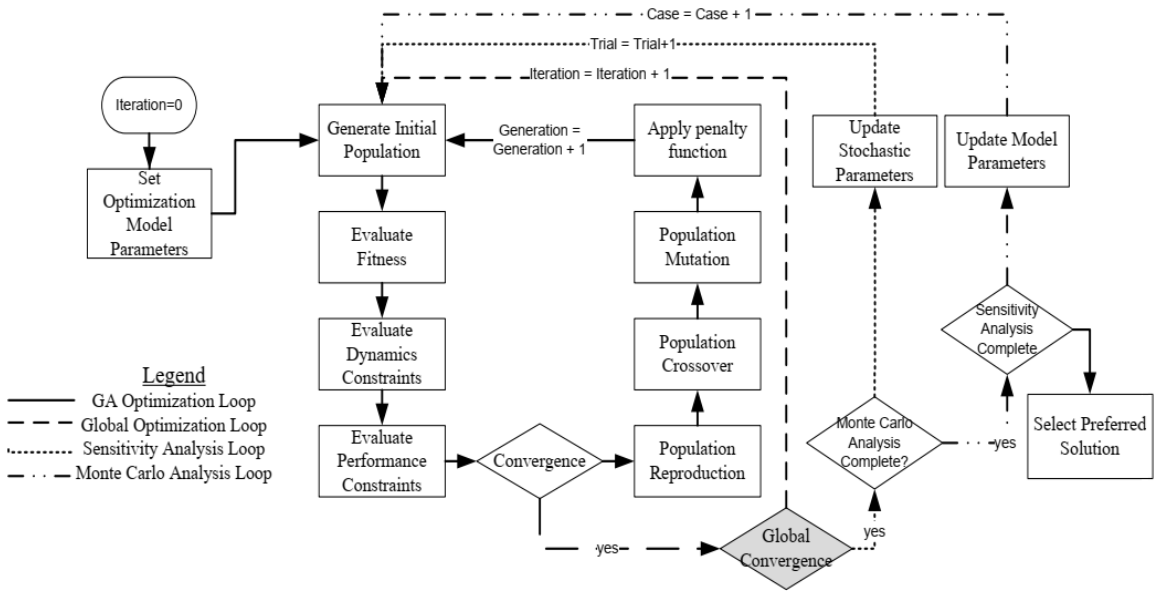

Figure 16. DISCO process [98, p. 6].

Value-Focused Model for C4 Network (Davis et al., 2000)

Davis et al. developed a quantitative method to evaluate objectives in the development of alternative upgrades to a Command, Control, Communications, Computer, and Information (C4I) architecture [99]. The researchers first identified typical bottlenecks in the C4I process; employed Value-Focused Thinking and reviewed regulations to identify relevant objectives; interviewed senior decision-makers to validate objectives and obtain relative weightings; and computed values for multiple architectures.

The system value hierarchy is depicted in Figure 17. Evaluation measures, which are the non-blocked quantities, were calculated by mapping real values onto ranges by measure-specific scaling functions. Seven alternate architectures were compared to a baseline. A plot of final architecture values vs cost identified several alternatives with varying utility for a similar price, validating the usefulness of the tradestudy.

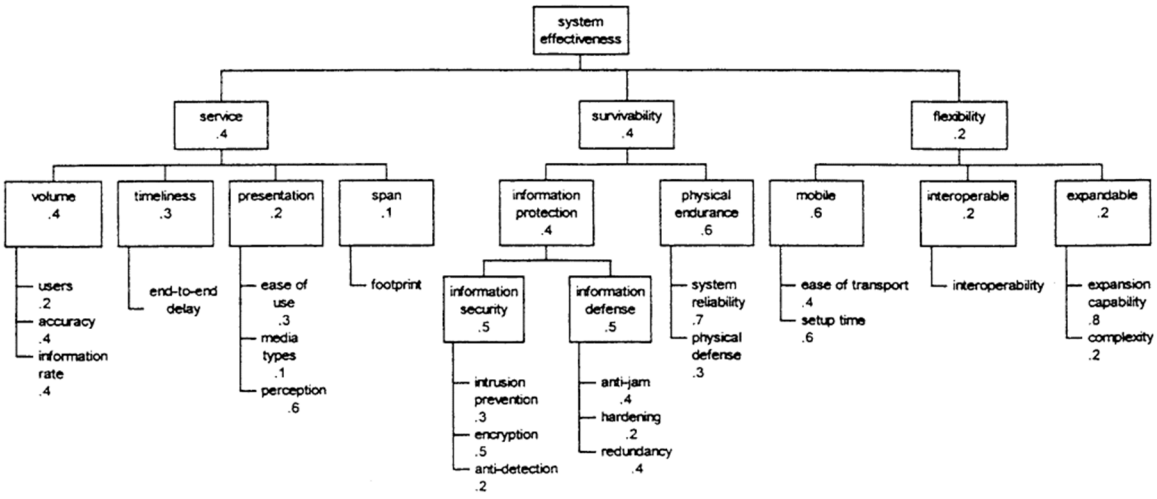

Figure 17. Davis' C4I network expanded value hierarchy [99] .

NOAA Satellite Observing System Architecture (Anthes, 2018)

Anthes provided the final report of the National Oceanic and Atmospheric Administration's (NOAA's) Space Platform Requirements Working Group in support of the NOAA Satellite Observing System Architecture (NSOSA) study [100]. NOAA examined the prioritization of measurements for its operational needs in the next generation of satellites. The group used an internal value model which identified the most important objectives for meeting observations from space, performance attributes at different levels of capability, and priorities for improving performance objectives from threshold to maximum effect. Architectural choices were subjected to alternative scenarios which included critical operations in global locations under normal and contingency conditions. An iterative approach was used to develop the architectures to meet value model objectives at different levels. After a baseline was developed by the working group, the work was reviewed with managers and stakeholders for feedback and updated. A final round considered projected budget constraints and left senior leaders with decision alternatives.

The group identified 44 total objectives across terrestrial and space weather categories with performance attributes for each objective. Objectives were ranked by the working group with preference given to functions resulting in government action that affect public safety or economic livelihood ahead of actions which only increase the state of knowledge. Through trial and error, weights on objectives were eventually assigned using a hyperbolic tangent function. A range of desirable attributes for each objective were identified. A fixed budget constraint of $2.2B per year was set with the understanding that if all architectures failed to meet this constraint attribute lower thresholds would be reevaluated.

Representative architectures were designed which met objectives at different performance attributes, then subjected to various weather scenarios. The simulation sought to elicit: the timeline to provide accurate forecasts in advance; the ability to warn 24 hours in advance; the ability to provide emergency managers necessary information; and if sufficient notice was given to the affected public. Operational impacts of each architecture, how performance differed when moving from baseline to maximum attribute capabilities, conflicts between mission elements, and bottlenecks were also of interest. Specifics on the architectural candidates, simulation performance, and the final architecture decisions were omitted from the report.

SDA Requirements

A review of open-source literature was unable to locate any authoritative documents on requirements for the future AN. Therefore, requirements from similar systems were reviewed to infer likely requirements as detailed in Chapter III.

Determining SSN Operational System Capability (Daw & Hejduk, 1999)

A review of open-source literature was unable to locate any historical or contemporary regulations detailing specific SSN requirements. However, in their 1999 study on improving the reporting of the operational capability of the space surveillance mission Daw & Hejduk claimed to have adapted requirements from AFSPC's Space Surveillance Requirements Document [101]. This work is posited as the best proxy to actual SSN requirements. The researchers considered suitability parameters, associated effectiveness parameters, and performance requirements in their study as listed in Table 7.

Table 7. Space surveillance parameters and requirements [101] .

Suitability Parameters	
All-Weather Accessibility	Multiple Search Capability
24-Hour Accessibility	Correlation Capability (track integrity)
Range Capability (NE, DS)	Routine Accessibility (12 hrs DS/18 NE)
Compatibility	Availability
Connectivity	Dependability
Spot Search Ability	Reliability
Event Search Ability	Responsiveness
New/Lost Object Search Capability	Discrimination Ability (pieces)
Metric Capability (accuracy, precision)	Track Capacity Rate
Basic SOI Capability (fidelity)	Throughput
Enhanced SOI Ability (resolution, fidelity)	Communications Integrity
Small Size Acquisition Ability	Processing Speed
Multiple Object Tracking Capability	
Effectiveness Parameters	
Coverage	Detectability (prob of acquisition/success)
Capacity	Accessibility (operating time)
Responsiveness	
Performance Requirements	
Timeliness	Unambiguity (correct correlations, discrete products)
Quality (accuracy, resolution, fidelity, stability)	Completeness (no lost/unidentified satellites or true UCTs)

Aiding GEO SSA with COTS Telescopes (Moomey, 2015)

Moomey's work on designing an optical tracking network to augment SSN needs has already been detailed. However, during his work he also developed mission requirements to address the AFSPC Commander's goals along with measures of effectiveness, design parameters, and measures of performance. These are depicted in Table 8.

Table 8. SADSS architecural requirements [30].

MR1 System shall be able to create observations with the capability to produce element sets for GEO objects, which are as accurate or more accurate than element sets created using observations from the current SSN (addresses goal 1)

MR	MOE & Effect	Design Parameters & Specifications		MOP
MR1	MOE 1-1 High accuracy sensor metrics	Pixel field of view *2 arcsec (12 micrometer pixel pitch)*	Precision of image time *< ±0.133 sec*	MOP 1-1-1 Sensor sigma
				MOP 1-1-2 Sensor bias
	MOE 1-2 High confidence and accuracy of generated ephemeris	Sun angle limits *0°–100°*	Sensor sigma *Timing precision + imaging precision = 5 arcsec (est.)*	MOP 1-2-1 Orbit solution covariance matrix
				MOP 1-2-2 RMS of orbit solution

MR2 System shall be capable of observing high-value space assets at all longitudes of the geosynchronous belt (addresses goal 1 and 2)

MR2	MOE 2-1 High probability of detection	Aperture diameter *25 cm*	RSO area *≥ 4 m²*	Band avg. CCD QE *75%*	MOP 2-1-1 Detected signal
	MOE 2-1 High probability of detection	CCD Noise *Read 8 e-/pix* *Dark .2 e-/pix/sec*	Sky noise *Diego Garcia + 2vm/arcsec²*		MOP 2-1-2 Detected noise
	MOE 2-2 Large coverage area	Focal length 1.25 m	Film format *30.5 x 30.5 mm*		MOP 2-2 FOV

MR3 System shall be capable of providing persistent coverage for targets of interest anywhere along the geosynchronous belt (addresses goal 2)

MR3	MOE 3-1 Coverage time	Sun angle limits *0°–100°*	Number of sites 5	MOP 3-2-1 Observed orbit
				MOP 3-2-2 Minimum elevation

MR4 System shall be capable of providing near-real-time observations of high-value GEO RSOs to the JSpOC (addresses goal 3)

MR4	MOE 4-1 Increased observation rate	Exposure time *1 sec*	Processing time *< 6.5 sec*	MOP 4-1 Exposure time + Processing time
	MOE 4-2 High astrometry solution ratio	FOV *2°² (1.4°x1.4°)*	Aperture diameter *25 cm*	MOP 4-2-1 no. of stars detected
	MOE 4-2 High astrometry solution ratio	Focal length *1.25 m*	Aperture diameter *25 cm*	MOP 4-2-2 Image distortion

MR5 System shall be capable of providing observations in a format ingestible to its customers (addresses goal 4)

MR5	MOE 5 Successful differential correction	Calibrated data *Requires validation*	Compatible message *GEOSC format*	MOP 5 Residual rejection %

MR6 System shall be capable of providing information useful for determining capabilities and purpose of the observed RSOs (addresses goal 5)

MR6	MOE 6 Actionable information	SNR sample rate *Observation sample rate*	SNR error *Requires customer input*	MOP 6 Quality of light curve metrics

AFSPCI 10-610 Military Utility Assessments (AFSPC, 2019)

AFSPCI 10-610 mandates that Military Utility Assessments (MUAs) be performed when considering augmenting the SSN with commercial data "to determine if any system provides sufficient added value to the SDA mission to justify inclusion in SPADOC, ASW or any other AFSPC-owned SSA system" while "consideration…[is] made for cost, uniqueness, timeliness, throughput, cyber security, and other factors" [59, p. 19]. The criteria used in the MUAs must include [59, Ch. 4]:

- Accuracy: arcseconds (Right Ascension/Dec) for optical tracking and degrees (azimuth/elevation), km (range), and km/s (range-rate) for radar tracking
- Capacity: number of tracks per day, observations per day, and RSOs per day
- Sensitivity: visual magnitude for optical and RSO diameter (meters) for radar data
- Field of Regard (FOR)/Orbit Coverage: steradians of solid angle or percentage of an orbital regime that may be observed
- Search Rate: square degrees per day for a particular orbital regime
- Tasking Responsiveness: data latency of the response to tasking to collect observations on a specific object that is within the sensor's FOV (minutes)
- Unique Capability: qualitative, but can be measured as the number of RSOs or space events for which the sensor provides unique or significantly better data than the rest of the SSN and may include small RSO tracking, low inclination/NE coverage, NE coverage in the southern hemisphere for perigee south orbits, daytime IR for optical systems, unique geographic location, coverage of high area-to-mass ratio RSOs, and persistent track/rapid maneuver detection

- Availability and Reliability: generally measured as the percentage of time the sensor or data source is operational and available for use in SDA operations
- Cost: millions of dollars per year

The MUAs also seek to characterize sensors by compatibility, utility, and quality in order to move away from historically high-quality standards which may not be needed for all mission sets [59, p. 20]. AFSPCI 10-610 also makes a point that "sensors that are tasked by other sources should make every attempt to transmit data at the soonest possible opportunity, preferably within 8 hours of collection, and within 5-30 minutes for high priority objects" [59, p. 64].

Literature Gap

The preceding literature illustrates the need to improve USG SDA processes and the availability, capability, and interest in using non-traditional SDA data. However, no end-to-end study based on system architecting and optimization techniques detailing the outcomes from incorporating non-traditional sensors into the SSN is extant. No AN requirements, MOEs, MOPs, nor measures exist for future architects and decision-makers to use as a foundation for evaluations. No M&S study rooted in optimization, fusing models of SSN sensors with representative commercial and scientific capabilities, and simulating the DS regime has been conducted. No consideration towards selection of competing commercial capabilities based on an analytical framework exists. In short, the USG's best chance to improve its SDA capabilities remains objectively unstudied.

It is noted that contributions by researchers such as Colombi et al., Bateman, Felten, Moomey, and Raley have addressed similar questions. Their work has paved the way for

this study. Raley's demonstration of a true AN represents the spirit of this research, but it failed to capitalize on using measures to track improvements and optimization to fine-tune AN capabilities. Colombi et al. and follow-on researchers conducted thorough research in creating optimal alternative optical networks to the SSN, but failed to consider the more realistic case that the USG will merely augment its existing sensors with non-traditional capabilities due to budget and mission constraints. Their M&S was also limited by considering only the GEO regime; assuming all scheduled observations were in fact collected; and implementing a rudimentary scheduling routine which did not explicitly capitalize on the geographic diversity of the AN. This research adapts Moomey's approach to system architecting and Colombi et al.'s baseline methodology in pursuit of better addressing the future AN possibilities envisioned by Raley.

Several members of the SDA community have acknowledged the need, and expressed their support, for this research. In Jan 2020 this research was discussed with SMEs in a USG SDA SPO who responded decidedly that no one to their knowledge is investigating this subject. Stakeholders working on the CAMO project, the UDL development, commercial SDA providers, and former associates of the DARPA OrbitOutlook program were also solicited and substantiated the research's relevance. A dialogue amongst the body at large at the 2020 Small Telescope Workshop illuminated a prevailing opinion that the USG should be doing more to capitalize on the use of non-traditional capabilities. The following year, upon being briefed on preliminary findings, a representative of a USG SDA SPO and the Chief Executive Officer (CEO) of a commercial SDA company both lauded the approach and results. Clearly, the dearth of literature on

this subject combined with stakeholder interest implies the completion of this research will further understanding of this subject matter.

Summary

This chapter has provided the necessary background and has thoroughly outlined the relevant literature related to the problem. Applications of this literature will become evident in the proposed methodology presented in Chapter III.

III. Methodology

Chapter Overview and Introduction

A thorough literature review has shown the relevance of the SDA problem. This chapter reviews the methodology and covers the seven fundamental steps previously outlined in the Introduction. Figure 18 overviews the approach. The methodology is executed in an iterable manner, depicted in Table 9, such that successive refinements to the baseline are made in publishable increments until the final results are obtained and presented herein. In general, only results from the final iteration are highlighted in this document. One notable exception is a comparison of the final three iterations' results in the Analysis and Results section, presented to show the relative changes as M&S assumptions improve.

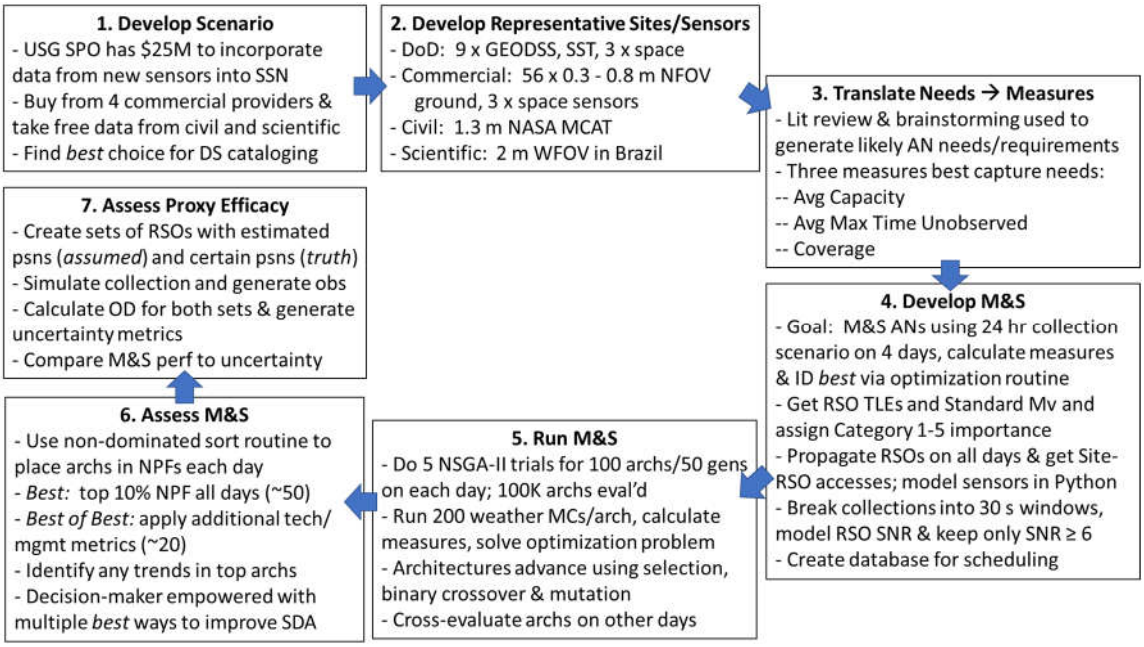

Figure 18. Methodology used to resolve the problem.

Table 9. Major project iterations broken into research aspects.

Iteration (Start Date and Eventual Publication)	Research Aspect																#Cmrcl Ntwks	Perf	Notes
	Orbit Regime			Sensors			Wx	OD	Sim Days				Measures						
	GEO	MEO	HEO	Grd	SST	Sp			SS	VE	WS	AE	Cov	Cap	Time	Std Mv			
1. Jan 2020, Small Telescope Workshop	X			X					X				X	X	X	X	1	Wtd Sum	Also studied how to use scientific collections. Non-Python.
2. Mar 2020, Dayton-Cincinnati Aerospace Sciences Symposium	X			X					X				X	X	X		2	Pareto	Also studied utility of shifting bright collections to commercial.
3. Sep 2020, Advanced Maui Optical Surveillance Conference	X			X					X				X	X	X		3	Pareto	Final ground sites/sensors chosen. Added category weighting to perf measures but proved unhelpful.
4. Dec 2020, Journal of Defense Analytics and Logistics	X			X			X		X	X			X	X	X		3	Normal-ized Pareto Front	Changed coverage to geographic measure and time to include scenario endpoints.
5. Mar 2021, Journal of Defense Modeling and Simulation	X			X	X	X	X		X	X	X	X	X	X	X		4	Normal-ized Pareto Front	
6. Jun 2021, Dissertation	X	X	X	X	X	X	X	X	X	X	X	X	X	X	X		4	Normal-ized Pareto Front	

Step 1. Develop Scenario

Recognizing the need for more SDA data to alleviate near-future burdens, the following scenario is proposed. An SDA SPO is charged with improving the USG's SDA cataloging capabilities. Conscious of the inability to construct new sensors around the world on short order, and knowing the general capabilities of non-traditional sensors, the SPO pursues incorporating data from non-traditional sensors into the SSN architecture. Due to these sensors' prevailing use of optical telescopes for DS tracking missions, only DS RSO tracking is considered.

To maximize control of scheduling and tasking, the SPO decides to purchase fully-taskable sensors from commercial providers and essentially add them as dedicated SSN sensors. Civil and scientific sensors are solicited for their willingness to contribute relevant and/or serendipitous no-cost data to the DoD space tracking mission without influencing OPCON over their tasking and scheduling. The volume of additional data which could be ingested into the current system is assumed to be acceptable, and information assurance

concerns are minimized through direct control of the commercial sensors and agreements with civil and scientific sensor owners/operators.

The SPO is allocated $25M for purchase options; this number is based on a proposed 10% increase to the 2016 GAO estimate of AFSPC's FY2020 budget for new sensors and systems [102, p. 45]. It is assumed four commercial companies with varying capabilities, locations, and costs compete for business while one civil and one scientific sensor each contribute no-cost data; these are detailed in the next sub-section. The sum total to purchase of all commercial options is expected to be well above this threshold, so a selection must be held. In lieu of selecting one single company's proposal for the commercial contribution to the AN, the SPO desires the commercial contributions be formed from some *best* set drawn from all commercial sensors. The SPO must therefore select, in some objective manner, which set of commercial sensors shall comprise the AN while meeting yet-unknown performance requirements and the cost threshold.

This problem is approached using system architecting methods. First, representative capabilities are deduced. The problem then turns to identifying what the SPO values in order to generate AN needs and requirements. The parameters most reflective of the system are next reduced into quantifiable measures. Applying Crawley's approach, a large-scale optimization tradestudy is conducted via a M&S to evaluate many possible architectures, identifying high performers based on the measures. Each architecture is a particular permutation of the AN which includes all USG sensors, all civil and scientific sensors, and some selection of commercial sensors. The end result of the evaluation identifies several strong candidates for the AN which meet needs in different ways.

Step 2. Define Representative Sites and Sensors

Overview

Table 10 summarizes the sensors[12] considered in this study while Figure 19 illustrates the locations. Consult Appendix A for exact technical parameters used in the M&S. The previously-outlined DoD systems are chosen to form the baseline DoD architecture, while one scientific and one civil telescope serve as contributors. Three separate hypothetical commercial companies with several 0.3 to 0.8 m ground-based telescopes, and one hypothetical company possessing three space-based optical assets in near-polar orbit modeled loosely on the Sapphire system, are developed based on representative parameters from open-source literature. The majority of the telescopes are assumed to be Narrow FOV (NFOV) and use a task-based search method with notable exceptions including BIGGO, a WFOV sensor serendipitously collecting on RSOs; SST, a WFOV survey asset; and ORS-5, a fixed-position NFOV collector. Further details on the collection methods are handled in a subsequent subsection.

Table 10. Summary of sensor owners, capabilities, and collection methods.

	DoD					Commercial		Civil	Sci
	GEODSS	**SST**	**SBSS**	**ORS-5**	**Sapphire**	**Co 1,2,3**	**Co 4**	**MCAT**	**BIGGO**
Capability	NFOV 9x 1m	WFOV 1x 3m	WFOV 30 cm	NFOV 10 cm	NFOV 15 cm	NFOV 56x 0.3-0.8 m	NFOV 3x 15 cm	NFOV 1.3 m	WFOV 2 m
Collection	Task	Survey	Task	Fixed	Task	Task	Task	Task	Seren

[12] In general, the words *sensor* and *telescope* are used interchangeably in this discussion and describe the device performing SDA collections.

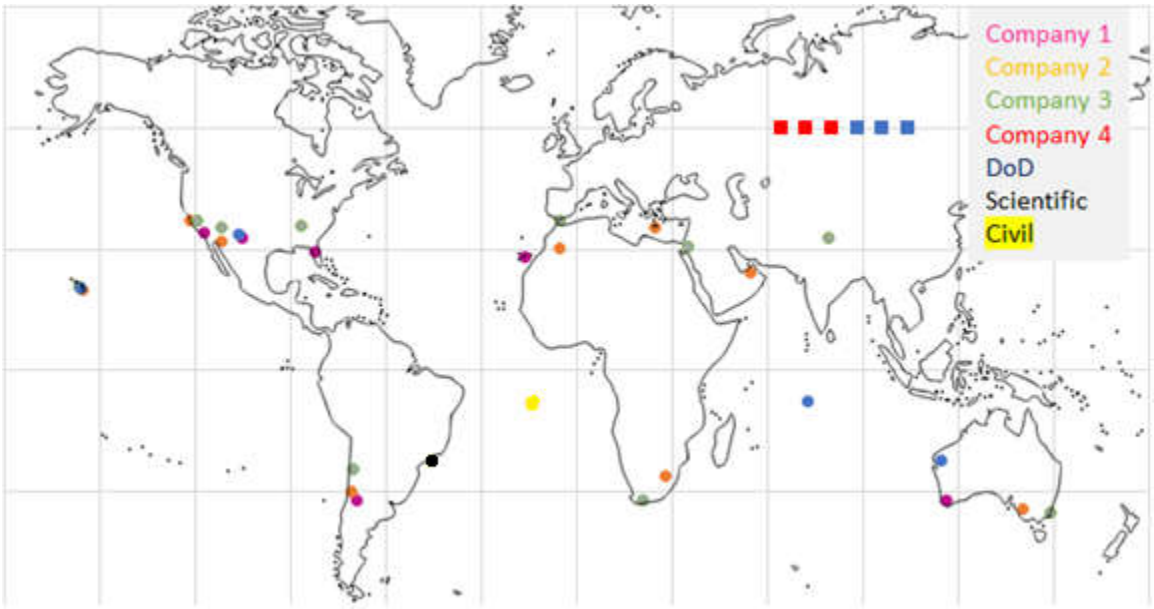

Figure 19. Locations of sensors used in the scenario; ground sensors are spheres while space-based platforms, which are not representative of their true positions, are squares.

DoD Sensors

The suite of ground sensors chosen to represent the DoD include the nine GEODSS sensors and SST. Space-based DoD sensors include ORS-5, SBSS, and Sapphire. These sensors have already been detailed in the Literature Review.

Civil and Scientific Sensors

A sensor similar to NASA's 1.3 m MCAT on Ascension Island is chosen to be a civil contributor, providing information mostly on debris [103]. A hypothetical large-aperture Wide Field of View (WFOV) telescope, the Brazil-Internacional Gigante Global Observatorio (BIGGO), is developed as a scientific contributor which serendipitously collects on RSOs while performing an astronomy mission at a fixed sky position.

Commercial Sensors

Three hypothetical, representative commercial ground-based networks and one space-based network are designed. To aid in the assignment of sites and sensors, four

business cases are developed and summarized in Table 11. Ground sites are chosen using publicly-available locations of commercial SDA sites and sites deemed favorable by other researchers, then allocated based on the hypothetical business cases. Three space-based near-polar satellites are assumed for Company 4.

The space-based platforms' sensors are modeled after those of Sapphire. All ground sensors are determined using the following approach inspired by Ackermann et al.'s COTS study [104]. Market research aggregates various COTS cameras and telescope specifications. Previously-developed equations are used to determine the FOV and plate scale of all possible camera/telescope permutations; a filter is then applied to identify small-aperture NFOV sensors as those with a FOV between 0.5° x 0.5° to 1.5° x 1.5° with apertures between 0.3-0.8 m and plate scales closer to 1 arcsec/pixel. Appropriate telescope/camera options are then allocated to ground sites to fulfill the business cases. Note that many ground sites employ multiple telescopes, while only one telescope is present on each satellite.

Commercial costs are assigned based on estimates of existing capabilities. ExoAnalytic sells its one-telescope capability for $0.5M and its ten-telescope site for $5.5M. Moomey estimates a site of 60 telescopes to cost at least $3.5M. It is logical to assume the companies will charge differently based on telescope capability and locations as well as offer incentives for selecting multiple telescopes. Space-based capabilities are set to cost more due to the fielding and operations cost of space systems as well as their inherent benefits over ground-based collections.

Table 11. Hypothetical company capabilities and business cases.

Company (#Sensors)	Business Case
1 (12)	• Limit number of sites/sensors & use mostly 0.3 m telescopes ($1M) • Offset high costs w/expensive, exquisite capabilities in high-interest locations • Use 0.6 m in Teide, Canary Islands ($1.5M); 0.6 m in El Leoncito, Argentina ($1.5M); and 0.8 m in Perth, Australia ($2M) • A discount of $0.2M is awarded if either all three large telescopes or all telescopes in the network are picked
2 (21)	• Mix 0.3 m and 0.4 m with different FOVs • Charge more for 0.4 m ($0.75M) than the 0.3 m ($0.50M) • Charge $0.25M extra for any site in the southern hemisphere
3 (23)	• Charge a low cost for a standard sensor (0.40 m, $0.50M) • Charge more for its locations in Israel and India (0.6 m in India) • Charge additional $0.2M if multiple sensors are used at one site
4 (3)	• Charge $3M per satellite

Step 3. Translate AN Needs into Measures

Several researchers conducting similar studies noted a lack of requirements as a challenge in vectoring their work. Therefore, potential needs and requirements for the future AN are developed to guide the creation of performance measures, from which some will serve as optimality criteria in the M&S. Moomey's requirements-driven approach to architecting an SDA network is largely adopted. AFSPCI 10-610 MUA criteria are also considered, while holistic findings from other research is incorporated. Several performance measures are identified using this approach. Appendix B reproduces this study.

In keeping with Crawley's approach to system architecting, only a few key measures which are felt to best assess the AN's performance are maintained. Over the project iterations, these measures are reduced from four to three, and recast using different

mathematical formulations until the below are settled on. Cross-review with Daw & Hejduk's study shows the three criteria tie well to SSN effectiveness parameters. The final architectural measures chosen are: *average capacity*, *average maximum time unseen*, and *coverage*. Formulations appear in a subsequent subsection.

Capacity is defined as the number of observations on a particular RSO. The *average capacity* is the average of this quantity amongst all RSOs tracked by an architecture. Greater capacity is more desirable. The maximum[13] time unseen is defined as the maximum time between observations on a particular RSO, while including the endpoints of each scenario. The *average maximum time unseen*[14] merely averages this value for all RSOs seen by the architecture such that a lower value is desirable.

Coverage represents the ability of an architecture's sensors to track regions of the GEO belt with an amount of redundancy[15]. The ±15° latitude region defining the GEO belt is broken into 1° x 1° bins. Each bin is assigned a value based on the number of sensors in the architecture capable of viewing it, then a diminishing returns formula is applied to discourage selecting an architecture with all sensors in one location. SBSS, Sapphire, and the three commercial space-based sensors achieve complete coverage of the GEO belt due to their orbital profiles while ORS-5, a NFOV asset in a circular equatorial plane, is assumed to view only the ±1° latitude region. An architecture's coverage measure is then computed by summing the values in all bins. A larger value is more desirable.

---

[13] AFIT SDA architecting researchers struggle with the measure of central tendency to best quantify this distribution. A maximum is felt to be more useful than an average in this study, because any RSO with even one large observational gap poses an unacceptable SDA challenge which must be minimized.

[14] Previous AFIT SDA researchers, as well as this researcher in past publications, have used the terms *latency* and *Mean of the Maximum Observational Time Gap* as a similar expression.

[15] Coverage was initially defined as the number of RSOs observed by the architecture out of all RSOs simulated, but this proved easily achievable. Because coverage seemed an important measure, it was recast.

Step 4. Develop M&S

Overview

The M&S is represented as the sequence of supporting tasks and an assessment depicted in Figure 20. Fundamentally, the work is driven using various Python-based scripts and routines which pulls together information using Structured Query Language-(SQL-) like joins via the Pandas library; uses the NumPy and SciPy libraries for mathematical computations; employs Python-based routines for optimization, non-dominated sorting, and orbit determination; and makes use of the Numba compiler and the Multiprocessing library for speed enhancements and parallelization. The notable exception includes the generation of astrodynamics information via STK.

Information on all RSOs, sites, and sensors are collated from source material and/or analyst judgement. Data flows into four separate STK scenarios, one for each evaluation day, from which reports are generated. Physics equations are applied to estimate the SNR of all sensor-RSO collections and retain only those meeting a threshold. Several tasking and scheduling routines are then employed to create a master list of observations, which are then recast as lookup matrices. A series of Monte Carlo simulations to be run on each architecture are devised by using cloud-based probabilities. The assessment is detailed in the next subsection. Note that fundamental assumptions, equations, and references for modeled quantities have been previously detailed in the Literature Review, hence they are only highlighted in this portion.

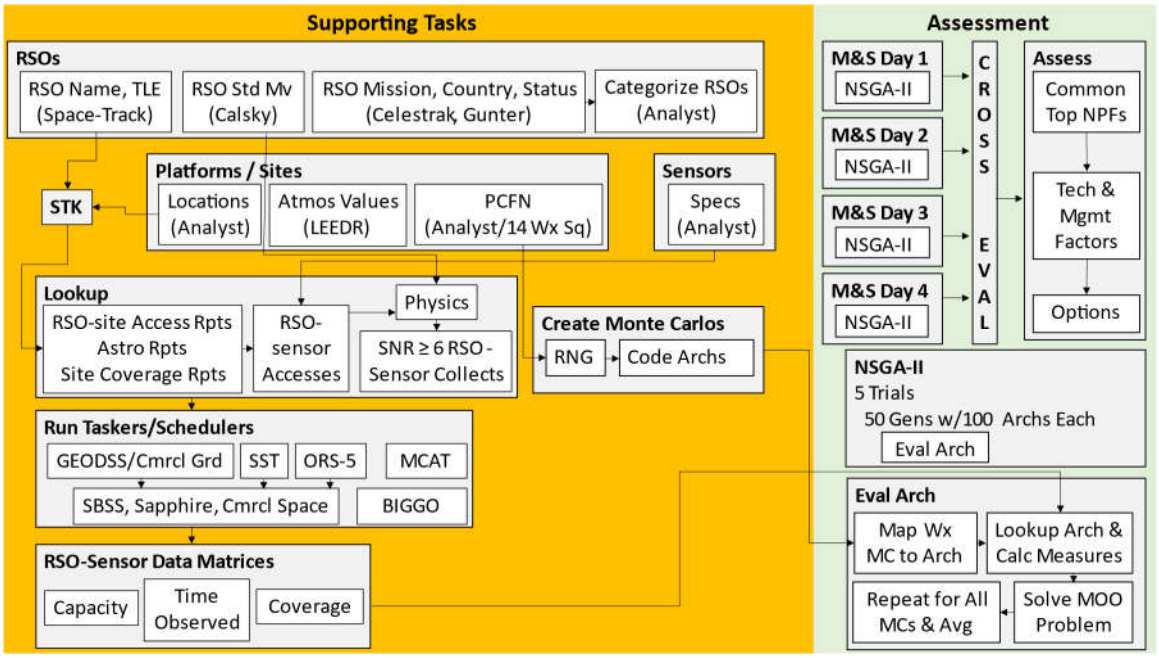

Figure 20. Core M&S codeflow; supporting tasks are completed prior to the assessment.

Model RSOs

954 GEO, 244 MEO, and 189 HEO RSO TLEs are pulled from Space-Track on 7 Mar 2020 for a total of 1,387 simulated RSOs. Figure 21 shows this distribution as plotted by inclination vs semi-major axis. RSO brightness is pulled from the Calsky webpage's $M_{v_{RSO,std}}$ data when available or inferred from other sources[16]. RSOs are then categorized in a Category 1 to Category 5 ranking system, where Category 1 is most important, in proportion to values previously cited in Dararutana's work. This ranking is based on the researcher's judgment and is informed by each RSO's country of origin, mission, mission

[16] All GEO values were pulled from Calsky, but the site's unexpected closure in Sep 2020 before the research incorporated MEO and HEO RSOs necessitated an alternate source for these values. When possible, data from the Heavens-Above and N2YO databases were used. Values for the remaining RSOs were inferred from extant values based on similarity in orbit regime, constellation, mission, owner/operator, and/or bus. Future researchers are cautioned to find an alternate source or to model brightness differently.

status, and other factors ascertained from online databases. In general, RSOs perceived to be of more interest to the USG are ranked more importantly.

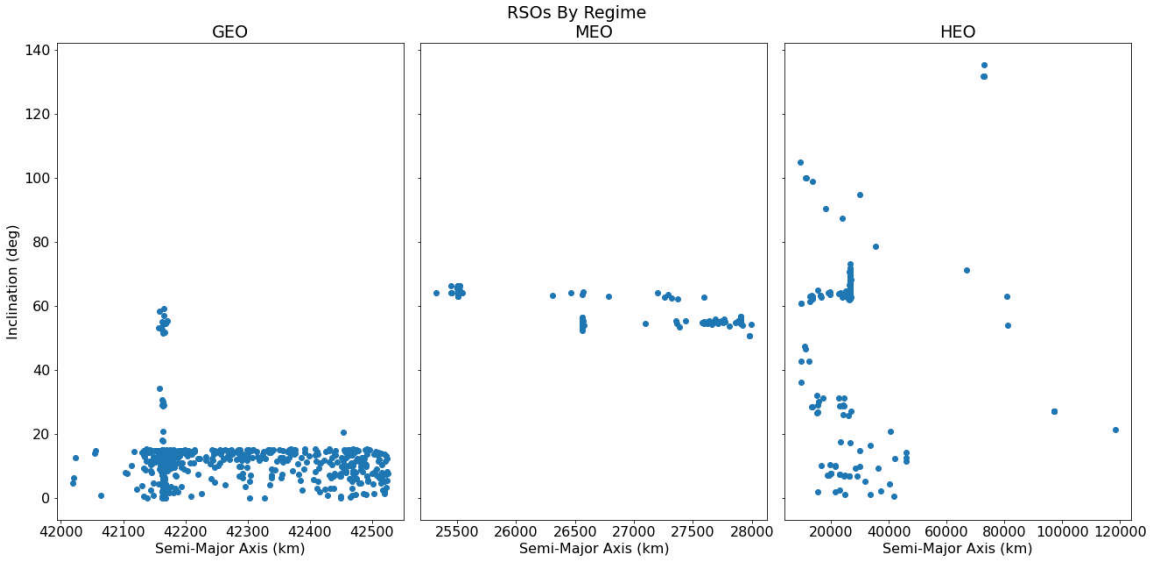

Figure 21. RSOs in GEO, MEO, and HEO as plotted by orbital parameters.

Four evaluation days, requiring four STK scenarios, are chosen: Vernal Equinox (VE, 20 Mar), Summer Solstice (SS, 21 Jun), Autumnal Equinox (AE, 23 Sep), and Winter Solstice (WS, 22 Dec). These dates are chosen to test architectural performance in all seasons as well evaluate stressing conditions. RSO TLEs are imported into each scenario. Because the TLEs are pulled from a single day, the true anomaly is modified for each day so as to generate unique comparative data. RSOs are set to be propagated using the Two-Body Propagator (2BP) which assumes perfect propagation using equations of motion without covariance information.

Model Sites

Ground sites are input into STK based on latitude and longitude and constrained to operate only in umbra and track RSOs at an elevation $\geq 20°$. The DoD space-based collection platforms are input using TLEs obtained from Space-Track while the three

Company 4 commercial satellites are represented by adding three evenly-spaced RSOs in one circular, 575 km altitude orbit inclined at 86.4°. Both ground and space-based platforms are constrained to a solar exclusion angle of 40° and a lunar exclusion angle of 10°. Sensors at each site and space-based platforms are handled in Python and detailed in the next subsection.

Physical quantities at all sites are estimated. Atmospheric transmittance and extinction values for ground sites are estimated using AFIT's Laser Environmental Effects Definition and Reference (LEEDR) software. Nighttime values in three-hour blocks using the summer and winter models are returned, which are later used in a join on observational data. A standard background radiance of 21 M_v/arcsec^2 on a clear moonless night is assumed for all ground sites, and lunar contributions are modeled using Krisciunas and Schaefer's work. Space-based sites employ lunar and zodiacal models posited by Dressel.

Run Lookup and Model Sensors

An assumption is made that all collections require 30 seconds to settle, take observations, and slew to the next target. This allows each day to be broken into 2880 finite intervals, greatly simplifying the scheduling discussed later. Reports outlining astrodynamically-possibly access times, azimuths, and elevations from every site and space-based collection platform to every RSO in 30 s increments are output via calls to STK Connect in a Python script. Various other reports estimating ranges, angles, and angular velocities necessary for the physics portion are also generated. Lastly, to create the coverage metric the FOR of each sensor is inferred by a custom report binning the world into 1° x 1° regions and denoting all viewable regions.

The reports are amalgamated into databases which allow for easy SQL-like operations using Python's Pandas library. Sensor information is then considered by using the underlying site reports and applying previously-derived technical parameters and the physics of the problem. Two modifications to that approach are applied. Equations with integration time t_{int} are modified to accommodate transit time t_{sig}, and a per-pixel SNR is calculated in lieu of managing the number of pixels in each sensor's aperture such that n_p in all calculations is effectively one. Each sensor-RSO access' SNR is calculated by estimating the RSO's brightness and accounting for environmental, sensor, site, and detection parameters. Only those accesses with an acceptable SNR are retained, thus leaving a pool of feasible collections for scheduling. Figure 22 illustrates the process.

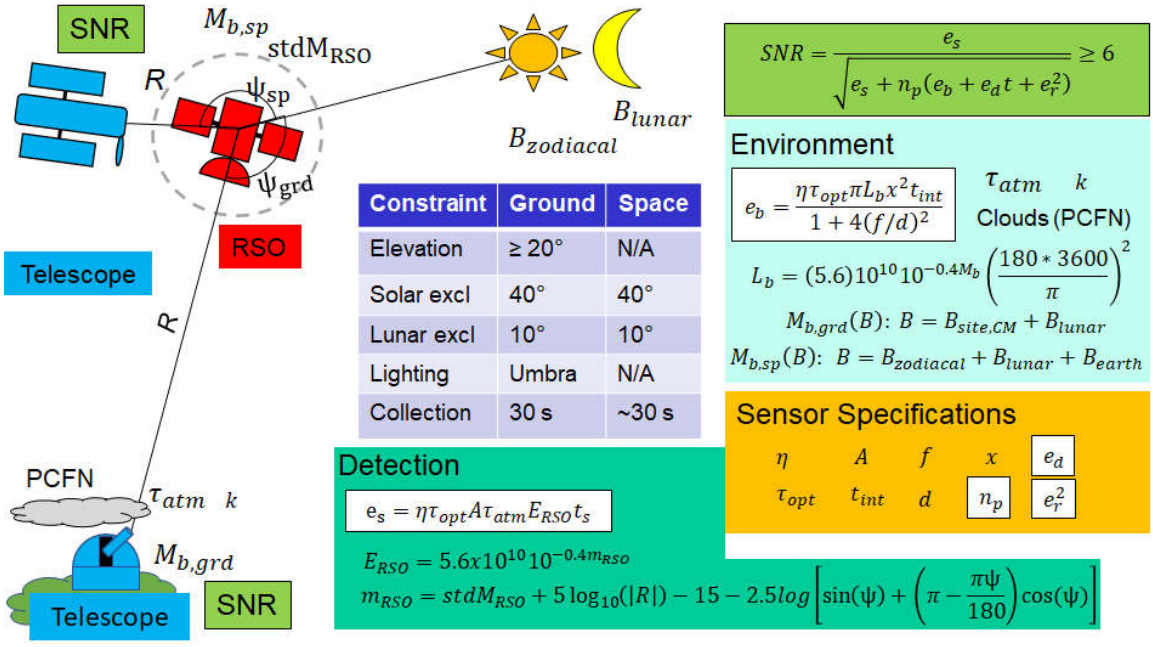

Constraint	Ground	Space
Elevation	≥ 20°	N/A
Solar excl	40°	40°
Lunar excl	10°	10°
Lighting	Umbra	N/A
Collection	30 s	~30 s

Figure 22. Physics calculations in the problem, which drives towards finding SNR.

Schedule Observations

Research shows the SSN employs a centrally-tasked, decentrally-scheduled approach to sensor management, such that each sensor is free to choose its own scheduling routine. This approach is moderately adhered to, sidestepping the employment of a mathematically-rigorous scheduling program to return reasonable results using some amount of randomness. Figure 23 outlines the approach.

Prior to discussing this implementation, one major assumption must be highlighted. Ideally, the scheduling routine would be run on every one of the thousands of individual architectures evaluated. However, computational constraints and the lower order of complexity of this architecting study prompts an alternative approach. In lieu of scheduling each architecture individually, all possible sensors in the scenario are scheduled once on each day. This forms a master database from which a particular architecture under evaluation pulls only observations from those sensors in the architecture. This process, while imperfect, is computationally-efficient and is still suggestive of using a different scheduler, as different architectures will in fact pull different observations.

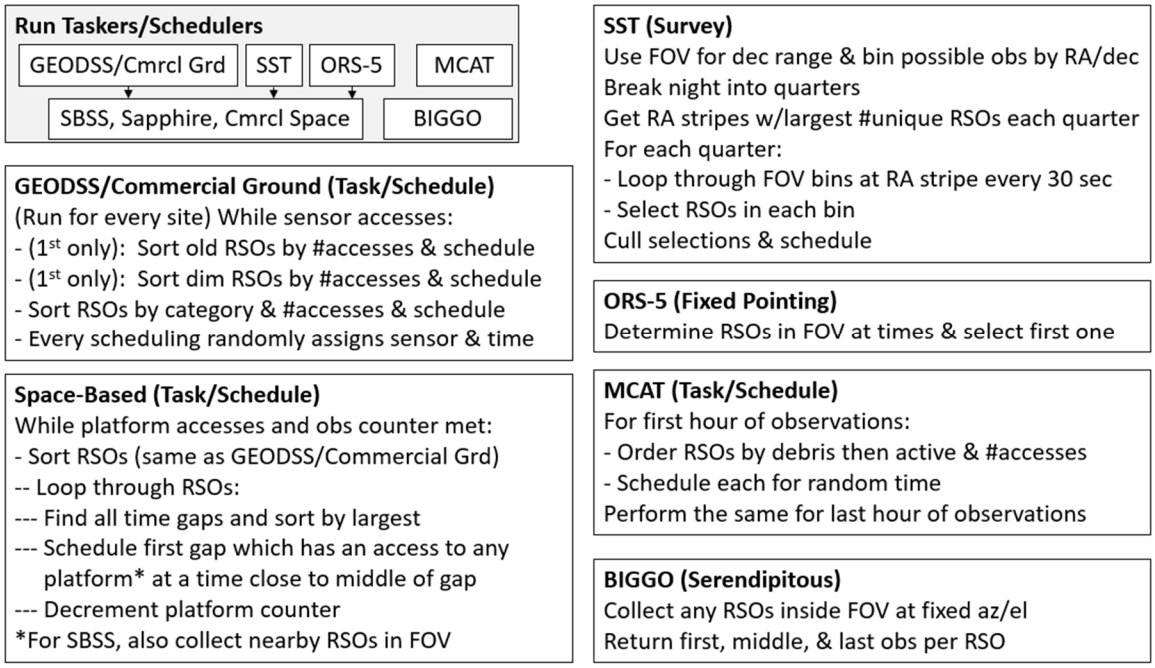

Figure 23. Tasking and scheduling approach.

GEODSS and the commercial ground sensors are scheduled in tandem, and flow into collections for the taskable space-based platforms along with SST, which uses a survey method, and ORS-5, which has a fixed pointing collection regime. This process is enacted because the limited accesses of taskable space-based assets are felt to be best used to reduce the maximum time between observations for RSOs, which can only be accomplished after some scheduling order exists. Both MCAT and BIGGO employ their own collection techniques. Each assumed technique is discussed next in-turn.

The GEODSS/commercial ground routine conducts prioritized, geometrically- and temporally-dispersed collections of all RSOs. Sites are scheduled in parallel, and all sensors at a site are scheduled in each parallel evaluation. RSOs are ordered based on the five categories; on the first iteration only, RSOs with very old epochs as identified from TLE data and those with a dim luminosity are processed first. Each grouping is further

sorted to encourage scheduling of RSOs with fewer remaining accesses first. Upon encountering an RSO, the routine schedules the collection for a random time on a random sensor at the site, then removes the sensor-time availability for future use. The routine continues until no accesses are available.

SST's WFOV survey capabilities are simulated using a modified stripe collection routine adopting aspects from Frueh [105]. The sensor is pointed at a fixed topographic right ascension (RA) range and the FOV is cycled in declination over time such that any RSOs present in the FOV cell are collected. The night is broken into quarters, and projected data is used to determine the RA stripe with the largest number of unique RSOs collected each quarter. The routine cycles through FOV cells every 30 s at the specified RA stripe each quarter, simulating potential collections. Due to known data transmission limitations of SST, collections on specific RSOs are reduced by only collating observations spaced at least 60 min apart.

ORS-5 is a NFOV, fixed-pointing collector. A small conical sensor is added to the ORS-5 model in STK, allowing for reports to output sensor-RSO accesses. In the case of multiple RSOs being accessible during a 30 s interval, only the first RSO is selected to be consistent with the assumption that NFOV sensors may only view one RSO at a time. Upon completion of the three routines, all data is combined and used to inform the following space-based tasking and scheduling.

The space-based routine is explicitly designed to use the limited space-based assets, which are unhindered by terrestrial considerations, to reduce the average maximum time RSOs go unseen. RSOs are sorted in a manner similar to the GEODSS/commercial scheduler, then assessed via a loop. For each RSO, the durations of time unseen are

identified, and the largest are prioritized. The first space-based sensor which is available and capable of collecting on the RSO at a time close to the middle of the duration is selected. A further constraint is placed on the sensors to simulate the realities of onboard storage capacity and downlink speeds expressed in literature by capping the maximum number of observations to 3000 for SBSS and 400 for all other space-based platforms [52]. Additionally, since SBSS is a WFOV asset a minor modification is made to account for serendipitous collections by adding observations taken on RSOs within a portion of its FOV.

MCAT, a multi-mission contributing sensor, is scheduled by assuming only the first and last hours of possible collections are dedicated to RSO monitoring. During each hour RSOs are ordered by inactive then active mission types, grouped by the number of accesses, and scheduled for a random time. BIGGO, the serendipitous scientific contributor, is pointed at a fixed azimuth and elevation for the entire 24-hour duration on the four days under study. Any RSOs passing through the aperture are assumed collected; as the collections occur over a long time interval, only the first, middle, and last observations on each RSO are returned.

Upon completion of all routines, a master scheduling file is developed which holds the site/platform, sensor, RSO, and collection time information. The data is reshaped into Python matrices and/or databases to allow quick calculations during the M&S.

Simulate Weather

To simulate the effects of clouds, several Monte Carlo simulations are run on the architectures. Different conditions are simulated by merely blacking out sites for an entire night if randomly-generated numbers exceeds a threshold. This threshold, the Probability

of Cloud Free Night (PCFN), estimates how many nights in a particular month have low cloud coverage at a location, thus representing acceptable telescope collections. The measures are derived using 30 years' of METAR data made available by the 14th Weather Squadron[17]. Data from stations closest to the ground sites are pulled. At each ground site, data for every night in a particular month across all years is evaluated, e.g. all nights in January from 1990 to 2020. Sky okta measurements from hourly reports are interpolated to determine an average cloud coverage each night. Any night with an average sky coverage of less than five oktas, or about half the sky clear most of the night, is assumed cloudless enough to collect observations. The PCFN measure is thus the number of cloudless nights out of all nights considered that month at the site[18], where larger numbers indicates the site at that time of year will more likely have cloud-free conditions.

Each Monte Carlo effectively computes a random number for every site in the M&S, compares it to the PCFN, and if the thresholds are not met all sensors at the affected sites are assumed to be blacked out for that Monte Carlo. In other words, multiple ways a 24-hour weather scenario may unfold are modeled and applied to architecture evaluations, turning sites off if conditions are simulated to be too cloudy.

Two different methods to determine the appropriate number of Monte Carlos are employed, both of which test a small set of architectures using 10,000 Monte Carlos with

[17] The cloud modeling approach used by previous AFIT researchers employed the PCFLOS for this estimate; however, since LEEDR is only able to generate these values for actual observatories with available empirical data, missing values were supplemented with mean annual cloud coverage data from ISCCP. This was felt to be inappropriate for this study, so various alternate options were considered. The approach taken is felt to better model the parameter as well as avoid the need to parse massive data files presented by other options.
[18] This concise summary belies the challenge of processing thousands of reports generated at non-standard times while handling errors and missing data. Although not an insurmountable challenge, this portion of the M&S may be reduced if a better metric or an extant, easy-to-use, relevant database is identified.

that assumption that a large number of simulations better approximates the problem. Oberle's percent error formula determines that, for a 95% confidence interval ($z = 1.96$) and a two percent error ($\varepsilon = 2$), at least 90 Monte Carlo simulations are necessary. A second calculation to illustrate the percent change of the measures' averages as the number of Monte Carlos is increased shows the point at which the percent change is consistently less than 0.5% occurs with 200 simulations. 200 Monte Carlos are felt to be appropriate, such that a list of 200 distinct permutations is generated for each day and applied to every architecture in the M&S, then results are averaged per architecture.

Step 5. Execute M&S

AN architectures are composed of the DoD, civil, and scientific sensors plus some set from the 59 sensors in the four commercial networks. This choice may be represented as a string of sensors which are either used or not used, naturally cast as a binary chromosome in a GA. A heuristic method is needed to evaluate the large tradespace of 10^{17} possible architectures and identify high-performing options in a reasonable amount of time. NSGA-II is selected due to its acceptance in the greater optimization community; use in similar problems; and its availability in the open-source Inspyred Python package.

Five NSGA-II trials are run on each day, in which 50 generations of 100 architectures each are executed. The number of generations is chosen after simulations of different sizes showed this to be an appropriate number. The population size is set to 100 per previous recommendations in literature. In all, 25,000 architectures are evaluated each day, for a total of 100,000 total evaluations.

Each trial begins with 100 random feasible architectures; feasibility is ensured by adding to the set only those architectures meeting the cost constraint of $25M. The cost is computed using a lookup based on the commercial sensors and prices determined in the business cases. Each architecture is evaluated using the weather Monte Carlos, evaluating 200 individual architectures by changing certain *1* bits in the chromosome into *0*, and returning the average to the optimizer. The pseudo-optimization problem solved is

$$
\begin{aligned}
Maximize\ c &= \begin{cases} \frac{1}{m}\sum_{j=1}^{m}\left(\sum_{b=1}^{b}\left(\sum_{s=1}^{s}\frac{1}{s}\right)\right), & d \le 25 \\ penalty, & d > 25 \end{cases} \\
Maximize\ \bar{p} &= \begin{cases} \frac{1}{m}\sum_{j=1}^{m}\left(\frac{1}{n}\sum_{i=1}^{n} r_i\right), & d \le 25 \\ penalty, & d > 25 \end{cases} \\
Minimize\ \bar{l} &= \begin{cases} \frac{1}{m}\sum_{j=1}^{m}\left(\frac{1}{n}\sum_{i=1}^{n} \max\left(\Delta t_0 \ldots \Delta t_f\right)\right), & d \le 25 \\ penalty, & d > 25 \end{cases}
\end{aligned}
\tag{3.1}
$$

where c is coverage, s is the sensor capable of observing the 1° x 1° bin, b represents all bins covering the GEO belt, m is the number of Monte Carlos, d is the cost in millions of dollars, $\bar{p}$ is average capacity, r_i is the observed RSO, n is the total number of RSOs observed by the architecture, $\bar{l}$ is the average maximum time unobserved, and Δt represents all unobserved durations for each RSO. A large penalty is applied if the $25M cost constraint is exceeded, making the value unfavorable to the optimizer.

The underlying values are computed by conducting operations on efficient arrays containing schedule-derived data. All values returned to NSGA-II are internally evaluated using a Pareto routine. The next generation is determined through selection, cross-over,

and bit-flip mutation. The process continues until the number of generations is reached. The final result is four databases, one for each day, listing the architecture evaluated on that day, performance measures, and cost.

An assumption is made, along the lines of Epoch-Era Analysis, that top-performing architectures are those which perform very well on all four days. However, due to the inherent randomness of NSGA-II and the large tradespace the same architectures are not in fact evaluated on all four days. To permit a fair comparison, a cross-evaluation stage is needed in which all architectures evaluated on one day in the M&S are ideally evaluated on all other days, without the need to employ NSGA-II. However, this is time-prohibitive and would result in cross-evaluation of many nonvaluable architectures, because cross-evaluating a poor-performing architecture is wasteful. Therefore, Blank & Deb's non-dominated sort routine from Pymoo[19] is applied on each day's architectures to determine those in the top 20% of fronts, and only these high-performers are cross-evaluated on all other days. This results in around 14,000 architectures available for comparison.

Some discussion on the code routine is warranted. The routine encapsulates around a dozen Python scripts, most of which construct or otherwise pivot the supporting data discussed in Steps 1 through 4. The actual optimization script makes use of Python's Multiprocessing library to evaluate individual architectures in parallel on a multi-core workstation, while employing the Numba[20] just-in-time compiler on numerically-intensive

[19] Blank & Deb's freely-available source code is modified in lieu of executing in Pymoo. Although there are several code routines available, this is amongst the few which enable easy output of Pareto fronts per architecture. Note that this routine as-written requires a substantial amount of RAM for array allocation.
[20] Numba is a nearly drop-in library for Python which substantially speeds code routines on the order of 20x. Despite notable limitations, it is possibly the best technique for speeding numerically-intensive code and should be considered by any Python adherent. Timely completion of the proxy efficacy portion of this research would not have been possible without the combination of Numba and parallel processing.

portions for speed increases. Completion of a single NSGA-II trial requires 2-3 hours. The end-to-end time to runtime all evaluations and cross-evaluations is around one week.

Step 6. Analyze M&S Results

To aid in comparison between days, the Normalized Pareto Front (NPF) concept is developed. A non-dominated sort is applied to place the 14,000 comparative architectures in Pareto fronts on each day. The fronts are normalized by the total number of fronts f of that day such that the best architectures are on front $1/f$. Top performing architectures are defined as those in the top 10% of fronts on all days, such that NPF ≤ 0.1 on all four days. Analysis is discussed in the next section.

Step 7. Assess Efficacy of Proxy Measures

While results of the core M&S identify top-performing architectures, it is insightful to determine if the best-performing architectures do in fact attain a major objective of fielding an SDA network, which is knowing the orbital positions of RSOs with a low uncertainty. The null hypothesis is formed that better architectures found in the core M&S will have lower architectural-wide positional uncertainty. Should this be shown true, it implies the architectural performance measures are a fair proxy for attaining a key technical consideration without the need to explicitly conduct orbit determination, a challenging and at times computationally-intensive requirement. To test this claim, the performance of all architectures found from the core M&S are compared to the aggregate positional uncertainties found in the study. Figure 24 outlines this approach while Figure 25 shows the codeflow.

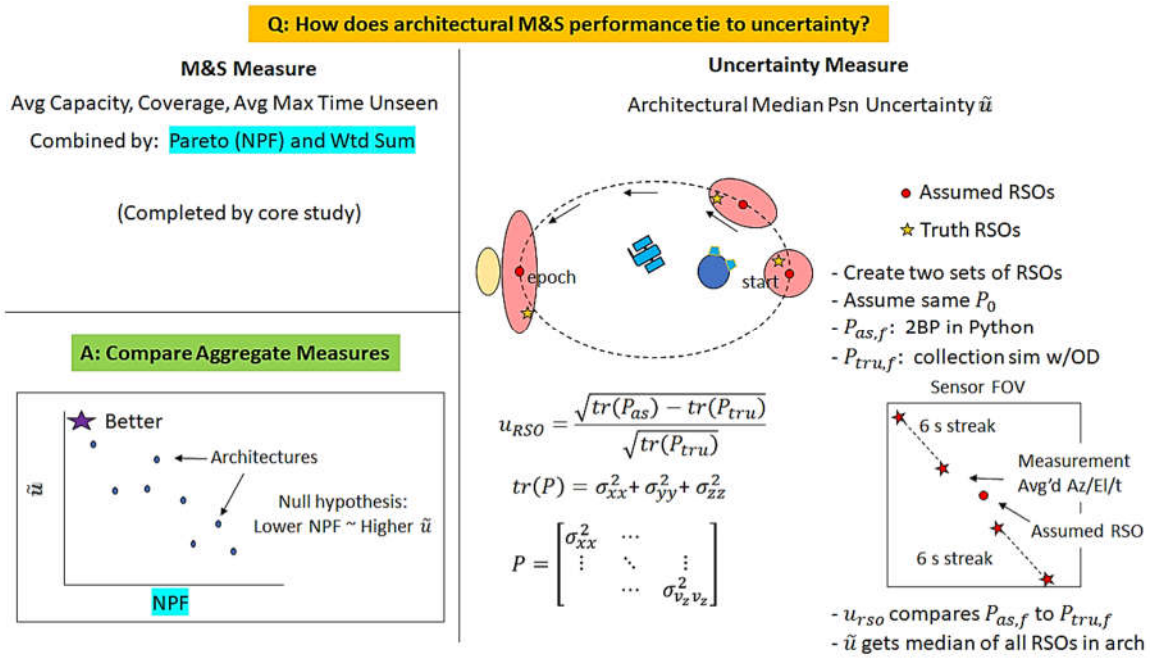

Figure 24. Proxy study approach, where M&S and covariance values are compared.

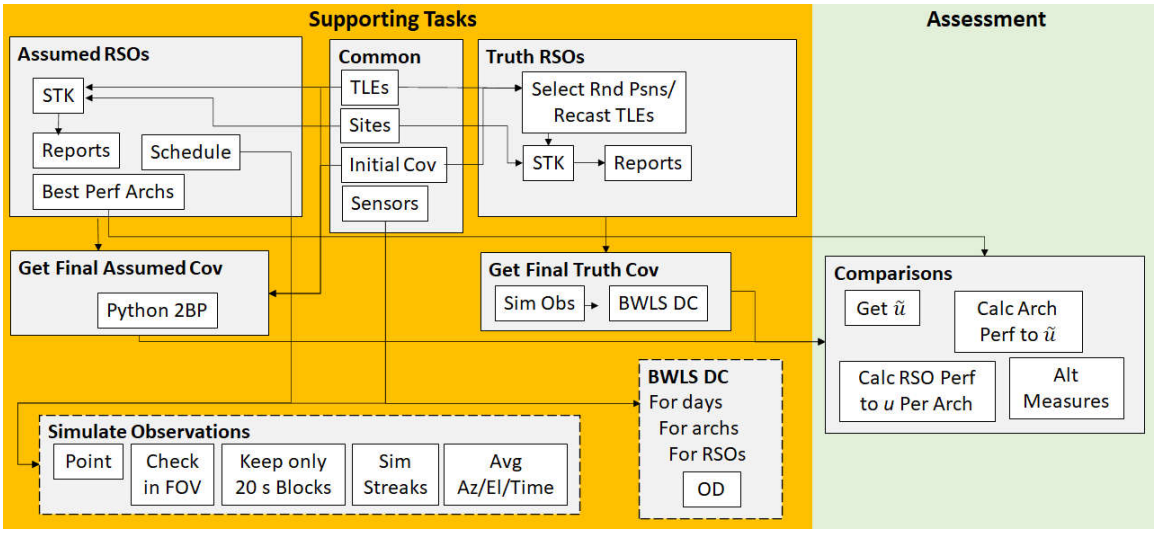

Figure 25. Proxy study workflow, where *assumed* and *truth* covariances are calculated.

On each day, for each architecture, the positional uncertainty of RSOs as measured by *assumed* and *truth* data are calculated and compared. The *assumed* set of RSOs use the reports, schedule, and quantified architectural performance generated from the core M&S. An initial covariance for both sets is set using a spherical covariance based on the largest

positional element from Floeher's assumptions. The *assumed* set is propagated to the end of the day using a Python-based Two-Body Propagator and final covariances retained. The *truth* set of RSOs is intended to simulate the true positions of all RSOs, and is generated by setting a random position inside the covariance of all RSOs, recasting the new state vectors, and outputting reports in STK. This results in two separate databases with azimuth, elevation, and time information for RSO locations from the *assumed* set and actual locations from the *truth* set as measured from all sensors.

A collection routine is simulated to ascertain observational data needed for the *truth* set covariance calculation. All sensors use the core M&S schedules and are assumed to center their FOV on the *assumed* RSO position. Recall that the core M&S allocates 30 s for every collection. The *truth* RSO positions during the collection times are determined each second, and only those RSOs inside the FOV for at least 20 uninterrupted seconds are kept. Astronomical streak data is insinuated by pulling azimuth and elevation at the endpoints of two six-second intervals separated by a six second pause. Azimuths and elevations are averaged to represent one observation at the start of the second streak, such that only one observation is reported for each scheduled access. In the end, a master database of all observations containing sensor, RSO, azimuth, elevation, and time information is created.

Vallado's BWLS Differential Correction routine is utilized to calculate the final covariance information for the *truth* set[21]. The routine ingests the observational database

[21] Vallado's routine is chosen after reviewing alternatives such as Orbit Determination Tool Kit (ODTK), Orekit, and various Python and C++ routines. This option offers the best balance of execution speed, adaptability, low learning curve, parallelizability, and credibility. However, it requires manually porting to Python. A future researcher is cautioned that adapting Vallado's routines requires enacting many code optimizations and advanced techniques such as Numba and parallelization if speed is essential.

and, for each architecture of interest, pulls data only from sensors in the architecture before running the OD routine on each RSO. Representative sensor noise and biases are incorporated in the weighing process. With both sets' covariance information available, various comparisons are run to test the null hypothesis, which are presented in the next section.

The uncertainty metric per RSO u_{RSO} is formed to quantify the positional uncertainty in terms of both the *assumed* and *truth* covariance values. It is defined as

$$u_{RSO} = \sqrt{\frac{tr(P_{as}) - tr(P_{tru})}{tr(P_{tru})}}$$

where P is the covariance matrix. A larger u_{RSO} equates to a lower uncertainty[22]. For architectural-level comparisons, a review of the data suggests a median is appropriate; therefore, the median architectural uncertainty $\tilde{u}$ is devised to permit direct comparison to the architectural performance found in the core M&S.

Computational requirements to complete the *assumed* portion of this assessment are minor, while those of the *truth* portion are substantial. Simulating the *truth* RSOs effectively duplicates most of the core M&S supporting work, including the generation of multiple large-sized databases, and combined with the OD routine imposes additional software architecting and database management challenges. Completing Vallado's routine for one day on all 14,000 architectures requires at least one week after highly-optimizing

[22] This creates unintended confusion in the study, as a lower aggregate positional uncertainty is the desire but the metric u as formulated posits higher values as better achieving this. This metric was chosen after comparing various alternate formulations, which found others reported differences beginning at the 1e-5 level, while the current approach returns more relatable values.

the underlying routine, incorporating Numba's speed enhancements, and parallelizing the problem.

One major omission during this routine is the handling of weather parameters during the uncertainty calculations. To permit a fair comparison between architectural performance derived from the core M&S, which relies on averaged data from Monte Carlo-evaluated architectures, all architectures require enacting a similar plan to omit data from clouded-out sensors in Vallado's routine and return an averaged architectural uncertainty measure per architecture. As before, this requires evaluating each architecture 200 times. Regrettably, the greater computational time required for the uncertainty routine makes this untenable, adding a caveat to the final conclusions. One alternative assessment which sidesteps weather calculations in both portions, however, is undertaken and described in the Analysis and Results section.

Summary

This chapter has outlined the methodology. The seven-step process fully explores the questions at hand. Analysis and results found by executing this plan are discussed in the next chapter.

IV. Analysis and Results

Chapter Overview

With the problem and methodology understood, the data is interpreted with analytical conclusions. Foundational work and analysis are completed on an Intel Core i5 Sandy Bridge laptop with four logical cores and 8 GB of RAM operating at 2.5 GHz. The majority of analysis is completed using Python and the Pandas, NumPy, and SciPy libraries with Matplotlib and Microsoft Excel used for graphical output. Computationally-intensive tasks in this and the previous steps are executed on a Xeon Sandy Bridge workstation with 32 logical cores and 56 Gb of RAM operating at 2.0 GHz. The end-to-end computational time required to complete the core M&S is around one week, while the architectural performance/position uncertainty efficacy study requires an additional 7-10 days. Intermediate data generation, margin to re-execute incorrectly handled portions, and interpretation requires at least one additional week.

Results from Core M&S

General Results

Of the 100,000 total architectures evaluated, only 69% are feasible due to the cost constraint. Results for the 14,000 architectures evaluated on all four days are collated. Figure 26 illustrates the results on Vernal Equinox, where the average maximum time unobserved and average capacity are plotted and a color spectrum depicts coverage. The highest performers are those towards the bottom right colored purple. Clustering or sparse data is observed in the distribution. Results on the other days are holistically similar.

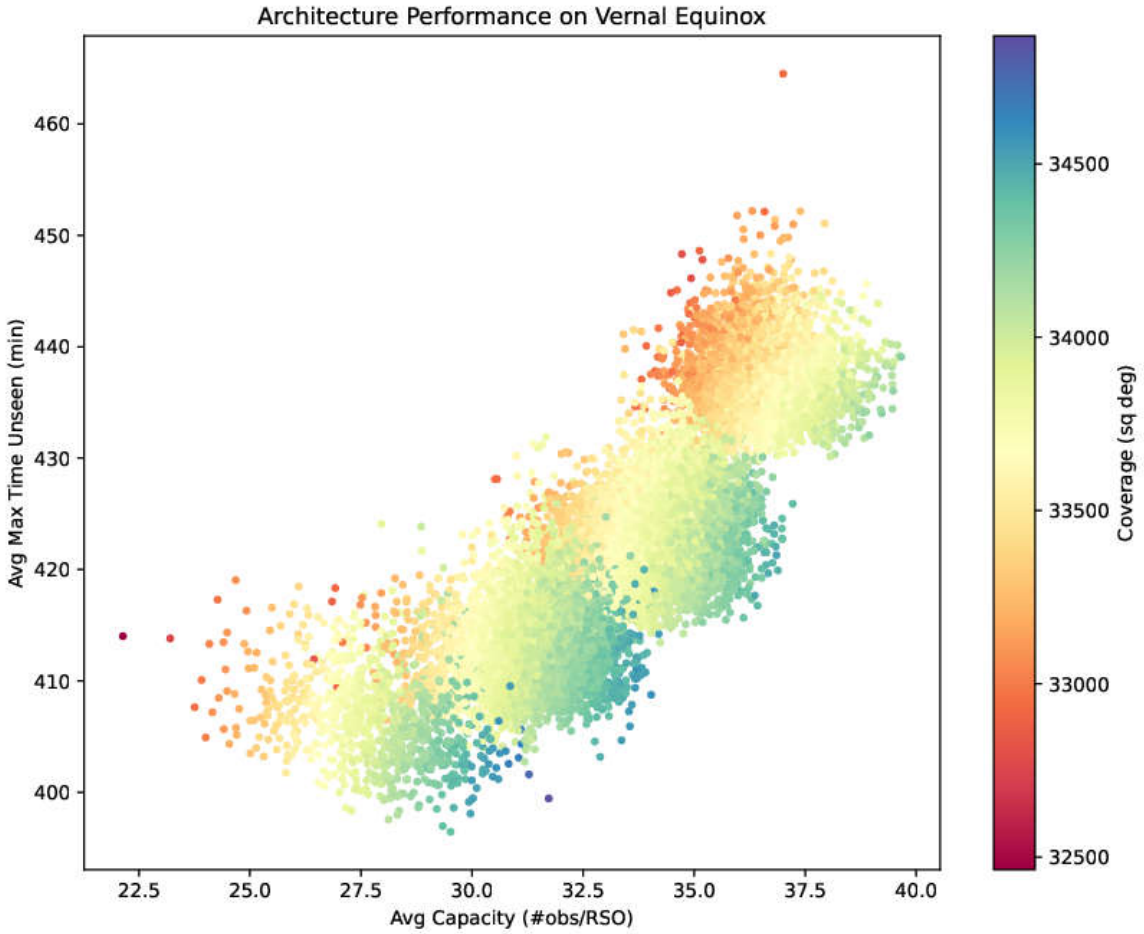

Figure 26. Architectural performance on Vernal Equinox.

To conceptualize the difference in performance on multiple days, Figure 27 plots individual architectures' NPFs on Vernal Equinox and Summer Solstice. Similar performance on both days occurs when an architecture's ratio of NPFs is near one, such that the points are closer to the equality line. Best architectures on the two days are defined as those with NPFs ≤ 0.1 on both days, shown in the circled region. Lastly, architectures are color-coded by cost which shows that better-performing architectures approach the $25M cost constraint. The graph indicates many architectures do not have similar performance on both days and that better performance costs more.

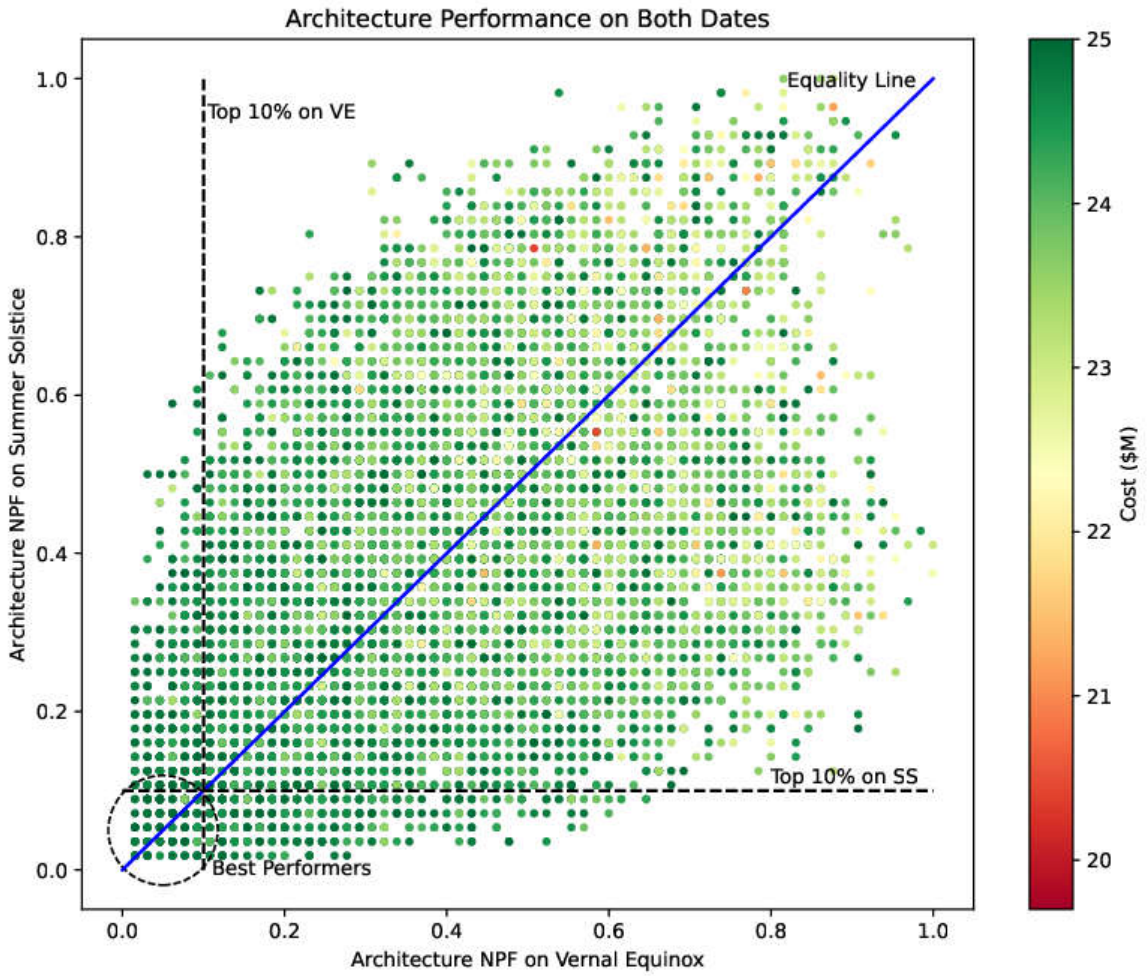

Figure 27. Architectural performance on Vernal Equinox and Summer Solstice.

Best Performers

As noted previously, *best* performers are defined as those architectures with top 10% NPFs on all four days studied. Only 59, or less than 0.5% of the 14,000 comparative architectures, meet this threshold. Figure 28 illustrates the performance of these architectures; seasonally-dependent trends are evident. On average, the best performers have 33-35 average observations per RSO, with RSOs going unseen for an average maximum time of 6.6-6.9 hours while achieving redundant coverage of the GEO belt.

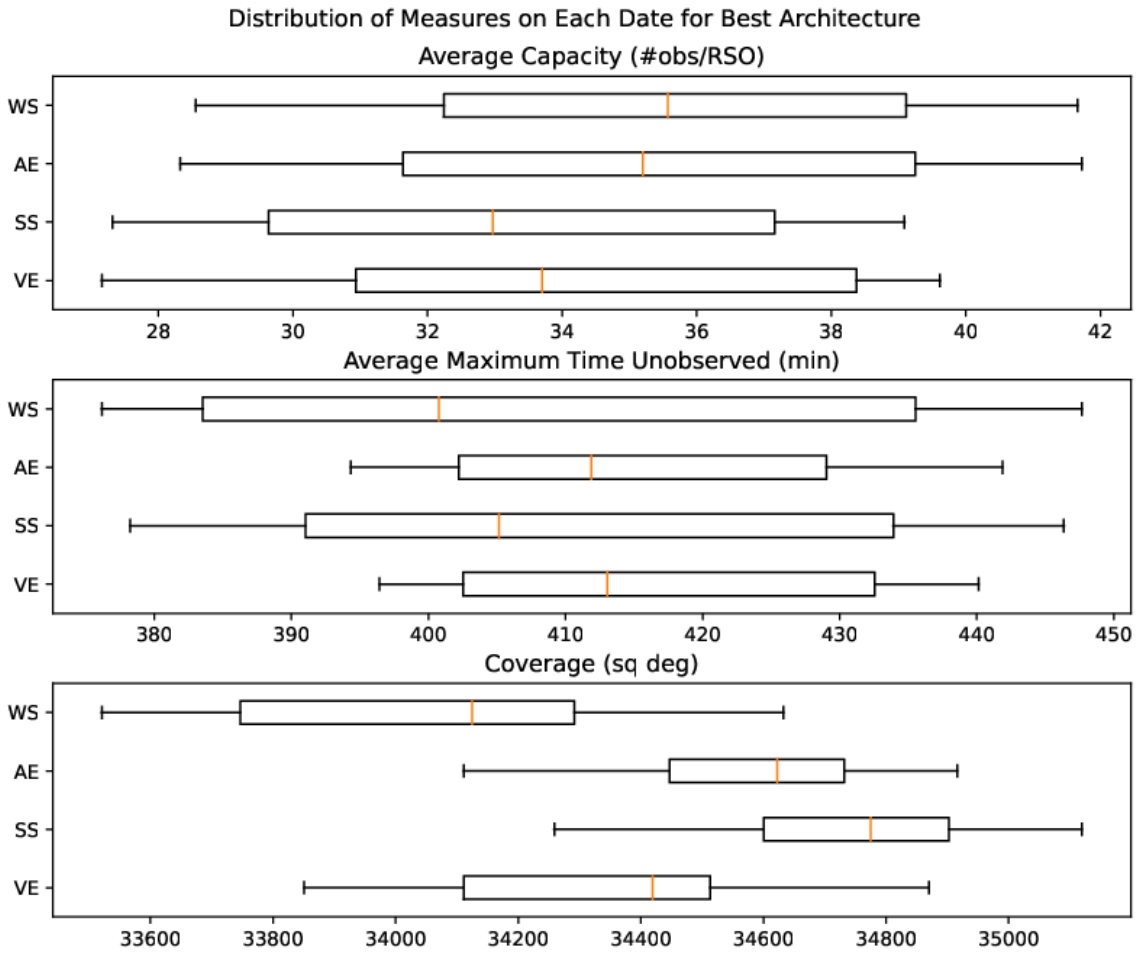

Figure 28. Performance of best architectures on Winter Solstice, Autumnal Equinox, Summer Solstice, and Vernal Equinox.

The lowest-cost architecture in the best set costs $24.2 M, while ten of the 59 expend total cost. Notably, nine specific sensors are used in 80% or more of the set: three sensors at Al Sadeem and sensors at Mauna Kea, Riverland, Kitt Peak, and Sahara Sky. Four sensors in the following locations are utilized in 20% or less of the set: El Leoncito, Perth, Teide, and the Indian Astronomical Observatory. It is inappropriate to make sweeping conclusions tying sensor parameters to success in the larger problem as the best performers are themselves pulled from only a small sample of the large tradespace. However, factors contributing to the selection include weather conditions at the site, the

ability to improve geographic diversity of the GEO belt, the ability to achieve an acceptable SNR, and the accessibility of RSOs over sites due to inherent orbital profiles.

Despite the diversity in capabilities, data explorations finds the best architectures may be binned into four groups based on the number of commercial space-based sensors present in the architecture, with values from zero to three. Figure 29 illustrates this grouping, visible by the patterns in the first and third subplots. The first three subplots merely sum the performance measure values found on all four days on the horizontal axis, while the fourth subplot indicates the number of sensors in the architecture color-coded by ground- and space-based sensors.

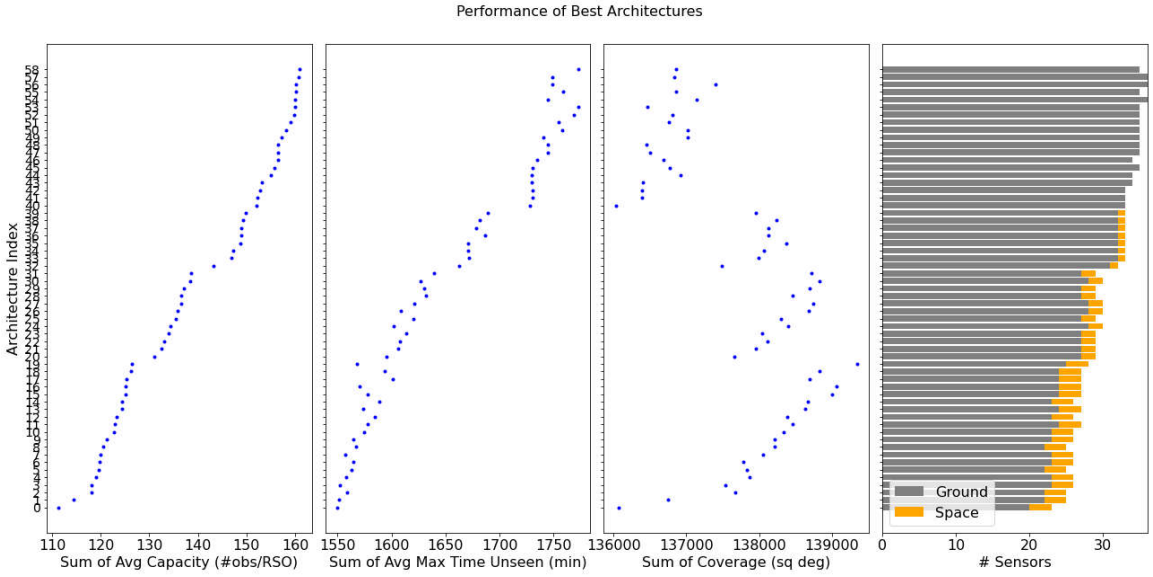

Figure 29. Performance of best architectures. Four distributions based on the number of space-based sensors employed are evident.

Architectures with more space-based sensors are able to employ fewer, generally ten less, total sensors than those with fewer space-based sensors. This seems intuitive as space-based capabilities are generally regarded to be better than ground capabilities due to fewer physics restrictions. This is partly reflected in the figure as architectures with more

space-based sensors are shown to have lower average maximum time unseen and higher coverage. Conversely, architectures employing fewer space-based sensors seem to earn their place amongst the best by focusing on higher capacity at the expense of the other two measures. Review of the underlying data also found these higher-capacity sensors to pull more predominantly from United States, Hawaiian, Mediterranean, and Middle East sensors.

Table 12 shows how the performance of the best architectures compares to the baseline as-modeled DoD architecture, as well as changes between different iterations of this study. Iteration 4 included ground contributions only, excepting SST, on Summer Solstice and Vernal Equinox; Iteration 5 included ground and space contributions on all four days; and Iteration 6 expanded Iteration 5 to include MEO and HEO RSOs. The improvement gained by the AN over the DoD architecture is shown in the green cells; on average, a 3.5 times increase in average capacity, a 3.4 hour or 33% decrease in the average maximum time unseen, and 1.5 times or 55% improvement in coverage are achievable by incorporating around 25-35 additional sensors at a cost of $25M.

Changes between iterations are noted in the delta columns. Notably, the addition of SST and space-based contributions in Iteration 5, the latter explicitly scheduled to reduce RSO maximum time unseen, resulted in a 17-34% decrease in the average maximum time unseen from Iteration 4. The 3-17% decrease in average capacity is believed to be due to a change in the scheduling routine which fully capitalized on parallelization at the expense of a rigorous centrally-tasked, centrally-scheduled algorithm. Between the final two iterations, an approximately 30% decrease in capacity is noted—which is attributed to the additional MEO and HEO RSOs in the problem.

Table 12. Performance of best AN architectures on all days, in final three iterations, compared to the DoD architecture. Green cells show AN improvements.

		Avg Capacity (#obs/RSO)			Avg Max Time Unobserved (min)			Coverage (sq deg)		
		It 4	It 5	It 6	It 4	It 5	It 6	It 4	It 5	It 6
VE	DoD	16.8	13.9	10	707	583.4	611.2	11213	22207	22207
	Δ		-2.9 (-17%)	-3.9 (-28.1%)		-124 (-17%)	27.8 (4.8%)		10994 (98%)	0 (0%)
	AN	51.5	49	34.4	592.1	451.9	416.7	31677	34338	34348
	Δ		-2.5 (-4.9%)	-14.6 (-29.8%)		-140.2 (-23.7%)	-35.2 (-7.8%)		2661 (8.4%)	10 (0%)
	Impr	206.5% (+3.1x)	252.5% (+3.5x)	244% (+3.4x)	-16.3% (-115 m)	-22.5% (-132 m)	-31.8% (-195 m)	182.5% (+2.8x)	54.6% (+1.5x)	54.7% (+1.5x)
SS	DoD	16.1	13.6	9.7	723.9	565	620.4	11317	22344	22344
	Δ		-2.5 (-15.5%)	-3.9 (-28.7%)		-159 (-22%)	55.4 (9.8%)		11027 (+2x)	0 (0%)
	AN	49.6	47.9	33.5	624.5	409.9	410.6	32174	34787	34750
	Δ		-1.7 (-3.4%)	-14.4 (-30.1%)		-214.6 (-34.4%)	0.7 (0.2%)		2612.7 (8.1%)	-37 (-0.1%)
	Impr	208.1% (+3.1x)	252.2% (+3.5x)	245.4% (+3.5x)	-13.7% (-99 m)	-27.5% (-155 m)	-33.8% (-210 m)	184.3% (+2.8x)	55.7% (+1.6x)	55.5% (+1.6x)
AE	DoD		14.4	9.8		603.5	621.9		22042	22042
	Δ			-4.6 (-31.9%)			18.4 (3%)			0 (0%)
	AN		52	35.7		446.7	415.7		34608	34577
	Δ			-16.3 (-31.3%)			-31 (-6.9%)			-31.3 (-0.1%)
	Impr		261.1% (+3.6x)	264.3% (+3.6x)		-26% (-157 m)	-33.2% (-206 m)		57% (+1.6x)	56.9% (+1.6x)
WS	DoD		15.6	10.8		538.5	619.7		22139	22139
	Δ			-4.8 (-30.8%)			81.2 (15.1%)			0 (0%)
	AN		51.6	35.7		387	407.7		34011	34058
	Δ			-15.9 (-30.8%)			20.7 (5.3%)			47 (0.1%)
	Impr		230.8% (+3.3x)	230.6% (+3.3x)		-28.1% (-152 m)	-34.2% (-212 m)		53.6% (+1.5x)	53.8% (+1.5x)
Avg Impr				246% (+3.5x)			-33% (-206 m)			55% (+1.5x)

Best of Best Performers

To further reduce the tradespace, five additional technical and managerial considerations are applied to the best performers. These include quantifying the realization of performance measures; pursuing minor cost savings and an award fee equity; and considering sensor utilization per company, which is felt to be a proxy for business sustainability.

The Sum of NPFs (SNPF) metric helps identify the architecture with best overall performance by summing the four days' NPFs, where lower values are more favorable. Percent Unrealized (PU) measures how far each architecture's performance measure values are from the best possible amongst the top performers by

$$PU = \frac{|best - achieved|}{best} \text{ x } 100 \tag{4.1}$$

Architectural comparisons are drawn by creating a sum of sum of PU (SSPU) metric for all three metrics on all days; lower sums indicate better relative performance. Cost savings off the $25M constraint is also tabulated.

The equity in award fee σ_{awd} is also considered as it helps a decision-maker understand the allocation of funding. This is computed by taking the standard deviation of the award fees to each company, where lower values are more equitable. Lastly, the sensor utilization equity metric σ_{SU} is created to help understand the allocation of business to each company. Sensor Utilization (SU) is defined as the ratio of sensors purchased to sensors proposed by a company, and is posited as a proxy for a company's business case fulfillment. A lower σ_{SU} suggests the four companies more equally meet their business cases.

Applying the five additional metrics to the best architectures, and identifying those architectures whose additional metrics are in the top 10% reduces the decision-space to 18 top architectures denoted as the *best of best* performers. Figure 30 illustrates the results for each architecture on all four days. Figure 31 provides additional summary data. The architectures with green highlights in the bottom five rows are recommended for the decision-maker with particular preferences. A notable reduction in the tradespace is thus achievable by applying modest additional conditions.

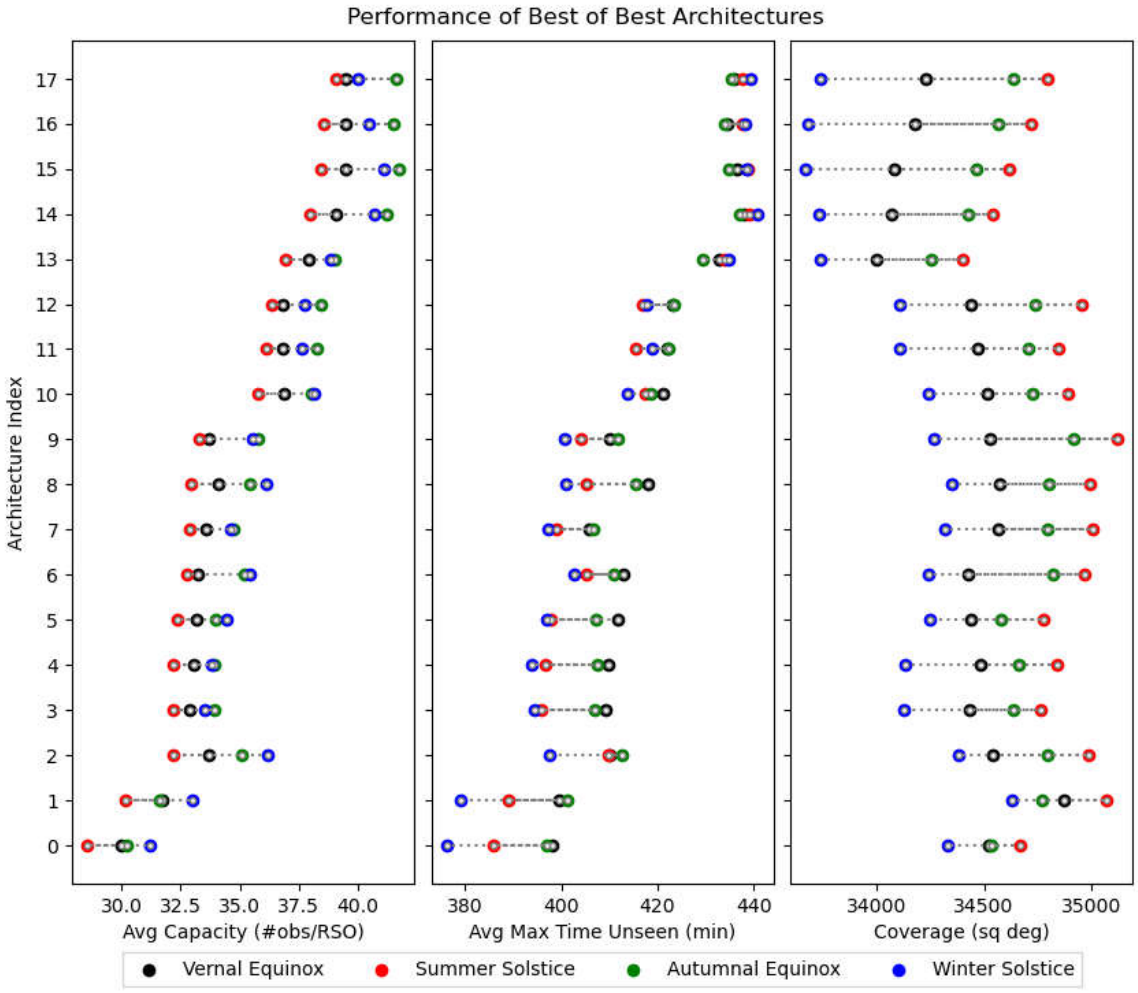

Figure 30. Performance of best of best on all four days.

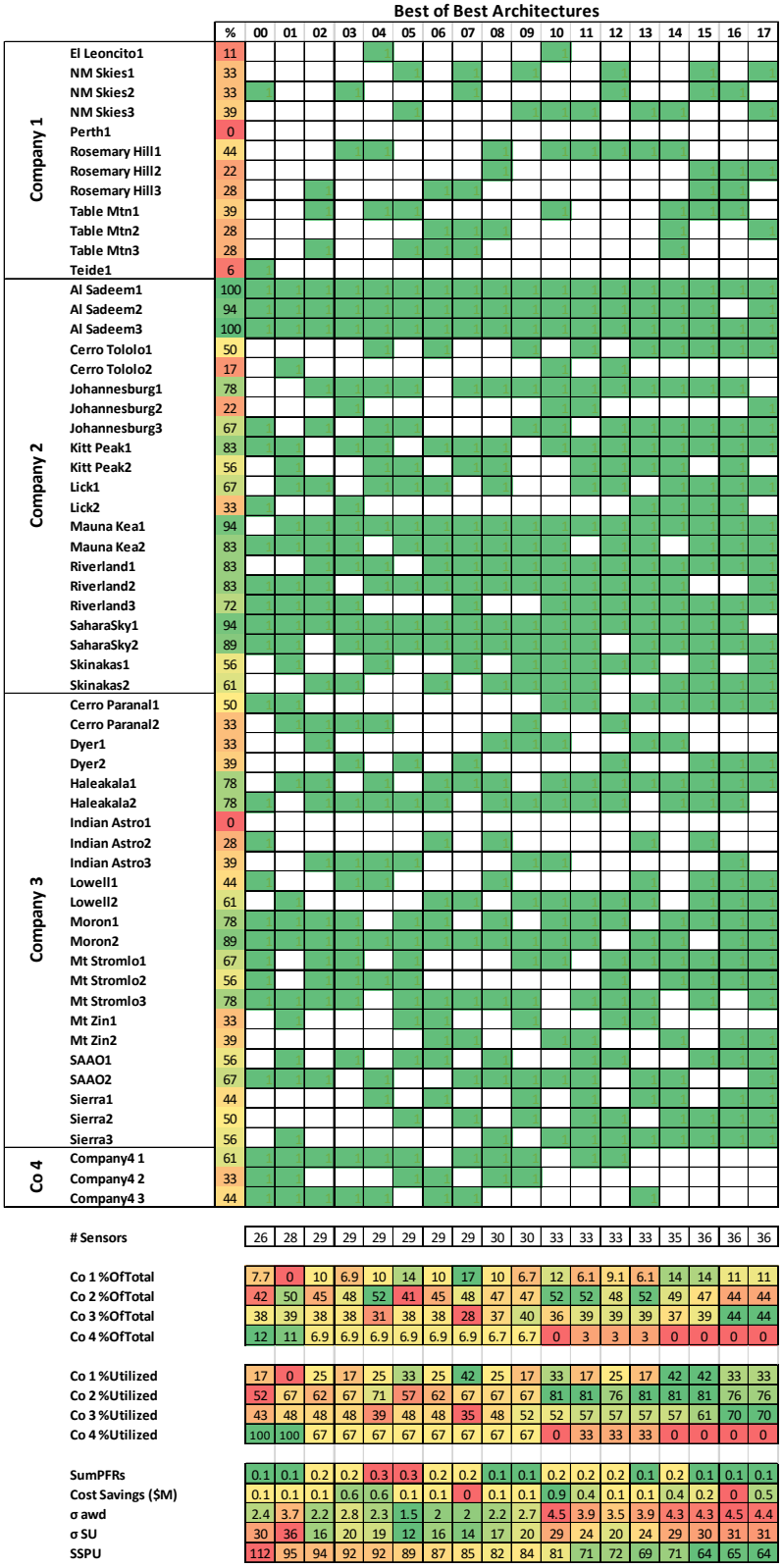

Figure 31. Performance of best of best. Green options in final rows are better.

Results from Proxy Efficacy Study

General Results

Due to the computational burden of OD calculations, it is decided to assess all 14,000 comparative architectures on Summer Solstice only, referred to as the single-day study, and to assess only 1,000 of the comparative architectures on all four days, referred to as the multi-day study. During analysis two interesting conclusions arise which prompt additional review. The first seeks to explore if alternatives to the three core M&S performance measures are better tied to positional uncertainty than the nominal three measures. The second attempts to minimize any loss of information when computing the median uncertainty by directly comparing RSO uncertainty with a new measure of RSO performance per architecture derived from the M&S. A comparison of results is presented at the end of this subsection.

Architecture Performance vs Median Uncertainty, Single Day

Prior to commencing the studies, a holistic comparison of architecture performance deduced from the core M&S and each architecture's median uncertainty $\tilde{u}$ is made for all 14,000 architectures on Summer Solstice as shown in Figure 32. On the first subplot, architectures are plotted on a scatterplot by their average maximum time unseen and average capacity, then color-coded by the architecture's NPF. The second subplot colors architectures by $\tilde{u}$ values. Should better-performing architectures equate to architectures with higher $\tilde{u}$, the coloring schemes would be expected to be similar; however, this is not the case. The second subplot does not follow a Pareto domination pattern, and best performance appears only in the northeast portion of the graph, possibly indicating certain performance measures are a better tie to uncertainty than others.

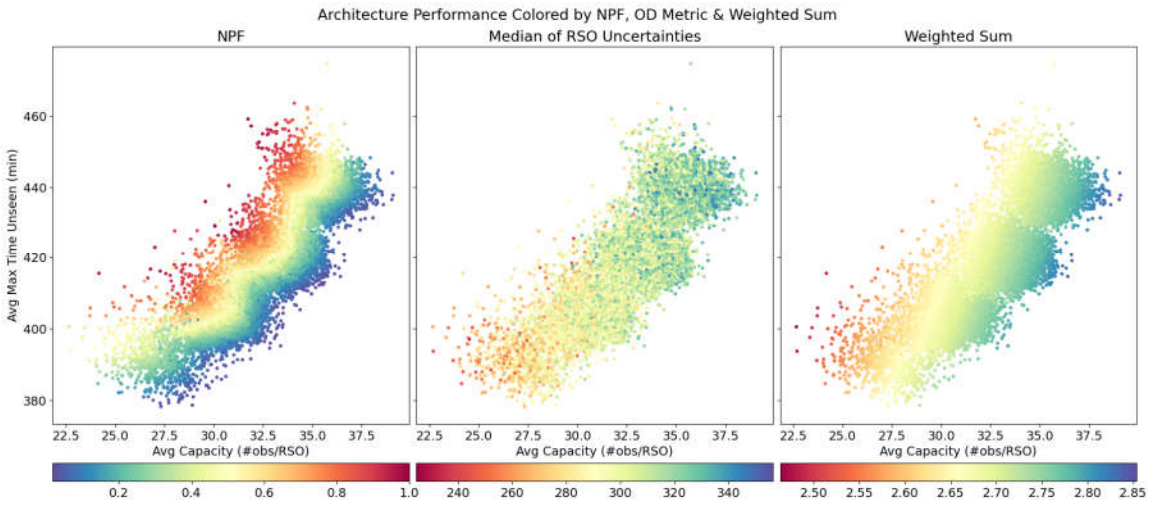

Figure 32. Architecture performance colored by NPF, $\tilde{u}$, and weighted sum. The weighted sum trends seem to tie better to $\tilde{u}$ than NPF.

Because the null hypothesis that better-performing architectures have higher $\tilde{u}$ is rational, it is conjectured that the core M&S's technique for collating performance, the NPF, may not be a good indicator for this comparison. Therefore, an alternative way to collate M&S performance is developed by recasting performance using an equally-weighted sum that considers normalized values of all measures

$$w = \frac{avgCapacity}{maxCap} + \frac{minAvgTime}{avgMaxTime} + \frac{coverage}{maxCoverage} \tag{4.2}$$

where the best possible value is three. The third subplot colors the architectures using M&S performance collated by this measure. This depiction aligns better to $\tilde{u}$ results while still showing Pareto-like behavior, implying the weighted sum may be a better way to collate performance than the NPF in addressing the research question. It is thus decided to quantify core M&S performance using both methods in the rest of this study.

Figure 33 shows the first-order comparisons using simple scatterplots of median uncertainty $\tilde{u}$ vs NPF and weighted sum. Both the Pearson correlation coefficient, R_p, and

Spearman correlation coefficient, R_s, are run to determine trend information. A linear trend is expected if strong correlation is evident. The striped behavior of the NPF graph on the first subplot is due to the discrete NPF values of the problem[23]. The correlation of the NPF to $\tilde{u}$ is near-zero, while the weighted sum subplot shows favorable dispersion but at best moderate correlation. The color-coding is based on NPF, indicating the weighted sum is a somewhat appropriate substitute for the NPF as the color spectrum generally cycles through increasing values.

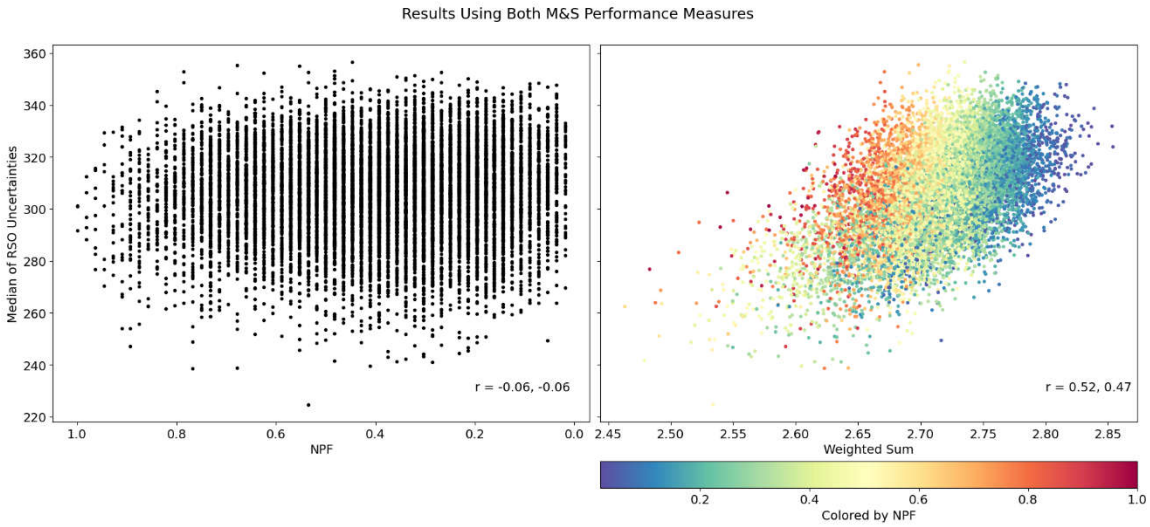

Figure 33. Architectural performance comparison. Collating performance by the weighted sum shows a stronger, but still moderate, correlation.

There is no strong correlation between the values. However, it is suspected the large amount of data may suffer from overplotting which masks general trends. To explore this, both datasets are aggregated using boxplots. For the NPF graph, boxplots bins are generated per NPF while Rice's Rule [106, p. 1]

$$n_b = 2\sqrt[3]{n_{archs}} \tag{4.3}$$

[23] All NPF graphs are plotted with the *x*-axis reversed to mirror behavior of the weighted sum portion.

is used to generate the number of appropriate bins n_b for the weighted sum. Figure 34 displays the results; the blue line plots the median of the median uncertainty, or Median $\tilde{u}$, of the bins.

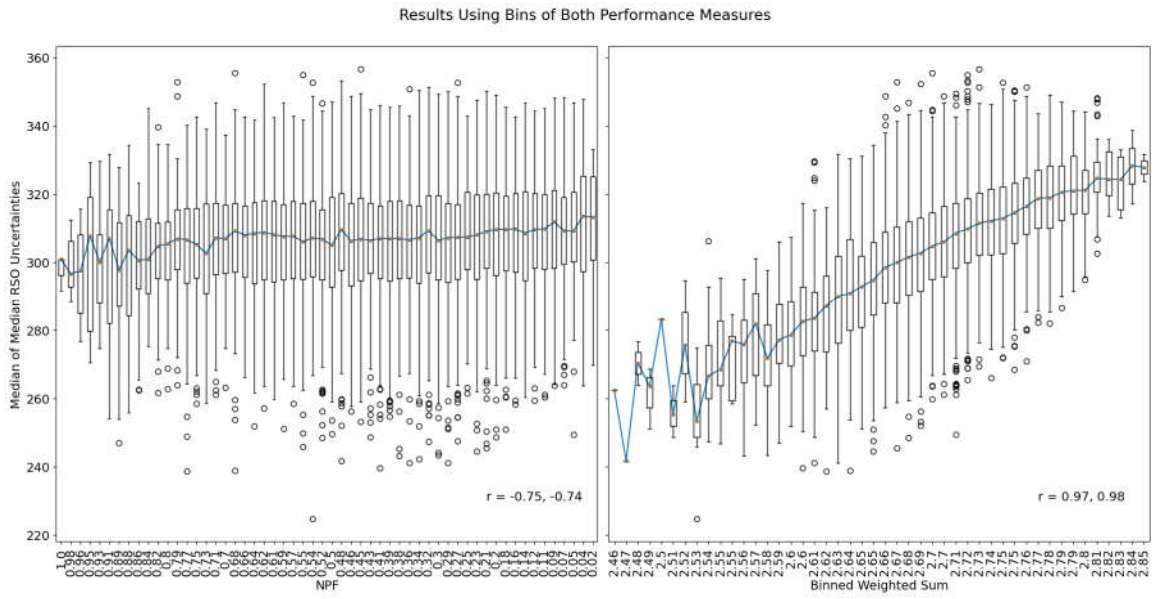

Figure 34. Architectural performance comparison after binning data into boxplots. Moderate to strong correlation of median of $\tilde{u}$ to binned performance is found.

Both subplots show a general improvement in Median $\tilde{u}$ as the architectural M&S performance improves. The NPF plot shows moderate correlation with a consistently tight interquartile range, while the weighted sum plot shows a strong correlation and tight interquartile range which shifts linearly with performance. Two interpretations are relevant. First, the weighted sum may be posited as better than the NPF in collating architectural performance when addressing the question of a tie to uncertainty. This is due to the strong correlation and behavior of the interquartile ranges, and because the best performing architectures as denoted by the weighted sum in fact have better Median $\tilde{u}$ values with a smaller spread than those denoted by the NPF.

An alternate interpretation emerges if the core question of tying performance to uncertainty is slightly disregarded. The poorest-performing architectures as measured using the NPF have similar Median $\tilde{u}$ to architectures performing at the 60% level when using the weighted sum. In other words, the typical architecture as measured using the NPF is guaranteed to have a fair Median $\tilde{u}$ despite its M&S performance, while a lower-performing architecture using the weighted sum will have always have worse Median $\tilde{u}$. Because the purpose of the larger research is to select better-performing architectures, and attaining lower positional uncertainty is desirable when fielding an SDA network, casting M&S performance using the weighted sum is posited as having better utility than the NPF in tying performance to uncertainty.

The above must be severely caveated due to the choice to aggregate data. Since the underlying data has weak correlation, it is not permissible to draw sweeping conclusions from the aggregated results. The results derived from the boxplots typify only interquartile range behavior; 25% of the architectures in each bin have worse uncertainty. Clark & Avery's caution is warranted: "the use of aggregate data may yield correlation coefficients exhibiting considerable bias above their values at the individual level…the estimates derived from aggregate data are valid only for the particular system of observational units employed" [107, p. 429]. At best, these results indicate conclusions which aid in understanding general, but not predictive, trends.

Architecture Performance vs Median Uncertainty, Multi-Day

A multi-day comparison similar to that already undertaken was also conducted. 1000 architectures are sampled from M&S performance tiers to ensure a representative swath of the dataset. All architectures are organized into bins based on the maximum NPF

values. All top-performing architectures are selected while architectures in the remaining bins are randomly selected in proportion to the bin sizes. The Sum of $\tilde{u}$ and the Sum of Weighted Sum are used in the comparisons in Figure 35. The data is also binned for an aggregate comparison in Figure 36. The results are similar to those of the previous study.

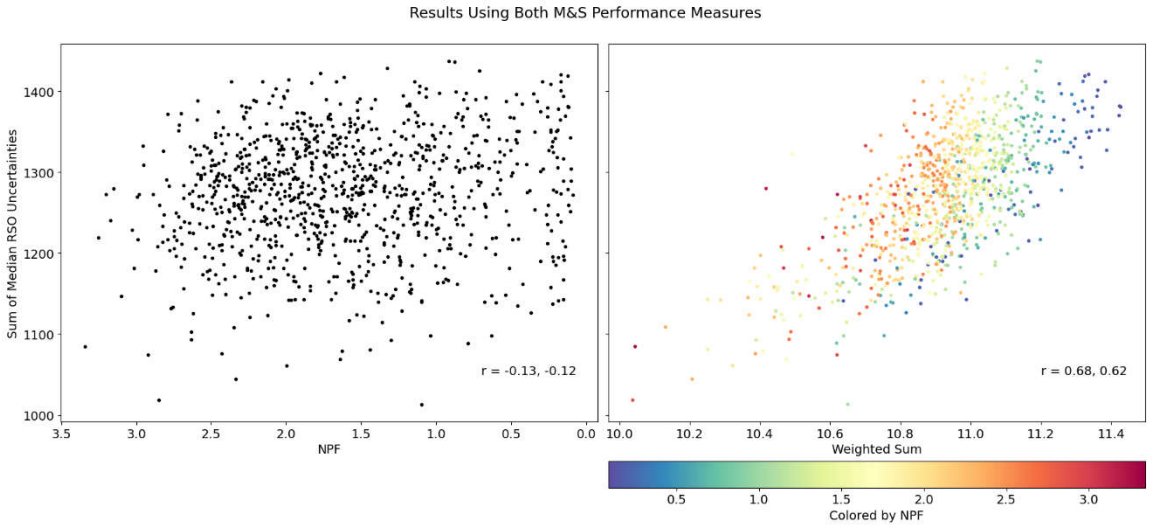

Figure 35. Architectural performance comparison; results are similar to the single day.

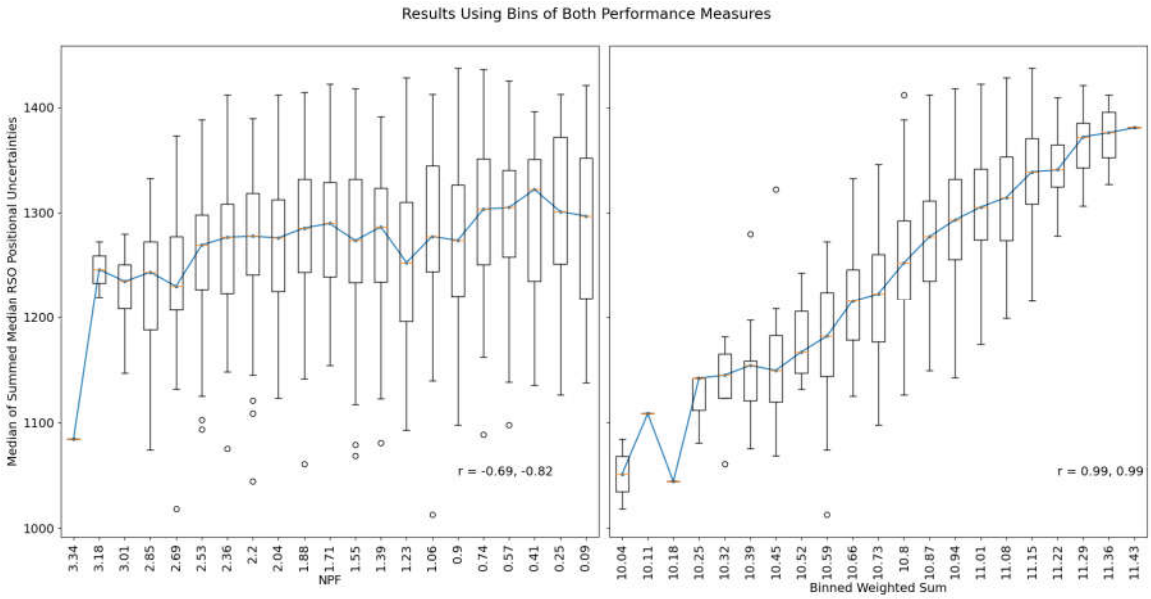

Figure 36. Architectural comparison using boxplots; results are similar to the single day.

Alternate Architecture Performance vs Median Uncertainty, Single Day

As alluded to earlier, particular M&S performance measures may be better tied to median uncertainty than the combination of all three. To test this hypothesis, a weighted sum is used to consider only one or two measures, forming six unique permutations. The study is conducted as before on all 14,000 architectures on Summer Solstice using scatterplots and boxplots to illustrate behavior. Figures 37 and 38 show the results, which indicate average capacity with average maximum time unseen, average capacity with coverage, and average capacity are similarly, if not better, tied to uncertainty.

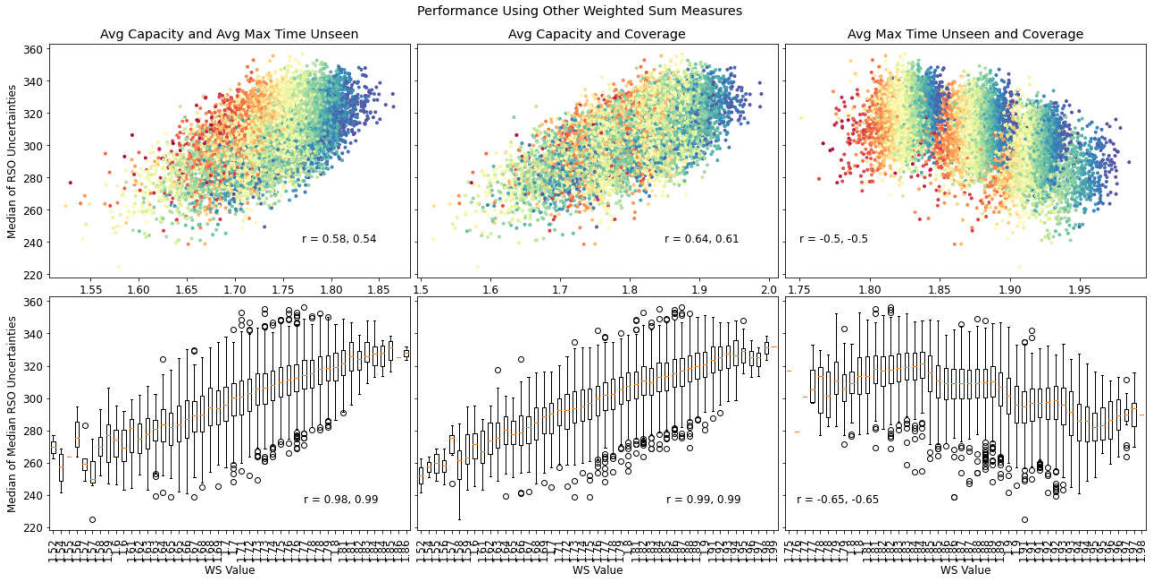

Figure 37. Comparisons using the weighted sum calculated by two measures only.

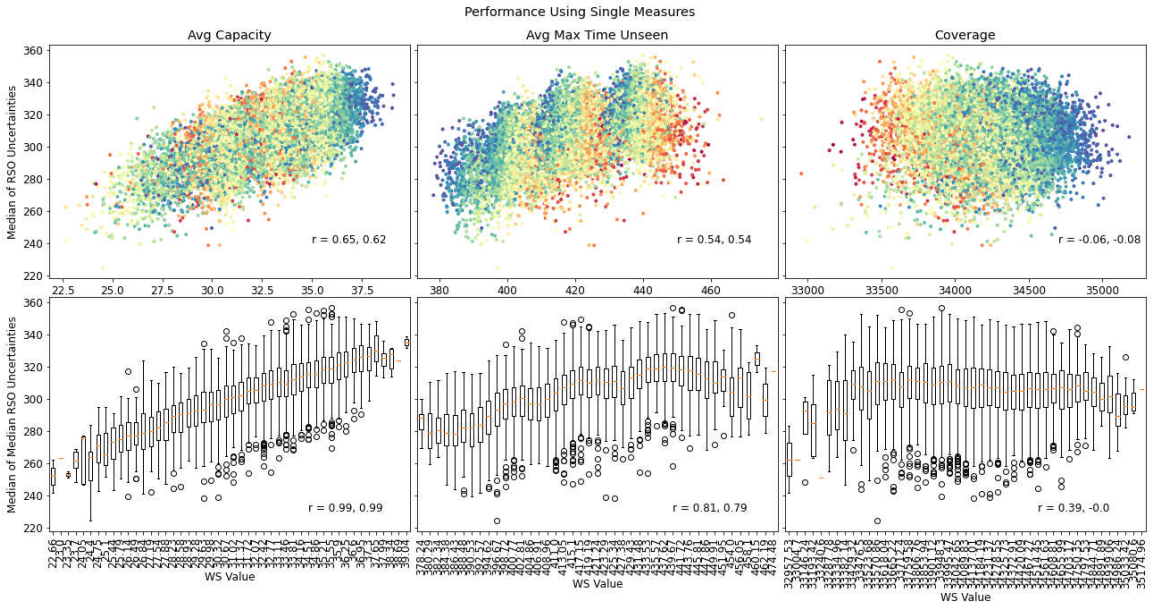

Figure 38. Comparisons using the normalized single measures only.

RSO Performance vs Uncertainty Results, Single Day

The median uncertainty metric $\tilde{u}$ was developed to aggregate RSO uncertainty values in each architecture so that a comparison to M&S performance, which was done at the architecture level, could be made. However, this aggregation is suspected of unduly influencing conclusions. Additionally, the inability to simulate weather effects by multiple Monte Carlo evaluations in the uncertainty portion, nor undo architectural performance values based on these evaluations in the core M&S, prompts an additional approach. The most basic comparison possible is sought to minimize the possibility of overly aggregating data while permitting a fair comparison.

In lieu of comparing architectural-level data, data is compared by RSO in a separate study. Each RSO is evaluated individually, and for every architecture viewing the RSO the RSO uncertainty u_{RSO} is compared to a measure of the architecture's ability to collect the RSO. This results in 1,400 scatterplots, one per RSO, with up to 14,000 datapoints comparing these values for all architectures on Summer Solstice.

The performance measure used to gauge the architecture's ability to collect on the RSO employs a weighted sum. Each RSO's number of observations, maximum time between observations, and coverage per architecture are calculated, normalized, and used in the weighted sum. The correlation coefficient for each RSO is calculated, and the median correlation coefficient amongst all RSOs is returned. Separate studies are also run to consider the six permutations of one or two of the performance measures.

The final median correlation coefficient values are found to have weak to moderate correlation; results are shown in the next subsection. This implies that, at the lowest-level comparison, architectural M&S performance is not strongly tied to positional uncertainty. It is noted, however, that clustering and non-linear behavior observed in the scatterplots detracts from the viability of this method. Nevertheless, it does help inform an assessment when viewed in context with the other studies.

Comparison of Results

Table 13 compares the results of the studies. The architectural performance measures used are listed in the columns, where the values used in the RSO study are indicated in brackets, and correlation coefficient values appear in the cells. Strong correlation is defined as values between 0.8-1 and are colored green; moderate correlation is between 0.6-0.8 and colored yellow, and weak to no correlation are values below 0.6 and colored red.

Table 13. Results of proxy efficacy study. Although the underlying data shows no strong correlation, aggregated data implies a trend.

Study	# Days		NPF		Weighted Sum													
					All		Avg Capacity & Avg Max Time		Avg Capacity & Coverage		Avg Max Time & Coverage		Avg Cap [NumObs]		Avg Max Time [Max Time]		Coverage [Coverage]	
	1	4	Rp	Rs	Rp	Rs	Rp	Rs	Rp	Rs	Rp	Rs	Rp	Rs	Rp	Rs	Rp	Rs
Arch Perf/$\tilde{u}$, Scatterplot	X		-0.06	-0.06	0.52	0.47	0.58	0.54	0.64	0.61	-0.5	-0.5	0.65	0.62	0.54	0.54	-0.06	-0.08
Arch Perf/Med$\tilde{u}$, Boxplot	X		-0.75	-0.74	0.97	0.98	0.98	0.99	0.99	0.99	-0.65	-0.65	0.99	0.99	0.81	0.79	0.39	0
Arch Perf/$\tilde{u}$, Scatterplot		X	-0.13	-0.12	0.68	0.62												
Arch Perf/Med$\tilde{u}$, Boxplot		X	-0.69	-0.82	0.99	0.99												
RSO Perf/u	X				0.49	0.53	0.49	0.53	0.68	0.70	0.08	0.12	0.68	0.70	-0.06	-0.08	0.16	0.15

The general conclusion is that architectural performance measures are a fair, but not statistically significant, proxy for positional uncertainty. The lack of statistical rigor is evident due to the weak correlation found in the scatterplot comparisons for both the 14,000 Summer Solstice architectures and 1,000 multi-day architectures, as well as the weak to moderate correlation in the RSO comparison. It is inappropriate to claim superior architectural performance as measured by the M&S as a good indicator or predictor of lower aggregate positional uncertainty.

However, when the data is aggregated a general trend is found to exist between architectural performance and positional uncertainty. The boxplots show that, for the median 50% of architectures, performance is moderately to strongly tied to positional uncertainty. The trend is more evident when using the weighted sum to collate performance rather than the NPF. Best architectures as codified by the weighted sum in fact have higher $\tilde{u}$ values than those deemed best when the NPF is used. Because deducing a conclusion about the larger group from aggregated data is a fallacy, it is posited these results support a general conclusion or rule of thumb.

In general, as better architectures are identified by the M&S the aggregate positional uncertainty becomes more favorable, more so when using a weighted sum to collated M&S performance than the NPF. An architect wishing to construct the AN using

the best performers as indicated by M&S data will, in general, attain lower architectural-wide positional uncertainty than poorer performing architectures. However, this is not predictive. A better architecture as determined from the M&S may, in fact, have worse architectural-wide positional uncertainty than lower-performing architectures and vice-versa.

An unexpected finding from the data is that using one or two of the performance measures may in fact be better than using all three. The correlation coefficients when using the average capacity with average max time unseen measures, average capacity with coverage measures, and only the average capacity measure, for both the direct scatterplots and RSO study show moderate correlation, besting all other permutations including use of all three measures. Their performance in the binned study also indicates a strong correlation. Future M&S studies may be bettered by merely using these measures to track performance. Interestingly, coverage is found to be a poor tie to uncertainty. In fact, the relatively higher correlation in the average capacity with coverage measures' result may rely more on the fact that capacity as a single measure shows higher correlation and coverage shows near-zero correlation.

Summary

The results of the core M&S and the proxy efficacy study have answered the fundamental research questions. The next chapter aims to succinctly restate findings throughout this project while recapping major assumptions which should be considered before implementing any actions. Lastly, several recommendations for future work are put forth to further address this and future SDA architecting questions.

V. Conclusions and Recommendations

Conclusions

This research strived to understand, develop a methodology for, and objectively evaluate a solution to SDA cataloging problems as recommended by national policy. Namely, the efficacy of augmenting the SSN with non-traditional sensors to improve performance was studied. Through development of a notional scenario, the AN concept was formulated and tested to understand performance gains by first defining likely needs and performance measures; then identifying probable capabilities; and applying system architecting, optimization, and decision analysis in a M&S to identify best solutions to the problem and holistic conclusions. Table 14 succinctly summarizes the answers to the three research questions proposed in the Introduction.

Table 14. Research questions with answers derived from the study.

Q1. Using system architecting, M&S, MOO, and decision analysis, how should the AN be optimally selected? - Craft AN concept and translate needs/requirements into measures - Create scenario for architectural comparisons and run M&S w/MOO - Compare architectures using NPFs and other factors to identify ~20 optimals which meet requirements in diverse ways, namely more/less space-based platforms
Q2. What are appropriate measures to gauge AN performance, and how should they be formulated to permit architectural comparisons? - Review policy/studies, pivot needs to measures: capacity, coverage, time unseen - Explore how formulating and employing measures affects problem - Develop additional technical/managerial metrics for final trades - Find measures are general proxy for arch position uncertainty and using weighted sum vs NPF has more apparent tie to uncertainty - Find M&S may be reduced to 1-2 measures while still finding strong performers - Proves architects may generally construct a low-uncertainty architecture by using weighted-sum best performers from M&S, averting need to run costly OD routine
Q3. How efficient and effective are non-traditional capabilities in augmenting USG SDA tracking? - For $25M: 3.5x better capacity, 55% better coverage, 33% drop in max time unseen - AN approach shows promising course of action to improve SDA cataloging

Applications and Contributions

The key take-away from this project is that, barring data volume and integrity challenges, non-traditional capabilities stand to greatly improve SDA objectives at modest cost. Expending only $25M to improve the number of observations per RSO by 3.5 times while reducing the average maximum time each RSO is unseen by 33%, or 3.5 hours, is posited as an effective and cost-efficient use of resources. Only data from around 30 sensors need be added to the existing network to achieve this increased performance.

The second major take-away from this project is a better end-to-end approach to resolving SDA architecting problems. The study's general flow and methodology illuminates how to approach future network-building problems at a high level. Additionally, improvements to typical SDA architecting approaches were made by improving optical collection constraints, developing a better M&S of weather conditions, and crafting a way to compare individual architectures' performance on multiple days.

The results from the assessment between architectural performance and uncertainty are compelling[24]. One way to demonstrably attain better SDA is by reducing RSO positional uncertainty; however, many models and simulations collate and optimize performance based only on traditional measures instead of using covariance data. For example, the performance measures chosen in this study were chosen more so to align with literature results and conjectured AN MOPs than to directly reduce positional uncertainty.

[24] The inability to simulate Monte Carlo weather data for the uncertainty portion detracts from this conclusion, although the RSO-only comparisons somewhat support the findings.

Analysis of architectural performance and uncertainty showed this to generally be the case, albeit as more of a rule of thumb than an explicit, predictive trend.

Top-performing architectures as found when using the weighted sum are shown to generally have the lowest uncertainty. An architect wishing to avoid the computational difficulty and execution time of incorporating an OD routine into an optimization algorithm may thus merely pick some set of best architectures and be reasonably assured they have lower uncertainty than the rest of the group. For additional confidence, an OD routine may be run on that small set to identify and retain those with the lowest uncertainties. In other words, using the best architectures found by the performance measures and assessed using the methods in this study is a fair way to ensure an architecture has a low aggregate RSO positional uncertainty, while running an OD routine on the simulated catalog data for this smaller set boosts confidence.

An interesting discussion point arises when the proxy efficacy study is considered in terms of verification and validation. Given that the measures as constructed identified better-performing architectures in the M&S, verification is fulfilled. However, because there is no stakeholder in this academic study, asserting program-level validation is difficult. If the major technical goal to be gleaned from the M&S is to identify networks with lower positional uncertainty, this is not entirely met. Comparisons of the NPF measurement to the median uncertainty somewhat show this, and the weighted sum illustrate a much better trend, but the lack of correlation in the underlying data and the spread evident in the boxplots suggest this is not entirely attained. However, if the stakeholder approved the performance measures with goals in mind not exclusive to finding the architectures with lowest positional uncertainty—for example, requesting high

coverage for the sake of building a world-wide redundant network only—validation may in fact be met. This is an important point to review with the stakeholder before, during, and after the assessment.

One incidental and unexpected finding is that the three originally-employed performance measures may not in fact be as effective as using only one or two of the measures. The results from the proxy efficacy study shows that using the average capacity with average maximum time, average capacity with coverage, or just the average capacity generally permits uncertainty results on par with or superior to those found when using all three measures. The potential for using one single measure, average capacity, is interesting as a single-objective optimization problem reduces computational burdens. It is cautioned, however, that simply using this single measure in any other study without context may be unwise. This is because the scheduling routine purposefully disperses observations around the world, akin to improving coverage, as well as using the space-based platforms to reduce average maximum time unseen. Therefore, a reported correlation between average capacity and positional uncertainty should not neglect the underlying methods used in generating this data.

Recommendations for Future Research

Overview

Direct and indirect results from this work, as well as discussions along the way, lend themselves to many ideas for future research. These are organized in the following manner. General improvements and modifications to the study are explored in the first section. Ideas which reconsider the core problem slightly, allowing for an extended or

derivative study, are then reviewed. Lastly, additional topics which materialized during execution but could not be reasonably incorporated are discussed.

Improvements of Aspects of the Problem

This project relies heavily on STK for astrodynamic propagation and report generation. Should STK become unavailable in the future or an alternate approach be desired, it may be possible to divorce the project from STK using a simpler Two-Body Propagation routine. Custom azimuth, elevation, range, time, and angular velocity routines would also be required. At present, the most promising way to pursue an STK-less problem is believed to be via custom-developed Python scripts as no other routine is as robust and menu-driven as STK, for which AGI also provides extensive customer support. One additional option is to explore use of the NASA Horizons database, which allows for some propagation of RSOs given TLEs as well as astrodynamic and radiometric values.

Making improvements to the weather portion of the M&S are evident. Clouds are challenging to model stochastically and turning off an entire site for a night may be unrealistic, especially since clouds may appear in only one patch of the sky for a few hours. A better method may be to stochastically simulate cloud conditions using some measures of positional data; however, during the research this information was not extant. Members of the AFIT Center for Directed Energy expressed their belief that this may be possible to generate in the future using results from research they are currently conducting. A future researcher is cautioned, in general, to consider the availability of supporting data for all proposed ground sites before committing to a path as the absence of only one set may provide unanticipated challenges as the research is scaled up.

Modeling and simulating the RSO SNR portion of SDA studies seemingly invites different perspectives on the appropriateness of assumptions. It is recommended any future architects overview an approach with a Subject Matter Expert (SME) early in the project to determine what may or may not be needed in the particular problem. The use of actual standard visual magnitude values to represent RSO brightness, instead of assuming a standard value for all RSOs as conducted in past research, was felt to be a good approach at the outset of the M&S. However, the unexpected loss of the primary data source for this information provided an unforeseen challenge. Obtaining another source for use in future work may be difficult, although it is conjectured data in the UDL may suffice. Either using a representative brightness value based on known regime and/or bus information, or simulating these from a distribution function, may be better approaches in the future.

The use of an alternative optimization method was briefly considered but decided against as NSGA-II is a proven, known tool employed in previous studies. However, it is believed that a Particle Swarm routine may perform equally well or better. It was supposed that the Particle Swarm would first require a list of feasible architectures, which are those meeting the cost constraint, prior to proceeding. Switching the optimization method, however, for the sake of using a different method when NSGA-II performed well may not add value to the research. However, if this or any other method is found to more swiftly search the solution space while providing similar results this may be worth considering.

Reconsidering Core Problem

The problem was conceived as a systems architecting study in which performance measures were to be optimized against a cost constraint and better performance delineated solely by those values. However, the proxy efficacy study revealed that merely optimizing

on some measure of architectural uncertainty computed during the M&S may be a better approach, depending on the stakeholder's desires. This is currently believed to be a computationally-expensive task, but if a stakeholder's main objective is achieving lowest uncertainty this approach will most directly accomplish it.

A major assumption at the outset of the project was that all commercial sensors were to be purchased and made fully-taskable. This significantly simplified the M&S, allowing the work to focus on optimally choosing sensors. However, the actual purchase decision may consider buying data-level information in aggregative, by time, or by the observation. Determining which purchase method to best employ, and/or how to design the AN using that particular decision constraint, forms an interesting study which would aid stakeholders in understanding the utility of the contracting options available.

A cost constraint was purposely added to this problem because budget concerns loom heavily. An alternate idea was proposed during the research in which the cost constraint be removed to permit the absolute best architectures to be identified. A cost and performance comparison could then be run to determine the point at which the *best bang for the buck* occurs. This is an interesting study which merits pursuit, as it helps a stakeholder justify a larger budget—especially if a mere $5M extra cost above the $25M cap is found to demonstrably improve capabilities—as well as identify diminishing returns.

This problem assumed all RSOs were perfectly-behaved, with no launches, trajectory changes, maneuvers, cross-tags, nor most deleterious behavior which complicates SDA operations. The schedule was also assumed fixed with no re-tasking during the M&S. An advanced study testing the robustness and resiliency of all

architectures by applying these considerations would boost the credibility of this or any SDA architecting study.

The omission of radars and RF detection assets in this study limits the applicability of the findings. However, given the short time and resources available this is an understandable omission. At a minimum, adding ground-based radars to track DS targets would improve the DS M&S. RF detection assets are believed to be easily simulated in the core M&S if accesses are assumed and a probability of RF intercept can be surmised.

A purposeful decision was made to omit LEO and cislunar RSOs from the study, but their inclusion would also bolster major findings. There are apparent difficulties in modeling cislunar trajectories and a dedicated architecting study regarding cislunar SDA capabilities may itself be prudent. Adding LEO RSOs, while having general utility, is expected to severely increase execution time due to the number of RSOs and possible need to perform refined orbit propagation. Simulation of ground-based radar and associated scheduling techniques, not yet explored by AFIT SDA architects, would also be required.

This study primarily called upon extant non-traditional capabilities to derive representative sensors. However, the next iteration may be bettered by including near-future and potentially beneficial sensors. In particular, adding telescopes performing daylight imaging of RSOs or accomplishing a separate architecting study with those assets may be valuable. An additional thought comes from Felten's conclusions that GPO collection satellites have utility [95]. Adding these into a future study has the potential to boost confidence in those results, and possibly encourage a USG or non-commercial provider to field a system in this regime.

The project originally called for employing OD at the 12-hour point of the problem to emulate SSN operations. However, this proved too difficult as devising a unique collection simulation, running the OD routine, and performing a rescheduling on every architecture in the problem required too much time and data management. However, performing this in some manner in a future iteration, especially one considering LEO RSOs, would enhance confidence in the proxy efficacy results.

The final idea involves adding additional layers of stochasticism to the project. Recall that the scheduling routine is run only once, and schedulers per architecture are pulled from the same file. Performing this process multiple times and aggregating results would negate the possibility of the scheduler unduly influencing results. However, this would be a substantial undertaking, requiring the entire problem be run multiple times. Additionally, due to randomness of the NSGA-II architecture selection process a comparison between multiple scheduling runs, as was accomplished when comparing performance on multiple days, would be required. Scaling back the problem would aid in accomplishing this study.

Additional Research Topics

Several additional ideas arose during the research which were disregarded as project complexity increased, yet they still merit mentioning. Commercial SDA providers solicited during the work believed that if the USG would offload bright and/or routine collections to them, it would aid their business cases while freeing USG assets for higher-priority tasks. This would form an interesting study which, if proven true, would help advance a case that the USG should, and now can, focus on other SDA goals.

Determining how to best incorporate data from contributing sensors is also pertinent. Contributor data in this study was assumed to be submitted without any influence on tasking; however, should the sensor have an exquisite capability of some form there may be utility in creating a partnership such that taskings occur on occasion. Should this be realistic, determining how to manage DoD tasking around these expected contributions, and to shuffle tasking if an observation is missed, may form an interesting study.

The challenges of data integrity were sidestepped in this study, but they remain a valid concern as indicated in AFSPCI 10-610 [59]. A study simulating the effects of a deleterious observation and/or some method to ascertain if an observation is flawed would help reduce USG reluctance in ingesting non-traditional data. Incorporating such a module into an extended version of this M&S would add credence to this research. Work by Raley [71] and the Trusat team [108] may be pertinent in this pursuit.

A proposal was made during the work that a scheduling routine incorporating cloud parameters be devised. The probabilistic azimuth and elevation of clouds at particular times of the year at given sites may be incorporated into a scheduler such that higher-probability locations are tracked. Such a routine may aid a site manager in better planning around missed observations.

A study comparing architectural performance when using multiple different criteria may illuminate better performance measures for use in a M&S scenario. As envisioned, several performance measures would be chosen and architectures subjected to the M&S and uncertainty routine. Trend information as gathered during the proxy efficacy study

would help identify which permutation of measures are better by executing the architectural-wide uncertainty study and comparing datasets.

Publications On This Topic

Iterations of this work have been frequently published in open-source literature. A paper accepted for the 2020 Advanced Maui Optical Surveillance conference representing Iteration 3 is extant on the venue website [109]. Iteration 4 is to be imminently published by the Journal of Defense Analytics and Logistics [110]. Iteration 5 has been accepted for publication in the Journal of Defense Modeling and Siulation. Conclusions from the proxy efficacy study are anticipated to be submitted to a third scholarly journal. This dissertation presents the final product on this topic.

Summary

SDA problems continue to challenge the USG as space usage and new threats increase. The topic addressed herein represents but one possible solution towards furthering space superiority. Additional critical review of the AN concept will bolster findings, while future research on related topics will help illuminate solutions to emerging SDA challenges.

Appendix A: Technical Parameters Used for Sites and Sensors in M&S

Tables 15 and 16 show amalgamated data for all sensors used in the M&S. All data is based on open-source information previously listed in the Literature Review, from specification sheets, best engineering judgement, and/or sources listed in Table 17.

Table 15. Owner, site, telescope, location, FOV, and collection method for all sensors.

Network	Site	Sensor #			Lat	Long	Capability	Collection
		1	2	3				
Company 1	El Leoncito	A			-31.8	-69.3	NFOV	Task
Company 1	New Mexico Skies	B	B	B	32.9	-105.53	NFOV	Task
Company 1	Perth	C			-32.01	116.14	NFOV	Task
Company 1	Rosemary Hill	B	B	B	29.4	-82.59	NFOV	Task
Company 1	Table Mtn	B	B	B	34.38	-117.68	NFOV	Task
Company 1	Teide	A			28.3	-16.51	NFOV	Task
Company 2	Al Sadeem	B	B	B	24.18	54.68	NFOV	Task
Company 2	Cerro Tololo	B	B		-30.17	-70.81	NFOV	Task
Company 2	Johannesburg	B	B	B	-26.18	28.07	NFOV	Task
Company 2	Kitt Peak	B	B		31.96	-111.6	NFOV	Task
Company 2	Lick	B	B		37.34	-121.64	NFOV	Task
Company 2	Mauna Kea	B	B		19.82	-155.47	NFOV	Task
Company 2	Riverland	B	B	B	-34.28	140.37	NFOV	Task
Company 2	SaharaSky	B	B		30.24	-5.61	NFOV	Task
Company 2	Skinakas	B	D		35.21	24.9	NFOV	Task
Company 3	Cerro Paranal	E	F		-24.63	-70.4	NFOV	Task
Company 3	Dyer	E	F		36.05	-86.81	NFOV	Task
Company 3	Haleakala	E	F		20.71	-156.26	NFOV	Task
Company 3	Indian Astro	G	E	F	32.78	78.96	NFOV	Task
Company 3	Lowell	E	F		35.2	-111.67	NFOV	Task
Company 3	Moron	E	F		37.15	-5.59	NFOV	Task
Company 3	Mt Stromlo	E	F	F	-35.32	149.01	NFOV	Task
Company 3	Mt Zin	E	F		30.6	34.76	NFOV	Task
Company 3	SAAO	E	F		-32.38	20.81	NFOV	Task
Company 3	Sierra	E	F	E	37.07	-119.41	NFOV	Task
Company 4	Satellite 1	L	[redacted]		Polar ~575 km		NFOV	Task
Company 4	Satellite 2	L	[redacted]		Polar ~575 km		NFOV	Task
Company 4	Satellite 3	L	[redacted]		Polar ~575 km		NFOV	Task
Scientific	BIGGO (Pico dos Dias)	H	[redacted]		-22.53	-45.58	WFOV	Serendip
Civil	MCAT (Ascension)	I	[redacted]		-7.97	-14.4	NFOV	Task
DoD	Diego Garcia	J	J	J	-7.41	72.45	NFOV	Task
DoD	Haleakala (DoD)	J	J	J	20.71	-156.26	NFOV	Task
DoD	Socorro	J	J	J	33.82	-106.66	NFOV	Task
DoD	Exmouth	K	[redacted]		-21.90	114.09	WFOV	Survey
DoD	Sapphire	L	[redacted]		SSO ~780 km		NFOV	Task
DoD	SBSS	M	[redacted]		SSO ~630 km		WFOV	Task
DoD	ORS-5	N	[redacted]		LEO Equatorial		NFOV	Fixed

Table 16. Telescope specifications.

Opt	Telescope & Camera	Dia (m)	FOV (°x°)	Focal Len (m)	f/#	Plt Scal (as/p)	Pixels	Pitch (um)	η_{625}	e_d (e-/p/s)	e_r (e-)
A	OSR Large Astrograph 600 F3.8 w/FLI ML09000	0.6	0.92 x 0.92	2.28	f/3.8	1.1	3056 x 3056	12	0.65	0.03	16
B	Takahashi FET-300 w/FLI ML09000	0.3	0.88 x 0.88	2.4	f/8	1	3056 x 3056	12	0.65	0.03	16
C	OSR Large Astrograph 800 F5 w/Apogee ALTA F4320	0.8	0.7 x 0.7	4	f/5	1.2	2048 x 2048	24	0.67	2	12
D	Astro Systeme Austria Astrograph 16N Reduced w/FLI ML09000	0.4	1.38 x 1.38	1.52	f/3.8	1.6	3056 x 3056	12	0.65	0.03	16
E	Takahashi C-400 w/Apogee ALTA F4320	0.4	0.5 x 0.5	5.6	f/14	0.9	2048 x 2048	24	0.67	2	12
F	Astro Systeme Austria Astrograph 16N Reduced w/FLI ML16803	0.4	1.39 x 1.39	1.52	f/3.8	1.2	4096 x 4096	9	0.52	0.01	15
G	OSR Large Astrograph 600 F5 w/Apogee ALTA F4320	0.6	0.94 x 0.94	3	f/5	1.7	2048 x 2048	24	0.67	2	12
H	Pico Dos Dias w/Spectral Instruments	2	0.63 x 0.63	5.6	f/2.8	0.6	4096 x 4096	15	0.65	6	12
I	MCAT w/Spectral Instruments Ascension	1.3	0.68 x 0.68	5.2	f/4	0.6	4096 x 4096	15	0.65	6	12
J	GEODSS w/Sarnoff MIT/LL CCID-16	1	1.25 x 1.64	2.15	f/2.15	2.3	1960 x 2560	24	0.65	6	12
K	SST w/ Custom CCD	2.9[25]	3.03 x 2.02	3.49	f/1	0.89	12288 x 8192	15	0.9	2	18.6
L	Sapphire w/E2V Tech CCD 47-20BI	0.15	1.4 x 1.4	0.545	f/3.6	4.9	1024 x 1024	13	0.85	250	8
M	SBSS w/Ball Kepler	0.3	4.0 x 1.9	0.851	f/2.8	6.5	2200 x 1044	27	0.80	1	120
N	ORS-5 w/MIT/LL CCID-51M[26]	0.1	1.0 x 0.5	1.41	f/14	1.8	2048 x 1024	12	0.85	12	1

[25] Although larger, literature indicated SST is better modeled with a 2.9 m aperture due to design parameters.
[26] FOV, focal length, and f/# for ORS-5 are based on engineering assumptions.

Table 17. Additional sources for sensor M&S.

Sensor	Additional References
GEODSS	Bruck & Copley [111]
SST	Ackermann et al. (2015) [52], Monet [112], Zingarelli [113], Ackermann & McGraw [114], Ackermann et al. (2014) [115]
Sapphire	Ackerman et al. (2015) [52], Leitch & Hemphill [116], CCD47-20 specification sheet [117], Scott et al. [118], Maskell & Oram [119], Qian [120, Ch. 34],
SBSS	Ackermann et al. (2015) [52], Vallado et al. [121], Kepler Homepage [122], Kepler Instrument Handbook [123]
ORS-5	Ackermann et al. (2015) [52], Kramer [124], Cunningham (2016) [125], Cunningham (2018) [126]

Appendix B: Augmented Network Requirements

The following is a list of mission requirements, MOEs, MOPs, and measures theorized to be important to a well-performing AN developed at the commencement of this research. This approach proved useful in identifying key measures prior to conducting the optimality portion. Upon conclusion of the research, it is evident this list requires refinement. The original is presently solely for informational purposes.

Requirement 1: AN shall meet or exceed SSN performance capabilities	
MOE 1-1: Capacity *average capacity*	MOP 1-1-1: # tracks/day or obs/day MOP 1-1-2: # RSOs/day MOP 1-1-3: #obs on RSO/day
MOE 1-2: Sensitivity *average size (or Mv or SNR)*	MOP 1-2-1: Mv for optical; RSO dia for radar MOP 1-2-2: SNR (unitless)
MOE 1-3: Accuracy & quality of sensor metrics and ephemeris generation *accuracy*	MOP 1-3-1: Sensor sigma MOP 1-3-2: Sensor bias MOP 1-3-3: Covariance MOP 1-3-4: RMS of orbit solution MOP 1-3-5: Track spacing MOP 1-3-6: Timing Accuracy
MOE 1-4: Orbital coverage and persistence *coverage*	MOP 1-4-1: Steradians of solid angle MOP 1-4-2: Percent of orbital regime observed MOP 1-4-3: Coverage time
MOE 1-5: Data reporting timeline *average latency*	MOP 1-5-1: Time to respond to tasking MOP 1-5-2: Observation rate MOP 1-5-3: Total time to create TLE
MOE 1-6: Unique capabilities *metric: unique RSOs*	MOP 1-6-1: RSOs SSN would not detect MOP 1-6-2: RSOs for which SSN sensitivity less MOP 1-6-3: Events GEODSS would not detect MOP 1-6-4: Coverages SSN would not detect
MOE 1-7: Availability/Reliability *network availability*	MOP 1-7-1: % time network is up/available

Requirement 2: Non-traditional sensors shall have minimal data integrity issues	
MOE 2-1: Confidence in transmission *bad actor influence*	MOP 2-1-1: Network meets IA requirements MOP 2-1-2: Network uptime MOP 2-1-3: Bad actor's influence on network MOP 2-1-4: Number of network infiltrations/mo
MOE 2-2: Confidence in data *data confidence*	MOP 2-2-1: Variation in sensor bias MOP 2-2-2: Demonstrably false data MOP 2-2-3: Incorrectly assessed events

Requirement 3: Non-traditional sensors shall demonstrate acceptable timeliness	
MOE 3-1: Tasking Responsiveness	MOP 3-1-1: Time to acknowledge tasking require MOP 3-1-2: Time until tasking fulfilled
MOE 3-2: Data transmission responsiveness	MOP 3-2-1: Time between collection/transmission

Requirement 4: AN shall be cost-efficient for the USG	
MOE 4-1: Operational cost *cost*	MOP 4-1-1: Sum of SSN operational cost and use of non-traditional means per year

Bibliography

[1] D. M. Buede and W. D. Miller, *The Engineering Design of Systems: Models and Methods*. John Wiley & Sons, 2016.

[2] E. Crawley, B. Cameron, and D. Selva, *System Architecture: Strategy and Product Development for Complex Systems*. Prentice Hall Press, 2015.

[3] M. W. Maier and E. Rechtin, *The Art of Systems Architecting*, 3rd ed. CRC Press, 2010.

[4] G. J. Roedler and C. Jones, "Technical Measurement," INCOSE, 2005.

[5] R. Bullock and R. Deckro, "Foundations for System Measurement," *Measurement*, vol. 39, Art. no. 8, 2006.

[6] G. S. Parnell, T. A. Bresnick, S. N. Tani, and E. R. Johnson, *Handbook of Decision Analysis*. John Wiley & Sons, 2013.

[7] K. Deb, *Multi-objective Optimization Using Evolutionary Algorithms*. John Wiley & Sons, 2008.

[8] J. S. Arora, *Introduction to Optimum Design*, 4th ed. Elsevier, 2017.

[9] M. S. Bazaraa, H. D. Sherali,, and C. M. Shetty, *Nonlinear Programming: Theory and Algorithms*. John Wiley & Sons, 2013.

[10] K. D. Jong, *Evolutionary Computation: A Unified Approach*. MIT Press, 2006.

[11] K. Y. Lee and M. A. El-Sharkawi, *Modern Heuristic Optimization Techniques: Theory and Applications to Power Systems*. John Wiley & Sons, 2008.

[12] D. H. Rhodes and A. M. Ross, "Five Aspects of Engineering Complex Systems," in *IEEE Systems Conference*, 2010, p. 3.

[13] A. Bal, "Demystifying Genetic Algorithms to Enhance Neural Networks," *Medium*, Jul. 2019. https://medium.com/intel-student-ambassadors/demystifying-genetic-algorithms-to-enhance-neural-networks-cde902384b6e (accessed Mar.2020).

[14] R. L. Haupt and S. E. Haupt, *Practical Genetic Algorithms*, 2nd ed. Wiley Online Library, 2004.

[15] C. R. Reeves, "Using Genetic Algorithms with Small Populations," in *Proceedings of the 5th International Conference on Genetic Algorithms*, 1993,

vol. 590, p. 92.

[16] "Genetic Algorithm Minimum Population Size," *Stack Exchange*, 2014. https://cs.stackexchange.com/questions/34019/genetic-algorithm-minimum-population-size (accessed Mar.2020).

[17] S. Chen, "What Is the Optimal/Recommended Population Size for Differential Evolution?," *Research Gate*, 2013. https://www.researchgate.net/post/What_is_the_optimal_recommended_population_size_for_differential_evolution2 (accessed Mar.2020).

[18] A. E. Eiben and J. E. Smith, *Introduction to Evolutionary Computing*. Springer, 2003.

[19] K. Deb, A. Pratap, S. Agarwal, and T. Meyarivan, "A Fast and Elitist Multiobjective Genetic Algorithm: NSGA-II," *IEEE Transactions on Evolutionary Computation*, vol. 6, Art. no. 2, 2002.

[20] T. Goel, "Elitist Non-Dominated Sorting Genetic algorithm: NSGA-II," University of Florida, 2011. [Online]. Available: https://mae.ufl.edu/haftka/stropt/Lectures/multi_objective_GA.pdf.

[21] D. A. Vallado, *Fundamentals of Astrodynamics and Applications*, 4th ed. Microcosm Press, 2013.

[22] A. F. Herz, F. Stoner, R. Hall, and W. Fisher, "SSA Sensor Tasking Approach for Improved Orbit Determination Accuracies and More Efficient Use of Ground Assets," in *Proceedings of the Advanced Maui Optical and Space Surveillance Technologies Conference*, 2013, vol. 1.

[23] M. R. Ackermann, R. R. Kiziah, P. C. Zimmer, and J. T. McGraw, "Weather Considerations for Ground-Based Optical Space Situational Awareness Site Selection," in *Proceedings of the Advanced Maui Optical and Space Surveillance Technologies Conference*, 2018, vol. 1.

[24] J. R. Shell, "Optimizing Orbital Debris Monitoring with Optical Telescopes," in *Proceedings of the Advanced Maui Optical and Space Surveillance Technologies Conference*, 2010, vol. 1.

[25] S. B. Howell, *Handbook of CCD Astronomy*, 2nd ed. Cambridge University Press, 2006.

[26] M. M. Schmunk, "Initial Determination of Low Earth Orbits Using Commercial Telescopes," Master's Thesis, Air Force Institute of Technology, 2008.

[27] K. Krisciunas and B. E. Schaefer, "A Model of the Brightness of Moonlight," *Publications of the Astronomical Society of the Pacific*, vol. 103, Art. no. 667, 1991.

[28] L. Dressel, "Wide Field Camera 3 Instrument Handbook, Version 12.0," Space Telescope Science Institute, 2019.

[29] H. Evans, J. Lange, and J. Schmitz, *The Phenomenology of intelligence-focused Remote Sensing, Volume 1: Electro-Optical Remote Sensing*. Riverside Research, 2015.

[30] National Weather Service, "Training Guide in Surface Weather Observations," National Oceanic and Atmospheric Administration, May 1998.

[31] T. S. Campbell, V. Reddy, J. Larsen, R. Linares, and R. Furfaro, "Optical Tracking of Artificial Earth Satellites with COTS Sensors," in *Proceedings of the Advanced Maui Optical and Space Surveillance Technologies Conference*, 2018, vol. 1.

[32] P. Zimmer, J. T. McGraw, and M. R. Ackermann, "Real-Time Optical Space Situational Awareness of Low Earth Orbit with Small Telescopes," in *Proceedings of the Advanced Maui Optical and Space Surveillance Technologies Conference*, 2018, vol. 1.

[33] D. Moomey, "A Call to Action: Aid Geostationary Space Situational Awareness with Commercial Telescopes," *Air & Space Power Journal*, vol. 29, Art. no. 6, 2015.

[34] M. Ackermann and P. Zimmer, "Telescopes and Optics for Space Surveillance," in *Proceedings of the Advanced Maui Optical and Space Surveillance Technologies Conference*, 2019, vol. 1.

[35] "Strategic Command Directive 505-1, Space Surveillance Operations—Basic Operations, Volume 2," United States Strategic Command, 2004.

[36] A. B. Poore *et al.*, "Covariance and Uncertainty Realism in Space Surveillance and Tracking," Numerica Corporation, 2016.

[37] K. Dararutana, "Comparison of Novel Heuristic and Integer Programming Schedulers for the USAF Space Surveillance Network," Master's Thesis, Air Force Institute of Technology, 2019.

[38] B. Tapley, B. Schutz, and G. H. Born, *Statistical Orbit Determination*. Elsevier, 2004.

[39] R. R. Bate, D. D. Mueller, and J. E. White, *Fundamentals of Astrodynamics*. Dover Publications, 1971.

[40] J. R. Vetter, "Fifty Years of Orbit Determination," *Johns Hopkins APL Technical Digest*, vol. 27, Art. no. 3, 2007.

[41] D. Vallado and P. Crawford, "SGP4 Orbit Determination," in *Proceedings of the AIAA/AAS Astrodynamics Specialist Conference*, 2008, vol. , p. 6770.

[42] A. M. Law, *Simulation Modeling and Analysis*, 5th ed. McGraw-Hill Education, 2015.

[43] "High Performance Computing Systems," *United States Air Force Research Laboratory Defense Supercomputing Resource Center*, 2020. https://www.afrl.hpc.mil/hardware/ (accessed Mar.2020).

[44] W. Oberle, "Monte Carlo Simulations: Number of Iterations and Accuracy," United States Army Research Laboratory, ARL-TN-0684, Jul. 2015.

[45] Joint Chiefs of Staff, "Joint Publication 3-14, Space Operations," Department of Defense, 2018.

[46] B. Lal, A. Balakrishnan, Caldwell, Becaja M, R. S. Buenconsejo, and S. A. Carioscia, "Global Trends in Space Situational Awareness (SSA) and Space Traffic Management (STM)," Science and Technology Policy Institute, 2018.

[47] Joint Chiefs of Staff, "Joint Publication 3-14, Space Operations," Department of Defense, 2013

[48] "Strategic Command Directive 505-1, Space Surveillance Operations—Basic Operations, Volume 1," United States Strategic Command, 2004.

[49] "Legend/Glossary/Definition of Terms & Products," *Space-Track*, 2019. https://www.space-track.org/documentation (accessed Nov.2019).

[50] T. Flohrer, H. Krag, H. Klinkrad, B. B. Virgili, and C. Früh, "Improving ESA's Collision Risk Estimates by an Assessment of the TLE Orbit Errors of the US SSN Catalogue," in *Proceedings of the 5th European Conference on Space Debris*, 2009.

[51] E. S. Nightingale, B. Lal, B. C. Weeden, A. J. Picard, and A. R. Eisenstadt, "Evaluating Options for Civil Space Situational Awareness (SSA)," Science and Technology Policy Institute, 2016.

[52] M. R. Ackermann, D. D. Cox, R. R. Kiziah, P. C. Zimmer, J. T. McGraw, and

D. D. Cox, “A Systematic Examination of Ground-Based and Space-Based Approaches to Optical Detection and Tracking of Artificial Satellites.,” in *Proceedings of the 30th Space Symposium Technical Track*, 2015, vol. 1.

[53] B. Weeden, “Going Blind: Why America is On the Verge of Losing Its Situational Awareness in Space and What Can Be Done About It,” Secure World Foundation, 2012.

[54] National Research Council, “Continuing Kepler’s Quest: Assessing Air Force Space Command’s Astrodynamics Standards,” National Academies Press, 2012.

[55] T. Chow, “Space Situational Awareness Sharing program: An SWF Issue Brief,” Secure World Foundation, 2011.

[56] D. J. Trump, “Space Policy Directive 3, National Space Traffic Management Policy,” The White House, 2018.

[57] B. L. Wilson, “Space Surveillance Network Automated Tasker,” *Advances in the Astronautical Sciences*, vol. 119, Art. no. Part 1, 2004.

[58] J. G. Miller, “A New Sensor Allocation Algorithm for the Space Surveillance Network,” JSTOR, 2007.

[59] AFSPC, “Air Force Space Command Instruction 10-610, Space Situational Awareness Metric Data Integration Guidelines for Non-Traditional Sensors,” United States Air Force Space Command, 2019.

[60] M. Wall, “US Military Satellite Explosion Caused by Battery-Charger Problem,” *Space*, 2015. https://www.space.com/29996-us-military-satellite-explosion-dmspf13-cause.html (accessed Mar.2020).

[61] “2009 Iridium-Cosmos Collision Fact Sheet,” Secure World Foundation, 2010.

[62] “Challenges to Security in Space,” Defense Intelligence Agency, 2019.

[63] J. Raymond, “Speech, Multi-Domain Command and Control Conference,” United States Air Force Space Command, 2017.

[64] M. Morton and T. Roberts, “Joint Space Operations Center (JSpOC) Mission System (JMS),” 2011.

[65] C. Clark, “What About JMS? Air Force Reanimates ‘Old Clunker’ Space Tracking System,” *Breaking Defense*, Apr. 2019. https://breakingdefense.com/2019/04/what-about-jms-air-force-reanimates-old-clunker-space-tracking-system/ (accessed Sep.2019).

[66] S. Erwin, "'Agile Software' to Replace Troubled JMS," *SpaceNews*, May 2019. https://spacenews.com/agile-software-to-replace-troubled-jms/ (accessed Sep.2019).

[67] C. Chaplain, "GAO-20-145 Space Command and Control: Comprehensive Planning and Oversight Could Help DOD Acquire Critical Capabilities and Address Challenges," Government Accountability Office, 2019.

[68] Office of the United States Air Force Chief Scientist, "Technology Horizons: A Vision for Air Force Science and Technology 2010-30," United States Air Force, 2011.

[69] "National Security Strategy," The White House, 2017.

[70] S. Curley, "GAO Decision B-413385, Analytical Graphics, Inc.," Government Accountability Office, 2016.

[71] J. Raley, R. Weisman, C. Chow, M. Czajkowski, and K. Sotzen, "OrbitOutlook: Autonomous Verification and Validation of Non-Traditional Data for Improved Space Situational Awareness," in *Proceedings of the Advanced Maui Optical and Space Surveillance Technologies Conference*, 2016, vol. 1.

[72] S. Erwin, "Military See Values in Commercial Data, But Needs to Figure Out How to Buy It," *SpaceNews*, Sep. 2019. https://spacenews.com/military-sees-value-in-commercial-data-but-needs-to-figure-out-how-to-buy-it/ (accessed Sep.2019).

[73] B. Houlton and D. Oltrogge, "Commercial Space Operations Center (ComSpOC): A Commercial Alternative for Space Situational Awareness (SSA)," in *Proceedings of the 30th Space Symposium Technical Track*, 2014, vol. 1.

[74] D. Oltrogge and S. Alfano, "ComSpOC Update and Operational Benefits," in *Proceedings of the 31st Space Symposium*, 2015, vol. 1.

[75] B.R. Flewelling, B. Lane, D. L. Hendrix, W. Therien, and M. W. Jefferies, "Recent Events and Highlights in Space Situational Awareness: Exploitation of Global Persistent, Real-time Optical Observations of Deep Space," in *Proceedings of the 34st Space Symposium*, 2018, vol. 1.

[76] "Products and Services," *ExoAnalytic Solutions*, Mar. 2020. https://exoanalytic.com/space-domain-awareness/commercial-price-list/ (accessed Mar.2020).

[77] J. Aristoff and N. Dhingra, "Non-Traditional Data Collection and Exploitation for Improved GEO SSA via a Global Network of Heterogeneous Sensors," in *Proceedings of the Advanced Maui Optical and Space Surveillance Technologies Conference*, 2018, vol. 1.

[78] C. Henry, "ExoAnalytic, NorthStar E&S Team up on Space Situational Awareness," *SpaceNews*, Apr. 2019. https://spacenews.com/exoanalytic-northstar-es-team-up-on-space-situational-awareness/ (accessed Mar.2020).

[79] D. O'Connell, D. R. Peddle, S. Bain, D. W. Bancroft, and K. Stakkestad, "The NorthStar System—A New Era in Earth Observation," in *Proceedings of the 2017 IEEE International Geoscience and Remote Sensing Symposium (IGARSS)*, 2017, vol. 1, pp. 451–454.

[80] J. Foust, "NorthStar Orders Three Satellites to Collect Space Situational Awareness Data," *SpaceNews*, Oct. 2020. https://spacenews.com/northstar-orders-three-satellites-to-collect-space-situational-awareness-data/.

[81] "Optical Measurements," *Orbital Debris Program Office*, 2020. https://orbitaldebris.jsc.nasa.gov/measurements/optical.html (accessed Mar.2020).

[82] C. T. Bellows, "Leveraging External Sensor Data for Enhanced Space Situational Awareness," Ph.D. Dissertation, Air Force Institute of Technology, 2015.

[83] "About LSST," *LSST*, 2020. https://www.lsst.org/about (accessed Mar.2020).

[84] "Extremely Large Telescope," *Wikipedia*, 2020. https://en.wikipedia.org/wiki/Extremely_large_telescope (accessed Mar.2020).

[85] "List of Largest Optical Reflecting Telescopes," *Wikipedia*, 2020. https://en.wikipedia.org/wiki/List_of_largest_optical_reflecting_telescopes (accessed Mar.2020).

[86] R. Stottler and A. Li, "Automatic, Intelligent Commercial SSA Sensor Scheduling," in *Proceedings of the Advanced Maui Optical and Space Surveillance Technologies Conference*, 2019, vol. 1.

[87] A. J. Warren, "Optimal Placement of a GEODSS Sensor," Air Force Environmental Technical Applications Center, 1991.

[88] T. H. Elio, "Optimal Placement of a GEODSS Sensor. A Follow-On Report for 14 Candidate Sites Worldwide," Air Force Environmental Technical Applications Center, 1991.

[89] T. E. Payne *et al.*, "Space Observation Network Study (SONS)," in *Proceedings of the 1998 Space Control Conference*, 1998, vol. 1, pp. 1–10.

[90] S. E. Andrews and R. C. Raup, "A Mechanism for Evaluating Space Surveillance Networks," in *Proceedings of the 1999 Space Control Conference*, 1999, vol. 1, pp. 1–10.

[91] W. Andress, "Space Surveillance Network (SSN) Optical Augmentation (SOA)," Air Force Space Battlelab, 1999.

[92] K. Morris, C. Rice, and E. Little, "Relative Cost and Performance Comparison of GEO Space Situational Awareness Architectures," in *Proceedings of the Advanced Maui Optical and Space Surveillance Technologies Conference*, 2014, vol. 1.

[93] J. M. Colombi, J. L. Stern, S. T. Wachtel, D. W. Meyer, and R. G. Cobb, "Multi-Objective Parallel Optimization of Geosynchronous Space Situational Awareness Architectures," *Journal of Spacecraft and Rockets*, vol. 55, Art. no. 6, 2018.

[94] M. G. Bateman, J. M. Colombi, R. G. Cobb, and D. W. Meyer, "Exploring Alternatives for Geosynchronous Orbit Space Situational Awareness," Unpublished, 2018.

[95] M. S. Felten, J. M. Colombi, R. G. Cobb, and D. W. Meyer, "Multi-Objective Optimization Using Parallel Simulation for Space Situational Awareness," *Journal of Defense Modeling and Simulation*, vol. 16, Art. no. 2, 2019.

[96] M. Daniels and E. Páte-Cornell, "Quantitative Analysis of Satellite Architecture Choices: a Geosynchronous Imaging Satellite Example," in *Proceedings of the 30th Space Symposium*, 2014, vol. 1.

[97] R. J. Diaz, "Enterprise Architecture for the Air Force Satellite Control Network," in *Proceedings of the 31st Space Symposium*, 2015, vol. 1.

[98] R. E. Thompson, "A Methodology for the Optimization of Disaggregated Space System Conceptual Designs," Ph.D. Dissertation, Air Force Institute of Technology, 2015.

[99] C. C. Davis, R. F. Deckro, and J. A. Jackson, "A Value Focused Model for a C4 Network," *Journal of Multi-Criteria Decision Analysis*, vol. 9, Art. no. 4, 2000.

[100] R. Anthes, "National Oceanic and Atmospheric Administration (NOAA) Satellite Observing System Architecture (NSOSA) Study," National Oceanic and Atmospheric Administration Office of System Architecture and Advanced

Planning, 2018.

[101] R. S. Daw and M. D. Hejduk, "Determining SSN Operational System Capability (SYSCAP)," in *Proceedings of the 1999 Space Control Conference*, 1999, vol. 1, pp. 24–34.

[102] "Space Situational Awareness Efforts and Planned Budgets," Government Accountability Office, 2015.

[103] S. M. Lederer *et al.*, "The NASA Meter Class Autonomous Telescope: Ascension Island," in *Proceedings of the Advanced Maui Optical and Space Surveillance Technologies Conference*, 2013, vol. 1.

[104] M. R. Ackermann, P. Zimmer, J. T. McGraw, and E. Kopit, "COTS Options for Low-Cost SSA," in *Advanced Maui Optical and Space Surveillance Technologies Conference*, 2015.

[105] C. Frueh, H. Fielder, and J. Herzog, "Heuristic and Optimized Sensor Tasking Observation Strategies with Exemplification for Geosynchronous Objects," in *Journal of Guidance, Control, and Dynamics*, 2018, vol. 41, no. 5, pp. 1036–1048.

[106] J. M. Cimbala, "Histograms," *Penn State University*, Aug. 2014. https://www.me.psu.edu/cimbala/me345/Lectures/Histograms.pdf.

[107] W. A. Clark and K. L. Avery, "The Effects of Data Aggregation in Statistical Analysis," *Geographical Analysis*, vol. 8, Art. no. 4, 1976.

[108] "TruSat White Paper, Version 3.0," Consensys Space, 2020.

[109] A. Vasso, R. Cobb, J. Colombi, B. Little, and D. Meyer, "Optimal Incorporation of Non-Traditional Sensors into the Space Domain Awareness Architecture," in *Proceedings of the Advanced Maui Optical and Space Surveillance Technologies Conference*, 2020, vol. 1.

[110] A. Vasso, R. Cobb, J. Colombi, B. Little, and D. Meyer, "Augmenting the Space Domain Awareness Ground Architecture via Decision Analysis and Multi-Objective Optimization," in *Journal of Defense Analytics and Logistics,* 2021, vol. 5, no. 1, pp 1-18.

[111] R. Bruck and R. Copley, "GEODSS Present Configuration and Potential," in *Proceedings of the Advanced Maui Optical and Space Surveillance Technologies Conference*, 2014, vol. 1.

[112] D. Monet *et al.*, "Rapid Cadence Collections with the Space Surveillance

Telescope," in *Proceedings of the Advanced Maui Optical and Space Surveillance Technologies Conference*, 2012, vol. 1.

[113] J. C. Zingarelli, E. Pearce, R. Lambour, T. Blake, C. J. Peterson, and S. Cain, "Improving the Space Surveillance telescope's Performance Using multi-hypothesis Testing," *The Astronomical Journal*, vol. 147, Art. no. 5, 2014.

[114] M. R. Ackermann and J. T. McGraw, "An Overview of Wide-Field-of-View Optical Designs for Survey Telescopes," in *Proceedings of the Advanced Maui Optical and Space Surveillance Technologies Conference*, 2010, vol. 1.

[115] M. R. Ackermann, R. R. Kiziah, B. J. Douglas, P. C. Zimmer, and J. T. McGraw, "Exploration of Wide-Field Optical System Technologies for Sky Survey and Space Surveillance," in *Proceedings of the 30th Space Symposium Technical Track*, 2014, vol. 1.

[116] R. Leitch and I. Hemphill, "Sapphire: a Small Satellite System for the Surveillance of Space," in *Proceedings of the 24th Annual AIAA/USU Conference on Small Satellites*, 2010, vol. 1.

[117] "CCD47-20 Back Illuminated High Performance AIMO Back Illuminated CCD Sensor," e2v Technologies, 2006. [Online]. Available: http://instrumentation.obs.carnegiescience.edu/ccd/parts/CCD47-20BI.pdf.

[118] A. Scott, J. Hackett, and K. Man, "On-orbit Results for Canada's Sapphire Optical Payload," in *Proceedings of the Advanced Maui Optical and Space Surveillance Technologies Conference*, 2013, vol. 1.

[119] P. Maskell and L. Oram, "Sapphire: Canada's Answer to Space-Based Surveillance of Orbital Objects," in *Proceedings of the Advanced Maui Optical and Space Surveillance Technologies Conference*, 2008, vol. 1.

[120] S. Qian, Ed., *Optical Payloads for Space Missions*. John Wley & Sons, 2016.

[121] D. A. Vallado, P. J. Cefola, R. Kiziah, and M. Ackermann, "Removing the Solar Exclusion with High Altitude Satellites," in *Proceedings of the AIAA/AAS Astrodynamics Specialist Conference*, 2016, p. 5433.

[122] "Kepler Science," *National Aeronautics and Space Administration*, 2020. https://web.archive.org/web/20201116141205/https://keplerscience.arc.nasa.gov/the-kepler-space-telescope.html.

[123] "Kepler Instrument Handbook," NASA Ames Research Center, KSCI-19033-001, 2009.

[124] H. J. Kramer, “ORS-5 (Operationally Responsive Space-5) / SensorSat,” *eoPortal*, 2020. https://directory.eoportal.org/web/eoportal/satellite-missions/o/ors-5.

[125] A. Cunningham, “Design of a CCD Camera for Space Surveillance,” in *Proceedings of the IEEE Aerospace Conference*, 2016, vol. 1, pp. 1–9.

[126] A. Cunningham, B. Buck, and K. Bojanowski, “Development of CCD Camera Electronics for Space Surveillance,” in *Proceedings of the IEEE Aerospace Conference*, 2018, vol. 1, pp. 1–8.

REPORT DOCUMENTATION PAGE

Form Approved
OMB No. 074-0188

1. REPORT DATE *(DD-MM-YYYY)*	2. REPORT TYPE	3. DATES COVERED *(From – To)*
16-09-2021	Doctoral Dissertation	Sep 2019 – Sep 2021

TITLE AND SUBTITLE

Optimal Incorporation of Non-Traditional Sensors into the Space Domain Awareness Architecture

5a. CONTRACT NUMBER

5b. GRANT NUMBER

5c. PROGRAM ELEMENT NUMBER

6. AUTHOR(S)

Vasso, Albert R. Maj, USSF

5d. PROJECT NUMBER

5e. TASK NUMBER

5f. WORK UNIT NUMBER

7. PERFORMING ORGANIZATION NAMES(S) AND ADDRESS(S)
Air Force Institute of Technology
Graduate School of Engineering and Management (AFIT/EN)
2950 Hobson Way
WPAFB OH 45433-7765

8. PERFORMING ORGANIZATION REPORT NUMBER

AFIT-ENY-DS-21-S-110

9. SPONSORING/MONITORING AGENCY NAME(S) AND ADDRESS(ES)
Intentionally left blank

10. SPONSOR/MONITOR'S ACRONYM(S)

AFRL/RHIQ (example)

11. SPONSOR/MONITOR'S REPORT NUMBER(S)

12. DISTRIBUTION/AVAILABILITY STATEMENT
DISTRUBTION STATEMENT A. APPROVED FOR PUBLIC RELEASE; DISTRIBUTION UNLIMITED.

13. SUPPLEMENTARY NOTES
This material is declared a work of the U.S. Government and is not subject to copyright protection in the United States.

14. ABSTRACT
The United States Government is the world's *de facto* provider of space object cataloging data, but is challenged to maintain pace in an increasingly complex space environment. This work advances a multi-disciplinary approach to better understand and evaluate an underexplored solution recommended by national policy, in which current collection capabilities are augmented with non-traditional sensors. System architecting and literature identify likely needs, performance measures, and contributors to a conceptualized Augmented Network. Multiple hypothetical telescope architectures are modeled and simulated on four separate days throughout the year, then evaluated against performance measures and constraints using optimization. Decision analysis and Pareto optimality identify a small, diverse set of high-performing architectures while preserving design flexibility. The efficacy of using the performance measures as proxies for reducing positional uncertainty is also explored. The results suggest a 3.5-times increase in average capacity, 55% improvement in coverage, and 3.5 hour decrease in the average maximum time a space object goes unobserved is achievable if decision-makers adopt the Augmented Network approach. A correlation between performance and positional uncertainty is found, suggesting top architectures can generally achieve a major Space Domain Awareness technical requirement without explicitly conducting an orbit determination routine on simulated collection data.

15. SUBJECT TERMS
Space Domain Awareness, Systems Architecting, Modeling and Simulation, Optimization, Decision Analysis

16. SECURITY CLASSIFICATION OF:			17. LIMITATION OF ABSTRACT	18. NUMBER OF PAGES	19a. NAME OF RESPONSIBLE PERSON
a. REPORT	b. ABSTRACT	c. THIS PAGE			Dr. Richard G. Cobb, AFIT/ENY
U	U	U	UU	197	19b. TELEPHONE NUMBER *(Include area code)* (937) 255-3636, ext 4559 (richard.cobb@afit.edu)

Standard Form 298 (Rev. 8-98)
Prescribed by ANSI Std. Z39-18